2007

ANALYTICAL METHODS FOR TRANSPORT EQUATIONS IN SIMILARITY FORM

Abhishek Tiwari
University of Kentucky, atiwa2@uky.edu

ABSTRACT OF THESIS

ANALYTICAL METHODS FOR TRANSPORT EQUATIONS IN SIMILARITY FORM

We present a novel approach for deriving analytical solutions to transport equations expressed in similarity variables. We apply a fixed-point iteration procedure to these transformed equations by formally solving for the highest derivative term and then integrating to obtain an expression for the solution in terms of a previous estimate. We are able to analytically obtain the Lipschitz condition for this iteration procedure and, from this (via requirements for convergence given by the contraction mapping principle), deduce a range of values for the outer limit of the solution domain, for which the fixed-point iteration is guaranteed to converge.

KEYWORDS: transport equations, analytical solutions, similarity variables, fixed-point iteration, Lipschitz condition

Abhishek Tiwari
April 4, 2007

ANALYTICAL METHODS FOR TRANSPORT EQUATIONS IN SIMILARITY FORM

By

Abhishek Tiwari

Kaveh A. Tagavi, PhD
Director of Thesis

James M. McDonough, PhD
Co-Director of Thesis

Lyndon S. Stephens, PhD
Director of Graduate Studies

April 4, 2007

RULES FOR THE USE OF THESES

Unpublished theses submitted for the Master's degree and deposited in the University of Kentucky Library are as a rule open for inspection, but are to be used only with due regard to the rights of the authors. Bibliographical references may be noted, but quotations or summaries of parts may be published only with the permission of the author, and with the usual scholarly acknowledgments.

Extensive copying or publication of the thesis in whole or in part also requires the consent of the Dean of the Graduate School of the University of Kentucky.

THESIS

Abhishek Tiwari

The Graduate School

University of Kentucky

2007

ANALYTICAL METHODS FOR TRANSPORT EQUATIONS IN SIMILARITY FORM

THESIS

A thesis submitted in partial fulfillment of the
requirements for the degree of Master of Science in Mechanical Engineering
in the College of Engineering at the University of Kentucky

By

Abhishek Tiwari

Co-Directors: Dr. Kaveh A. Tagavi, Professor of Mechanical Engineering
and Dr. James M. McDonough, Professor of Mechanical Engineering and Mathematics

Lexington, Kentucky

2007

Dedicated
To my parents(s) at Gwalior

Acknowledgments

I would like to express my deepest gratitude to my academic advisor Dr. Kaveh A. Tagavi, and co-adviser Dr. James M. McDonough for their enthusiastic supervision throughout the course of this work. This work would have been impossible without their support. I would like to thank Dr. Raymond LeBeau for taking the time to serve on the final examination committee.

I am grateful to my many student colleagues who have made my stay at RGAN 210A a memorable one. I am especially grateful to C. B. Velkur, Anand Palki, Chaitanya Penugonda, Narendra Beliganur, Daniel Reasor and Ying Xu for their stimulating discussions, emotional support, entertainment and caring they provided.

I am forever indebted to my friends Nilesh G. Raut and Smita Joel at 271, Kalmia Avenue, Lexington for being the surrogate family during my period of stay here at Lexington and for their moral support there after.

Table of Contents

List of Figures

List of Tables

List of Files

Chapter 1
Introduction

The nonlinear nature of the Navier–Stokes equations makes it difficult to achieve exact solutions. Researchers have been employing different methods to study them. Most existing exact solutions of the Navier–Stokes equations are for fluids with constant viscosity and constant thermal conductivity. The various methods employed and the exact solutions of Navier–Stokes equations can be found in Berker [1, 2, 3]. These equations, which have been known for more than 100 years in their complete form, are very difficult to solve, even on modern computers. In fact at high Reynolds numbers (turbulent flow), the equations are, in effect, impossible to solve with present mathematical techniques, because the boundary conditions become time-dependent. Nevertheless, it is very instructive to derive and discuss these fundamental equations because they reveal many important concepts, yield several particular solutions, and can be examined for modeling laws.

1.1 Transport equations

In fluid mechanics and heat transfer, these Navier–Stokes equations are also designated as *transport equations* because of the relation they bear to movement, or transport, of momentum, heat and mass. The three most important properties are viscosity, thermal conductivity and diffusivity. Each of the three coefficients relates flux or transport to the gradient of a property. Viscosity relates the momentum flux to velocity gradient, thermal conductivity relates the heat flux to temperature gradient, and the diffusion coefficient relates the mass transport to concentration gradient. An example of a simple transport equation can be expressed as follows:

$$u_t + cu_x = 0\,, \tag{1.1}$$

where u is a function of two variables x and t, and the subscripts denote partial derivatives. Here c is a fixed constant. Given an initial condition

$$u(x,0) = f(x)\,, \tag{1.2}$$

we would like to find a function of two variables that satisfies both the transport equation (1.1) and the initial condition (1.2). This equation can be used to model pollution, dye dispersion or even traffic flow, with u representing the density of the pollutant (or dye or traffic, respectively) at position x and time t. In general a "Generic transport equation" which can describe transport

phenomena such as heat transfer, mass transfer, fluid dynamics etc., can be written as

$$\underbrace{\frac{\partial \rho\phi}{\partial t}}_{Transient\ term} + \underbrace{\nabla\cdot(\rho\vec{u}\phi)}_{Convection\ term} = \underbrace{\nabla\cdot(\tau\nabla\phi)}_{Diffusion\ term} + \underbrace{S_\phi}_{Source\ term} \quad . \tag{1.3}$$

Upon inspection of the above equation, it can be inferred that all the dependent variables seem to obey a generalized conservation principle. In this respect, any differential equation addresses a certain quantity as its dependent variable and thus expresses the balance between the phenomena affecting the evolution of this quantity. The various terms in Eq. (1.3) represents the following:

- the *transient term*, $\partial\rho\phi/\partial t$, accounts for the accumulation of ϕ in the concerned volume ;
- the *convection term*, $\nabla\cdot(\rho\vec{u}\phi)$, accounts for the transport of ϕ due to the existence of the velocity field ;
- The *diffusion term*, $\nabla\cdot(\tau\nabla\phi)$, accounts for the transport of *phi* due to its gradients ;
- the *source term*, S_ϕ, acccounts for any sources or sinks that either create or destroy *phi*. Any extra terms that cannot be cast into the convection or diffusion terms are considered as source terms ;

This general transport equation in the form of N.-S. equations poses a formidable system of nonlinear partial differential equations. No general analytical method yet exists for attacking this system although the digital-computer numerical techniques [97, 98, 99, 100, 101, 102] show great promise for the future. No exact solutions are known for problems like the airfoil problems, flow past a flat plates, condensation over a vertical plates, stagnation flows and other boundary-layer flow problems. In accumulating exact solutions over the past 100 years, a considerable number of exact but particular solutions have been found which satisfy the complete equations for some special geometry. Almost all the known particular solutions are for the case of incompressible Newtonian flow with constant transport properties for which the basic equations of mass and momentum reduce to

Continuity:

$$div\boldsymbol{V} = 0\,, \tag{1.4}$$

Momentum:

$$\rho\frac{D\boldsymbol{V}}{Dt} = -\nabla\hat{p} + \mu\nabla^2\boldsymbol{V}\,. \tag{1.5}$$

There are basically two types of analytical solutions of Eq. (1.5):

1. Linear solutions, where the acceleration $\boldsymbol{V} \cdot \boldsymbol{\nabla}$ vanishes.

2. Nonlinear solutions, where $\boldsymbol{V} \cdot \boldsymbol{\nabla}$ does not vanish.

The existing exact solutions of the Navier–Stokes equations have been published in a wide variety of journals [12, 13, 15, 16, 18]. These exact solutions are for the following flows: Couette steady flows, Poiseuille steady duct flows, unsteady duct flows, unsteady flows with moving boundaries, duct flows with suction and injection, Ekman flows. All of these exact solutions are deduced by standard methods of solution, for example, method of separation of variables, Bessels functions, Laplace transformation etc. Some of these exact solutions are briefly discussed in the next chapter.

In all the above cases, the basic equations expressing physical laws as mentioned earlier are partial differential equations. In certain cases standard methods of solution (separation of variables, Laplace transforms, etc.) are of value, and the solution can be found. Nevertheless, there are a number of problems in which solutions cannot be found by the usual classical methods. This is particularly true if the equations encountered are nonlinear.

It is of interest to note that solutions of certain sets of partial differential equations occurring in these flows can be found quite readily inspite of the failure of the classical methods to yield results. Notable among such solutions are those that have been obtained by employing transformations that reduce the system of partial differential equations to a system of ordinary differential equations. These transformations are designated as "Similarity Transformations," and the resulting solutions are known as similarity solutions.

1.2 Similarity transformation

Symmetrical problems are the simplest ones to solve. The symmetry of the equilateral triangle and that of the circle are obvious because these figures can readily be visualized. Less obvious but equally real is the algebraic symmetry of ordinary and partial differential equations, which, if present, can facilitate the solution of the equations just as geometrical symmetry can facilitate the solution of geometrical problems.

Mathematically, an object is said to possess symmetry if performing certain operations on it leaves it looking the same. For example, rotating an equilateral triangle by 120° around its centroid does not change its appearance. We express the symmetry of the triangle by saying it is invariant to rotation of 120° around its centroid. Differential equations, both ordinary and partial, are sometimes *invariant* to groups of algebraic transformations, and these algebraic

invariances, like the geometric ones mentioned above, are also symmetries. One of the pioneers to come up with the idea of using algebraic symmetry to find the solution of ordinary differential equations was the mathematician Sophus Lie [103, 104]. In his course of works he achieved two important results; he showed how to use knowledge of the transformation group:

1. to construct an integrating factor for first-order ordinary differential equations, and
2. to reduce second-order ordinary differential equations to first order by a change of variables.

These two results are all the more important because they do not depend on the equation's being linear. Another important contribution to this theory was given by the Austrian physicist L. Boltzmann [105], who used the algebraic symmetry of the partial differential diffusion equation to study diffusion with a concentration-dependent diffusion coefficient. The crux of his method is using the symmetry to find the special solutions of the partial differential equation by solving a related ordinary differential equation. The American mathematician Garett Birkhoff [106] was first to recognize that Boltzmann's procedure depended on the algebraic symmetry of the diffusion equation and could be generalized to other partial differential equations, including nonlinear ones. Using the algebraic symmetry of the partial differential equation, he showed how solutions can be found merely by solving a related ordinary differential equation. This method of deriving similarity solutions by using group invariance property is known as *Group theory method* [4] . The other commonly used techniques to carry out similarity analysis are: free parameter method, separation of variables and dimensional analysis.

In the "free parameter method," it is assumed that the dependent variable occurring in a particular partial differential equation can be expressed as a product of two functions. One of the functions in this product is a function of all of the independent variables except one. The other function is assumed to depend on a single parameter, η, where η is a variable obtained from a transformation of the variables involving the independent variable not occurring in the first function. Hansen [6] has provided a very detailed discussion of this procedure.

A second method of performing a similarity analysis which incorporates the classical separation of variables method of solution has been formulated by D. E. Abbott and S. J. Kline [48]. This method is concerned with finding similarity transformations and takes boundary conditions into account. The form of the similarity variable is specified. Once a specific form of the similarity variable is chosen the original partial differential equation is transformed under the selected coordinate transformations. The dependent variable is considered to be a function of

new coordinates. It is at this point that the separation of variables concept enters the analysis. The dependent variable is expressed as a product of separable functions of the new independent variables. Substitution of the product form of the dependent variable into the equation generally leads to an equation in which the functions of one variable cannot be isolated on the two sides of the equation unless certain parameters are specified . Usually, these parameters can be specified quite readily and "separation of variables" is achieved.

Another important method of performing similarity analysis of partial differential differential equations is dimensional analysis. This method is discussed thoroughly by the Sedov [49]. This method shows how variables may be transformed. Furthermore, if the physical law is expressed as a differential equation, it may be clear from the transformed variables how the number of variables may be reduced.

Before moving further we would like to mention why these solutions are known as "similarity solution." Given below is the example of a 1-dimensional diffusion equation exhibiting similarity solution and its nature.

1.2.1 What is a similarity behavior?

Consider the following partial differential equation for a 1-dimensional diffusion equation:

$$\frac{\partial \theta}{\partial t} = c_1 \frac{\partial^2 \theta}{\partial y^2} \,. \tag{1.6}$$

Depending on the physical significance attached to the variables, Eq. (1.6) is representative of a wide range of physical phenomena. For example, if we define θ define as temperature, c_1 as thermal conductivity, t as time, and choose y as a coordinate normal to a wall, Eq. (1.6) describes the propagation of heat in a finite solid when the wall (of thickness l) is suddenly heated to a temperature exceeding that of its surroundings. Here, we have assumed that prior to the temperature change the wall is in *steady state condition* (T_w). The initial and boundary condition are taken as $\theta(y,\, 0) = T_w y/l$ and $\theta(0,\, t) = 0$, $\theta(l,\, t) = 0$ respectively.

Again, we might define θ as a velocity of a flow parallel to a plate, choose c_1 as the kinematic viscosity, let y be the normal distance from the plate, and t be time. Eq. (1.6) then describes the velocity variation of the flow if the wall is suddenly set into motion. Diffusion of vorticity in a fluid, slowing down of neutrons in matter, etc., are also represented by Eq. (1.6). Solutions to Eq. (1.6) can be found by applying rather standard mathematical methods. We will attempt to find a solution, however, based on the following technique.

Let us transform variables by choosing a new independent variable η, defined by

$$\eta = \frac{y}{2\sqrt{c_1 t}} \tag{1.7}$$

Suppose also that the dependent variable θ can be expressed as

$$\theta = \Theta(t) F(\eta)\,. \tag{1.8}$$

From Eqs. (1.7) and (1.8) we have

$$\frac{\partial \theta}{\partial y} = \frac{\partial \theta}{\partial \eta}\frac{\partial \eta}{\partial y} = \Theta F'(\eta)\frac{1}{2\sqrt{c_1 t}}; \quad \frac{\partial^2 \theta}{\partial y^2} = \Theta F''(\eta)\frac{1}{4c_1 t} \tag{1.9}$$

and

$$\frac{\partial \theta}{\partial t} = \Theta' F + \Theta F' \frac{\partial \eta}{\partial t} = \Theta' F + \Theta F' \left(-\frac{\eta}{2t}\right)\,, \tag{1.10}$$

where

$$\frac{\partial \eta}{\partial t} = -\frac{c_1 y}{4(c_1 t)^{3/2}} = -\frac{\eta}{2t}\,. \tag{1.11}$$

Substituting Eq. (1.11) and Eq. (1.10) into Eq. (1.6) we get,

$$\Theta(F'' + 2\eta F') = 4t\Theta' F\,. \tag{1.12}$$

Therefore if $\Theta = c_2 t^n$ Eq. (1.12) can be written as:

$$F'' + 2\eta F' - 4nF = 0\,. \tag{1.13}$$

Thus by transformation of variables, we have been able to reduce a partial differential equation in two variables to an ordinary differential equation in one variable. If the above equation is considered as an equation for momentum of a fluid motion over a suddenly accelerated plane, then the problem is to find the velocity of the fluid surrounding the plate as a function of time and distance from the plate. Thus in this case θ will become u and c_1 will become ν. The term $\Theta(t)$ in Eq. (1.8) is replaced by U_0 so that,

$$u = U_0 F(\eta)\,,$$

where

$$\eta = y/2\sqrt{\nu t}\,.$$

The boundary and initial conditions on u are are now applied to $F(\eta)$ and become

$$\lim_{\eta\to\infty} F(\eta) = 0\,,\ F(0) = 1\,. \tag{1.14}$$

The choice of $\Theta(t) = U_0 = constant$ implies $n = 0$ in Eq. (1.13). Thus the equation becomes,

$$F'' + 2F' = 0\,. \tag{1.15}$$

The solution of Eq. (1.15) is readilly found to be

$$F(\eta) = 1 - \frac{2}{\sqrt{\pi}} \int_0^{\eta} e^{-\eta^2}\, \mathrm{d}\eta = \operatorname{erfc}\eta\,. \tag{1.16}$$

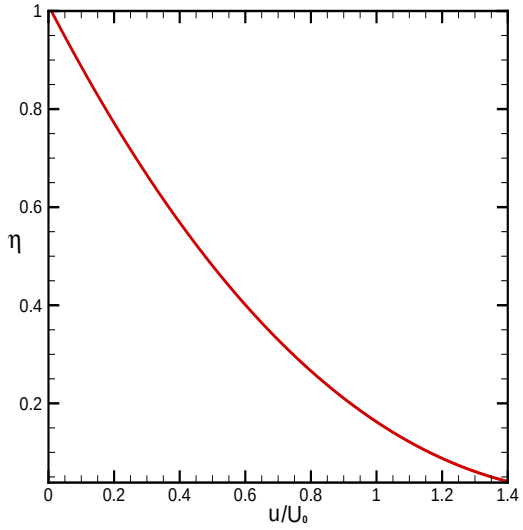

Figure 1.1 Graphical illustration of similarity behavior.

The function $\operatorname{erfc}\eta$ is the complimentary error funtion. Its value can be found from tabulations of the error function $\operatorname{erfc}\eta$ which are given in a number of standard reference tables [127]. The solution for u is, therefore, given by

$$u = U_0 \operatorname{erfc}\eta \tag{1.17}$$

or

$$u/U_0 = F(\eta)\,.$$

Thus the nondimensional velocity u/U_0 is a function of the single variable η. A plot of η versus u/U_0 is shown in Fig. (1.1). For any given time t_0, the parameter η can be replaced by a scalar multiple of y. Thus we see that if u/U_0 were plotted against y for various times, the velocity profiles would be all "similar" in form and collapse onto the single curve defined by Eq. (1.17). That is, the velocity profiles at various times differ only by coordinate scale changes . This geometry property is a characteristic of similarity solutions and is the reason for the choice of the name.

Chapter 2
Background

The characteristics of transport phenomena, as we have seen, are essentially nonlinear– a fact that has long been recognized. Indeed the advances in the analytic theory of fluid mechanics have rested heavily upon and have contributed greatly to our knowledge of nonlinear differential equations, both ordinary and partial. This chapter is primarily concerned with methods of solution for nonlinear differential equations arising from transport processes– which herein interpret to mean chemical kinetics, fluid mechanics, diffusion, heat transfer, and related areas. The exposition is a mixture of theory and examples. A section on the origin of some equations is followed by sections on exact solutions, detailed examples, approximate methods, and numerical methods.

2.1 What is nonlinearity?

In many engineering investigations, perhaps the most common procedure is to mention nonlinearities merely to dismiss them. In elementary studies, we often get the impression that everything is ideal, frictionless, inelastic, rigid, inviscid, incompressible, and the like.

What in fact is the complication that causes us to mutter these phrases? Recall that the derivative, denoted by D, possesses the fundamental property "the derivative of the sum of two functions f and g is equal to the sum of derivative of the functions;" that is, for any constants $a,b,$

$$D[af + bg] = a\,Df + b\,Dg. \tag{2.1}$$

This property is also possessed by the integral, all difference operators, and combinations of the above classes. However, the mere possession of linearity by the operators *does not ensure* that the complete equation will have this property. In general we say that an operator L is linear if

$$L[af + bg] = aLf + bLg \tag{2.2}$$

where f and g are functions, and a and b are constants. Logarithm operator, squaring operator, exponential operator are examples which do not possess this property. Recall that

$$\begin{aligned} \exp[af + bg] &= \exp[af]\,\exp[bg]\,, \\ &\neq a\exp f + b\exp g\,. \end{aligned} \tag{2.3}$$

Consider the linear ordinary differential equation

$$\frac{d^2x}{dt^2} + ax = 0 \tag{2.4}$$

where a is constant. If x_1 and x_2 are both solutions of Eq. (2.4), *i.e.*,

$$\frac{d^2x_1}{dt^2} + ax_1 = 0, \quad \frac{d^2x_2}{dt^2} + ax_2 = 0 \tag{2.5}$$

then it follows, by the linearity of the second derivative that $Ax_1 + Bx_2$ is a solution, where A and B are arbitrary constants. This fact is the foundation of the principle of superposition which has been essentially responsible for the great successes of the past in constructing effective theories for (linearized) physical phenomena.

Let us now suppose that Eq. (2.4) is modified to account for the nonlinear restoring force $ax + bx^2$. The equation now becomes

$$\frac{d^2x}{dt^2} + ax + bx^2 = 0\,. \tag{2.6}$$

If two solutions $x_1(t)$ and $x_2(t)$ of Eq. (2.6) have been found, is $x_1 + x_2$ also a solution? Upon substituting $x_1 + x_2$ for x we find

$$\left[\frac{d^2x_1}{dt^2} + ax_1 + b{x_1}^2\right] + \left[\frac{d^2x_2}{dt^2} + ax_2 + b{x_2}^2\right] + 2bx_1x_2\,. \tag{2.7}$$

The two bracketed expressions of relation (2.7) vanish by assumption, but the last term is not zero. Hence $x_1 + x_2$ is not a solution. *Thus the principle of superposition no longer holds and we have suffered a major setback.* It is the loss of this principle and the lack of an effective replacement that leads to many difficulties.

It should be noted here that the use of the phrases linear and nonlinear does not refer to the graphical character of a function. Rather they concern the properties of operators. If in an ordinary differential equation the dependent variable y and its derivetives are of the *first degree* only and no product of these terms, such as $y'y'''$, $yy'y''$, occur then the equation is clearly linear. Thus, $y''' + y'y'' = 0, (y'')^2 + y' + y^{1/2} = 0$ are nonlinear equations of third and second order, respectively. The nonlinear terms are $y'y'', (y'')^2$, and $y^{1/2}$. An immediate observation is that types of nonlinearities are legion. Some are more difficult to handle than others. Such a great variety leads one to suspect that no single theory of nonlinearity is possible.

2.1.1 Literature

Refinements and advances in science and technology, the demands of the space age and the availability of computing machines have created great interest in a whole range of nonlinear

problems. Much of this work originated in astronomy and nonlinear mechanics. In astronomy one encounters the Lane-Emden equation for the gravitational equilibrium of gaseous configurations. It originted with Lane [19] and has been further investigated by Emden [20] and Kelvin [21]. Chandrashekhar [22] and Davis [23] contributed in developing a general form.

Mechanical and electrical oscillations have concerned numerous researchers. Here we find the works of Andronow and Chaikin [24], Stoker [25], McLachaln [26], Kryloff and Bogoliuboff [27], Minorsky[28, 29, 30], Cunningham [31], and Malkin [32]. Stability and other theoretical concepts are explored in the monographs by Hale [33], Lasalle and Lefschetz [34] and Lefschetz [35].

The theory of elasticity and plasticity is rich in nonlinear equations. Probably the earliest problem was that of the "elastica" discussed by McLachlan [26]. Bickley [36] has modified the idea to characterize the drape of fabrics by means of a "bending length." A substantial number of pre-1940 papers are summarized by von Karman [37]. This excellent summary concerns the large-deflection of elastic structures as well as problems in plasticity and fluid mechanics. It is partially concerned with nonlinear partial differential equations.

In electricity, nonlinearity arises from saturation of ironcored apparatus. The triode oscillator is an example of a nonlinear device. Van der Pol and Appleton were leaders in triode problems and the Van der Pol equation has served as a fundamental model for many investigations.

Extensive research in connection with Newtonian and non-Newtonian fluids has been conducted by many authors. The pioneer work is done by Prandtl [38, 39], Blasius [40, 41], Goldstein [42], Bickley [36], Karman [37], Oseen [43], Reynolds [44] and Taylor (see Karman [37] and Schlichting [9]). Most of these conspicuous advances in fluid mechanics have occurred because of similarity solutions. Apart from these early contributions, theory and examples, in various disciplines, are given by Hansen [6], Ames [45, 46], Kline [47] and Sedov [49]. The ordinary differential equations which arise from the construction of similarity varibles are often of intractable form. The difficulties are compounded because the boundary conditions occur in part at infinity. The next section begins with several examples whose exact solutions are attainable. In the next section a comprehensive review of exact solutions to N.–S. equations is discussed.

2.2 Exact solutions of Navier–Stokes

Our discussion about the exact solutions of N.–S. can be divided into two categories. In the, first category, the nonlinear terms in the N.–S. equations are identically zero, or sum to zero, or are forced to linearize. In the second category we include the exact solutions that most fully take into account the nonlinearities of the convection terms.

2.2.1 Solutions without nonlinear convection terms

Parallel flows: For parallel flows, the nonlinear convection terms in the equations are identically zero. Superposition of solutions in the same domain is possible if the governing equations and boundary conditions are linear and homogeneous. The physical problem involves flows due to longitudinally moving boundaries. A well-known example is the Couette flow between two plates. Other examples can be found in Berker [1, 2, 3] and in potential theory literature. One important class of parallel flows is the flow in long cylinders driven by a pressure gradient. The governing equation is the Poisson equation. Exact solutions inlclude Poiseuille flow between plates and in a circular tube and other cross sectional geometries, such as annuli, eccentric circles, ellipses, confocal ellipses, equilateral triangles, cirlcles with circular notches, limacons, lemniscates, epitrochiods, etc. An excellent review has been given by Shah and London (1978) [11]. The following describe some flows closely related to parallel flows.

Concentric flows: Let (r, θ, z) be cylindrical coordinates. Concentric flows are those in which the velocity v is in the θ direction only. The Navier–Stokes equations give

$$v_{rr} + \frac{1}{r}v_r - \frac{v}{r^2} = 0. \tag{2.8}$$

Examples are the flow between concentric rotating circular cylinders and the flow due to a single rotating cylinder in an infinite fluid. Concentric flows and parallel flows can be superposed, provided that the boundaries coincide.

Flows that are Essentially Parallel or Concentric: These flows are governed by linear equations. There are two main categories: asymptotic suction flows and spiral flows.

If a constant normal velocity $-V$ is added to a parallel flow $w(y)$, the constant-pressure Navier–Stokes equations become

$$-Vw_y = \nu w_{yy} \tag{2.9}$$

A solution is the asymptotic suction profile

$$w = W[1 - exp(-Vy/\nu)], \tag{2.10}$$

where W is a constant. Equation (2.9) is also applicable to the flow between two porous plates with injection on one plate and suction of the same magnitude on the other plate Berman [50, 51]. The axisymmetric analogue of the asymptotic suction profile on a porous plate is the longitudinal flow over a porous circular cylinder with constant suction, was found independently by Wuest [52], Lew [53], and Yashura [54]. The flow in an annulus with radial velocity $-Va/r$ was studied by Berman [50], and that along a corner with suction was examined by Stuart [55]. Many other spiral flows and their solution can be found in Berker [3].

Other Linear Flows: These flows are neither parallel nor essentially parallel. They are governed by nondegenrate linear equations, i.e. the order of the governing equations is the same as in the original N.–S. equations. The solutions reviewed are pseudo-plane flows, where all path lines lie in their own plane, or essentially pseudo-plane flows. Other pseudo-plane flows can be found in Berkers's [1, 2, 3] works.

The most important of these flows is Ekman flow. In a coordinate system rotating with angular velocity ω, let the Cartesian velocities be $[u(z), v(z), 0]$. The governing equations become

$$-2\omega v = \nu u_{zz}, \quad 2\omega u = \nu v_{zz}. \tag{2.11}$$

Ekman [5] found the solution for a moving plate in a rotating system to be

$$u + iv = Uexp\left[-\sqrt{\frac{\omega}{\nu}}(1+i)z\right]. \tag{2.12}$$

Ekman flow was extended by Gupta (1972) [56] to include suction or weak injection on the plate. The flow due to a pressure gradient between two plates in a rotating system was studied by Vidyanidhi and Nigam (1967) [57] and Vidyanidhi *et al.* (1975) [58]. A related pseudo-plane flow is that between two noncoaxial rotating plates, studied by Abbott and Walters (1970) [59]. Nonunique solutions were found by Berker (1979,1982) [1, 3]. Addition of a constant suction was considered by Erdogan (1976) [60] and Rajagopal (1984) [8].

Beltrami flows or screw fields: These are the flows with the property $\zeta \cdot \mathbf{q} = \mathbf{0}$ (*i.e.* vorticity is parallel to velocity and the flow is necessarily three dimensional). Exact solutions for planar generalized Beltrami flows were first investigated by Kampé de Fériet (1930,1932) [61, 62] and by Strakhovitch (1934) [63]. For axisymmetric generalized Beltrami flows Weinbaum and O'Brien (1967) [17] provided the useful solutions. For Beltrami flows a comprehensive account can be found in Wang [12].

2.2.2 Solutions of Navier–Stokes with acceleration terms

Similarity solutions: So far we have discussed cases where the nonlinear terms in the N.–

S. equations are identically zero, or sum to zero, or are forced to linearize. Similarity solutions are the exact solutions that most fully take into account the nonlinearities of the convection terms. Phenomena such as nonexistence and nonuniqueness may occur, and analytic analyses of these and other phenomena, such as stability, are greatly facilitated by the reduction of N.–S. equations to ordinary differential equations. Several methods for example, separation of variables, integration factor, asymptotic expansion, power series expansion, Laplace transformation, Euler transformation etc., can be used to solve these ordinary differential equations. In what follows we describe steady similarity solutions of the Navier–Stokes equations.

Radial flows: Two-dimensional radial flow was first studied by Jeffrey (1915) [125].

In planar cylindrical coordinates (r, θ) let the radial velocity be given by

$$u = \frac{\nu F(\theta)}{r} \tag{2.13}$$

where ν is kinematic viscosity. The Navier–Stokes equations reduce to

$$F''' + 2FF' + 4F' = 0\,. \tag{2.14}$$

The solution to this nonlinear equation can be expressed in terms of elliptic functions.

Stretching flows: The flow due to stretching surface may be applied to the extrusion of sheet materials. Due to the zero tangential pressure gradient and the similarity transformation the Navier–Stokes equations reduce to

$$f''' + ff'' - (f')^2 = 0 \tag{2.15}$$

with the following boundary conditions:

$$f(0) = f'(\infty) = 0\,, \quad f'(0) = 1\,. \tag{2.16}$$

Crane (1970) [126] obtained the rare closed-form similarity solution

$$f = 1 - \exp(-\zeta) \quad \text{where } \zeta \text{ is a similarity variable}\,. \tag{2.17}$$

Axisymmetric, three-dimensional and other extensions of these flows can be found in Wang [14].

Free shear flows: Free shear flows are unaffected by walls and develop and spread in an open ambient fluid. There are mainly three types of free shear flows: (1) free shear layer between parallel moving streams, (2) plane laminar jet and (3) the wake behind a body immersed in a

stream. Out of these three types, only plane laminar jet flow exhibits a closed form of solution. Given below is the similarity form of plane laminar jet

$$f''' + ff'' + (f')^2 = 0 \tag{2.18}$$

with

$$f(0) = f''(0) = 0\,, \quad f'(\infty) = 0 \text{ as boundary conditions.} \tag{2.19}$$

The exact analytic solution of Eq. (2.18) (deduced by Schlitching [10]) is the following:

$$f(\eta) = 2a\tanh(a\eta) \tag{2.20}$$

where η is a similarity variable, and a is constant determined by momentum flux.

Point sink flow: This flow which is also known as flow into a convergent channel also yields to a closed form of solution. The similarity equation and the associated boundary conditions for this are as follows:

$$f''' + f'^2 + 1 = 0 \tag{2.21}$$

$$f(0) = f'(0) = 0\,, \quad f'(\infty) = 1\,. \tag{2.22}$$

The exact solution of which in terms of f' is,

$$f' = 3\tanh^2\left(\frac{\eta}{\sqrt{2}} + \tanh^{-1}\sqrt{\frac{2}{3}}\right) - 2\,. \tag{2.23}$$

In this brief review we have seen that very few closed form solutions exist for N.–S. equations. These solutions may be classified into three major types: parallel and related flows, generalized Beltrami and related flows, and similarity solutions. Among these three types the most interesting are the similarity solutions of N.–S. equations, which usually pose two-point BVPs in the form of a nonlinear ordinary differential equation. Generally these nonlinear ODEs cannot be solved analytically, so recourse must be made to a numerical approach; however no single numerical method is applicable to every nonlinear ODE. The large variety of possible problems precludes a well defined useful choice criterion. Some of the popular methods that are available to solve these two-point BVPs are discussed in the next few paragraphs. All these methods can be divided broadly into two main categories: numerical methods and approximate methods.

Approximate methods

By approximate methods we shall mean analytical procedures for developing solutions in the form of functions which are close, in some sense, to the exact solution of the nonlinear

problem. Therefore numerical methods fall into a separate category since they result in tables of values rather than functional forms.

Approximate methods may be divided into three broad interrelated categories; "iterative," "asymptotic," and "weighted residual." The iterative methods include the development of series, methods of successive approximation, etc. Some form of the repetitive calculation via some operation F whose character is $u_{n+1} = F[u_n, u_{n-1}, ...]$ successively improves the approximation. Transformation of the equation to an integral equation leads to a natural iterative method.

Asymptotic procedures have at their foundation a desire to develop solutions that are approximately valid when a physical parameter (or variable) of the problem is very small, very large or in close proximity to some characteristic value. Typical of these methods are the perturbation procedures both regular and singular.

The weighted residual methods, probably originating in the calculus of variations, require that the approximate solution be close to the exact solution in the sense that the difference between them (residual) is somehow minimized. Collocation insists that the residual vanish at a predetermined set of points while Galerkin's method is so formulated that weighted integrals of the residual vanish. Following are the brief accounts of prevalent approximate methods.

Variational methods: The two-point boundary-value problem is replaced by the variational problem of minimizing a certain integral, and the resulting variational problem is solved by the Rayleigh–Ritz methods [65, 66]. Many boundary-value problems (for the determination of some equilibrium state of a physical system, for example) can be formulated in terms of variational problems. That is, some functional (representing for example, the energy of the system) is to be minimized over an appropriate space of admissible functions, say $\mathcal{H}$ (Hilbert space). Or we may easily form some functional whose minimum value is attained for the solution of the boundary-value problem. As an *example*, consider the expression

$$I\{\mathbf{w}, \lambda, \sigma\} \equiv \int_a^b \|\mathbf{w}'(\mathbf{x}) - \mathbf{f}(\mathbf{x}, \mathbf{w}(\mathbf{x}); \lambda, \sigma)\|_I^2 \, \mathrm{dx} + \|\mathbf{g}(\mathbf{w}(\mathbf{a}), \mathbf{w}(\mathbf{b}); \lambda, \sigma)\|_{\mathrm{II}}^2 \,, \tag{2.24}$$

where $\|\cdot\|_I$ and $\|\cdot\|_{II}$ are some vector norms for n- and $(n + m)$-dimensional real vector spaces, respectively. Clearly $I\{\mathbf{w}, \lambda, \sigma\} \geq 0$ for all $\mathbf{w}(\mathbf{x}) \in \mathbf{C^1}(\mathbf{a}, \mathbf{b})$ and $I\{\cdot\} = 0$ for a solution of ,

$$\mathbf{y}' = \mathbf{f}(\mathbf{x}, \mathbf{y}; \lambda, \sigma) \,, \quad \mathbf{a} < \mathbf{x} < \mathbf{b} \,; \tag{2.25}$$

$$\mathbf{g}(\mathbf{y}(\mathbf{a}), \mathbf{y}(\mathbf{b}); \lambda, \sigma) = \mathbf{0} \,. \tag{2.26}$$

For any functional $I\{\cdot\}$, using an approximation of the form

$$\mathbf{w_N(x)} = \sum_{\mathbf{j=1}}^{\mathbf{N}} \zeta_{\mathbf{j}} \phi_{\mathbf{j}}(\mathbf{x})\,, \tag{2.27}$$

a scalar function of the N coefficient vectors, ζ_j, and the eigenvalue parameters λ, as well as σ is defined by

$$\Phi(\zeta_1, \zeta_2, ..., \zeta_N, \lambda, \sigma) \equiv I\{\mathbf{w_N(x)}, \lambda, \sigma\}\,. \tag{2.28}$$

The Ritz procedure is to minimize Φ with respect to the components ζ_{ij} of ζ_j and the components λ_k of λ . In general this leads to the system of (nN+m) equations

$$\frac{\partial \Phi}{\partial \zeta_{ij}}(\zeta_1, ..., \zeta_N, \lambda, \sigma) = 0\,, \quad i = 1, 2, ..., n, \quad j = 1, 2, ..., N; \tag{2.29}$$

$$\frac{\partial \Phi}{\partial \lambda_k}(\zeta_1, ..., \zeta_N, \lambda, \sigma) = 0\,, \quad i = 1, 2, ..., m\,. \tag{2.30}$$

For many special cases that frequently occur in physical applications, the systems (2.29) and (2.30) simplify in various ways. The most familar example occurs when the integrand in the functional $I\{\cdot\}$ is a homogeneous quadratic form in $\mathbf{w}$ and $\mathbf{w}'$ and the space $\mathcal{H}$ is such that the boundary conditions are automatically satisfied. In fact, under fairly common circumstances, the Ritz and Galerkin procedures are identical [Kantrovich and Krylov (1958) [68]].

Convergence of the Ritz method has been studied extensively for variational problems leading to linear boundary-value problems. An interesting exception, given by Ciarlet, Schultz, and Varga (1967) [69], leads to higher-order-accurate approximations to the solution of various nonlinear problems of second and higher order.

For linear boundary-value problems that come from variational problems, the Ritz procedure can lead to finite-difference methods. The basic idea here is to employ "basis" functions $\phi_j(x)$ which are piecewise-linear and continuous, and vanish at all but one point (at which it takes on the value unity) of some net. See, for example, Courant (1943) of Friedrichs and Keller (1966) [73].

Galerkin procedure: The approximating functions are chosen from some Hilbert space $\mathcal{H}$ of functions that are, say, piecewise continuously differentiable on [a,b]. Specifically let us assume that $\phi_j(x)$ is an orthonormal basis for $\mathcal{H}$, with

$$(\phi_j, \phi_k) \equiv \int_a^b \phi_j(x)\phi_k(x)w(x)\mathrm{dx} = \delta_{\mathrm{ij}} \quad \mathrm{i,j} = 1, 2, \ldots\,. \tag{2.31}$$

Here $w(x)$ is the (positive) weight function defining the inner product on $\mathcal{H}$. Then we may define an Nth-order approximation to a solution of Eqs. (2.25) and (2.31) as a combination of the form

$$u_N(x) = \sum_{j=1}^{N} \xi_j \phi_j(x)\,. \tag{2.32}$$

The N coefficient vectors ξ_j of dimension n are to be determined by requiring that

$$\gamma_k(\xi_1, ..., \xi_N) \equiv \int_a^b \left[\mathbf{u}'_{\mathbf{N}}(\mathbf{x}) - \mathbf{f}(\mathbf{x}, \mathbf{u}_{\mathbf{N}}(\mathbf{x}); \lambda, \sigma)\right] \phi_k(x) w(x) dx = 0\,, \quad k = 1, 2, ..., N-1, \tag{2.33}$$

and

$$\gamma_N(\xi_1, ..., \xi_N; \lambda, \sigma) \equiv \mathbf{g}(\mathbf{u}_{\mathbf{N}}(\mathbf{a}), \mathbf{u}_{\mathbf{N}}(\mathbf{b}); \lambda, \sigma) = \mathbf{0}. \tag{2.34}$$

Thus in Galerkin's method to "approximately satisfy the boundary-value problem" means to satisfy the boundary conditions exactly and, for the error, in satisfying the equation to be orthogonal to the first $N-1$ basis functions. That is, the measure of error to be made zero is the projection of the error in satisfying the equation on the subspace spanned by $\phi_1, ...\phi_{N-1}$. Of course any function orthogonal to all of the basis functions vanishes, and so in the limit as $N \longrightarrow \infty$ the functions $\mathbf{u}_{\mathbf{N}}(\mathbf{x})$ may very well converge to a solution.

If the differential equation and the boundary conditions are all linear, then the system (2.33) and (2.34) is linear in the components of the $\xi_j \equiv 0\,,\ j = 1, 2, ..., N$ is clearly a solution, and we have in fact an algebraic eigenvalue problem in which λ is to be determined so that nontrivial solutions exist. In the nonlinear case, Newton's method is again an excellent scheme for seeking accurate approximations to the roots of (2.33) and (2.34).

Method of Collocation: The solution of the two-point boundary-value problem is represented by a function of several parameters which satisfies the boundary conditions for any set of values of the parameters. The approximate solution is substituted in the differential equations, and the parameters are determined by the satisfaction of some error criterion [65]. In this technique we assume that the functions $\psi_j(x)$ form a complete set on some Banach space, $\mathbf{B}$, which includes $C^1(a, b)$. Further, let interpolation by linear combination of these functions converge, together with the first derivatives, for functions in $C^1(a, b)$. This means that for each finite set

$$\psi_1(x), \psi_2(x), ..., \psi_N(x) \tag{2.35}$$

there are corresponding points $x_{j,N} \in [a, b]$ such that for any $\phi(x) \in C^1(a, b)$ there exist (unique constants) $a_{k,N}$ such that

$$\phi(x_{j,N}) = \sum_{k=1}^{N} a_{k,N} \psi_k(x_{j,N})\,, \quad j = 1, 2, ..., N\,. \tag{2.36}$$

Further, for these combinations, it is required that:

$$\lim_{N\to\infty}\sum_{k=1}^{N} a_{k,N}\psi_k(x) = \phi(x)$$

$$\lim_{N\to\infty}\sum_{k=1}^{N} a_{k,N}\psi_k'(x) = \phi'(x)\,.$$

Approximate solutions of (2.25) and (2.31) are now sought, for a given value of N, in the form

$$\mathbf{v_N}(\mathbf{x}) \equiv \sum_{\mathbf{j=1}}^{\mathbf{N}} \eta_{\mathbf{j}}\psi_{\mathbf{j}}(\mathbf{x})\,. \tag{2.37}$$

The conditions for determining the coefficients η_j and the eigenvalues λ are that $\mathbf{v_N}(\mathbf{x})$ should satisfy the differential equation at $N-1$ distinct points $x_{j,N-1} \in [a,b]$ and should satisfy the boundary conditions. Thus we obtain the $(nN+m)$ equations in as many unknowns

$$\gamma_k(\eta_1,...,\eta_N;\lambda,\sigma) \equiv \mathbf{v_N'}(\mathbf{x_{k,N-1}}), \mathbf{f}(\mathbf{x_{k,N-1}};\lambda,\sigma) = \mathbf{0}\,,$$

$$k = 1,2,...,N-1; \tag{2.38}$$

$$\gamma_N(\eta_1,...,\eta_N;\lambda,\sigma) \equiv g((\mathbf{v})_\mathbf{N}(\mathbf{a}),(\mathbf{v})_\mathbf{N}(\mathbf{a});\lambda,\sigma)\,, \tag{2.39}$$

these equations can be solved by Newton's method. Specifically if $n=2, m=q=1$, so that all of the features of the system (2.25) and (2.26) are included in this example. The estimate $\lambda = \lambda^{(\nu)}$, say, of the eigenvalue is kept fixed, and Newton's method is employed on the $n(N-1)$ equations in (2.38) and some selected n of the $(n+m)$ equations in (2.39) to determine the (converged) vectors $\eta_1^{(\nu)},...,\eta_N^{(\nu)}$. This stage is referred as "inner iteration." After the convergence of these inner iterations, the function

$$\mathbf{v_N}(\mathbf{x}) \equiv \sum_{\mathbf{j=1}}^{\mathbf{N}} \eta_{\mathbf{j}}\psi_{\mathbf{j}}(\mathbf{x}) \tag{2.40}$$

is presumably an (accurate) approximation to the solution of some boundary-value problem for (2.25) with $\lambda = \lambda^{(\nu)}$. But it only satisfies n of the required $n+m$ boundary conditions (2.26).

The "outer iterations" are designed to change $\lambda^{(\nu)}$ so that the remaining m conditions in (2.39) are more nearly satisfied. Generally Newton's method is applied to these m equations in the unknowns λ.

Quasilinearization: In this method, applicable only to two-point boundary-value problems for systems of nonlinear ordinary differential equations, the original nonlinear problem is replaced by a sequence of more easily solved linear problems whose solutions converge under

appropriate conditions to the solution of original problem. Quasilineariztion is equivalent to Newton's method except in its specifics of its implementation [143]. In Newton's method we discretize the nonlinear equation and then locally linearize the nonlinear difference equations at each iteartion. By way of contrast in *quasilinearization* (often called the Newton–Kantorovich procedure) we first linearize the nonlinear operator(s), and then discretize the linear equations. Iterations are performed in a manner similar to that of Picard iteration, using a different iterative function. Mathematically, if we have the following nonlinear equation

$$Lu = f(x, u, u')\,, \tag{2.41}$$

where f is generally nonlinear in u and u'. We view u and u' as being distinct independent functions and expand f in Frechét–Taylor series in the following way:

$$f(x, u, u') = f(x, u^{(0)}, u'^{(0)}) + \left(\frac{\partial f}{\partial u}\right)^{(0)} (u - u^{(0)}) + \left(\frac{\partial f}{\partial u'}\right)^{(0)} (u' - u'^{(0)}) + \dots\,, \tag{2.42}$$

where $u^{(0)}$ and $u'^{(0)}$ are initial estimates of u and u' respectively. Thus equation () now can be written as,

$$\left[L - \left(\frac{\partial f}{\partial u'}\right)^{(0)} \frac{d}{dx} - \left(\frac{\partial f}{\partial u}\right)^{(0)}\right] u = f(x, u^{(0)}, u'^{(0)}) - \left(\frac{\partial f}{\partial u}\right)^{(0)} u^{(0)} - \left(\frac{\partial f}{\partial u'}\right)^{(0)} u'^{(0)}\,. \tag{2.43}$$

it is clear that this equation is linear in u and can be discretized in a usual manner.

Regular perturbation method: The method of regular perturbation should properly be called the "small parameter method" of Poincaré [75]. It is one of the outstanding approximate methods because it can be justified rigorously. That is to say, one can establish the existence of the solution and the convergence of the series expansion in the small parameter under rather general conditions (see e.g., Davies and James [107]). Their results are discussed in terms of following pair of equations.

$$\frac{dx}{dt} = f(x, y, t; \mu)\,, \quad \frac{dy}{dt} = g(x, y, t; \mu) \tag{2.44}$$

where μ is a parameter. *If f and g possess a Taylor series in x,y, and μ for all values of t in $0 \le t \le t_1$ then the pair of Eqs.* (2.44) *have solutions x and y which can be expressed in the form of Taylor series in the parameter μ. These series will converge when μ is sufficiently small.* Of course there is no reason why only one "small" parameter must be used. Nowinski and Ismail [76] have utilized a multiparameter expansion in electrostatics. Ames and Sontowski [77] have applied applied multiparameter procedures to solve algebraic problems.

Extensive use has been made of the regular perturbation method in nonlinear mechanics. Some of the pertinent references include Stoker [25], Mclachlan [26], Cunningham [31], and Kryloff and Bogliuboff [27]. As an example, we would consider the boundary-layer flow past a wedge where the flow outside the boundary-layer is

$$U(x) = u_1 x^m \,. \tag{2.45}$$

From Schlichting [9] the similarity equation is

$$f''' + f f'' + \beta(1 - f'^2) = 0 \tag{2.46}$$

with $f(0) = f'(0) = f'(\infty) - 1 = 0$. β is related to m through the relation

$$\beta = \frac{2m}{m+1}. \tag{2.47}$$

For $m << 1$ it follows that $\beta << 1$. Thus we suppose f can be expanded in the regular perturbation series in β

$$f = f_0 + \beta f_1 + \beta^2 f_2 + \dots \,. \tag{2.48}$$

Then the sequence f_n satisfies the equations

$$f_0''' + f_0 f_0'' = 0 \,, \tag{2.49}$$

$$f_1''' + f_0 f_1'' + f_0'' f_1 = (f_0'^2 - 1) \tag{2.50}$$

together with $f_0(0) = f_0'(0) = 0 \,, f_0'(\infty) = 1$, and $f_i(0) = f_i'(0) = 0 \, f_i'(\infty) = 0$ all $i > 0$. The nonlinear problem for f_0 is essentially that of the Blasius problem. The remaining equations are linear. Only the first equation is nonlinear, and it is identical with that for a flat plate at zero incidence. All remaining equations are linear and contain only the function f_0 in the homogeneous portion, whereas the non-homogeneous terms are formed with the aid of the remaining functions f_i. L. Howarth [7] solved the first seven differential equations (up to and including f_6), and calculated tables from them.

Modified perturbation methods: Various devices have been introduced to extend the range of validity of regular perturbation expansions. One of these is due to Shohat [78]; this useful device yields results that are accurate for large values of parameter μ. His method has been further amplified and applied by Bellman [79, 80]. The other modifications to the perturbation methods are applied with the view to address the equations of the following form:

$$\mu x^{(n)}(t) + F[x, x', x'', ..., x^{(n-1)}, \mu] = 0. \tag{2.51}$$

If a regular expansion is attempted we expect difficulties because the zero order equation, obtained by setting $\mu = 0$, is of lower order than the original equation. These problems can be solved by *singular perturbation method* suggested by Friedrichs [81]. In this method one of the boundary conditions is dropped, and an approximation is obtained. This approximation is a good appriximation except within the bounadry layer. This solution, which holds good outside the boundary-layer is known as *outer solution*.

What about the *inner solution* in the boundary-layer? Over the years since the end of WWII a philosophy and procedure has evoloved for treating these problems. The ideas underlying the " method of inner and outer expansions" or of "double asymptotic expansions" or "the method of matched asymptotic expansions" (Bretherton [84]) have been contributed to by many. It was used by Friedrichs [82] in the 1950s. It was systematically developed and applied by Kaplun [83], Lagerstrom and Cole [85]. A treatment of the developments and many more references is given by Van Dyke [86]. One of the guiding principles that should be kept in mind (Van Dyke [86]) is "*When terms are lost or boundary conditions are discarded for the outer solution they must be included in the development of the inner solution.*" Since the "inner" boundary condition was abandoned for the outer solution the "outer" boundary condition must be abandoned for the inner solution. This means that an overlapping domain exists between the two solutions. The inner solution must be *matched* to the outer solution in some fashion. Kaplun and Lagerstrom [83] assert that the existence of an overlapping domain between the two solutions implies that the inner expansion of the outer expansion should, to appropriate (perturbation) parameter orders of magnitude, agree with the outer expansion of the inner expansion. This general matching principle is usually bent to the investigator's taste—the asymptotic form found most useful by Van Dyke [86] is the *asympototic matching principle*.

Methods of iteration/Cauchy–Picard iteration: Approximate methods which generate a new estimate at the nth step in terms of one or more of the approximations in the preceding steps are called *methods of iteration*. Some of these methods have been extensively used by mathematicians in the development of existence theorems. Perhaps the best known of these iterative methods is the *Cauchy–Picard process*. Of less notoriety are some modifications of this process and those operational methods of Pipes [74].

Let L be a differential operator and

$$Lu = f\,. \tag{2.52}$$

If we wish to develop an iterative solution for Eq. (2.52) what is required is a *sequence*

$u_0, u_1, ...u_n, ...$ which converges to the exact solution as n increases indefinitely. Each iteration is based upon some relation of the form

$$u_{n+1} = F(u_n, u_{n-1}, ...) \tag{2.53}$$

where F is an operator intimately related to the equation to be solved.

Consider the set of n simultaneous differential equations

$$\frac{dy_j}{dt} = f_j(y_1, ..., y_n, t)\,, \quad j = 1, 2, ..., n \tag{2.54}$$

having the prescribed initial values $y_j(t_0)$. Upon integrating from t_0 to t and evaluating the integration constants we have the relation

$$y_j(t) = y_j(t_0) + \int_0^t f_j(y_1, ..., y_n, t)\mathrm{dt}\,. \tag{2.55}$$

The iteration process begins with a set of initial trial functions $y_j^{(0)}$ which may be arbitrarily chosen but usually are selected as the initial condition constants. A sequence of iterative approximations are then constructed according to the scheme

$$y_j^{(k+1)} = y_j(t_0) + \int_{t_0}^t f_j(y_1^{(k)}, ..., y_n^{(k)}, t)\mathrm{dt} \tag{2.56}$$

$k = 0, 1, 2, ...; j = 1, 2, ..., n$. The following observations concerning Cauchy-Picard iteration are worthy of note:

(a) If the system (2.54) satisfies the assumptions of the existence-uniqueness theorem in some neighbourhood of the initial data,—then the Cauchy–Picard iteration converges to the true solution.

(b) This iterative process constructs the power series expansion (if it exists) which agrees with the Taylor series. If the Taylor series does not exist, the iterative method can still be applied. Nonexistence of the Taylor series occurs if the expansion center is a singular point.

(c) Integrations are required. If the f_j are sufficiently complicated, analytic integration may be difficult. In such cases numerical or approximate integration may be necessary.

(d) This method is equivalent to replacing Eq. (2.54) by

$$\frac{dy_j^{k+1}}{dt} = f_j(y_1^{(k)}, ..., y_n^{(k)}, t)\,, \tag{2.57}$$

$$y_j^{k+1}(t_0) = y_j(t_0)\,. \tag{2.58}$$

The Cauchy-Picard iteration develops a sequence $y_j^{(k)}$ which converges to the true solution under the proper conditions.

Series solutions: For many boundary-value problems, especially those with a simple analytic formulation, a solution can be obtained in the form of an infinite series,

$$y(x) = \sum_{n=1}^{\infty} C_n \psi_n(x) \tag{2.59}$$

of given functions $\psi_n(x)$ whose coefficients C_n are initially undetermined. *The success of the method depends principally on the nature of the boundary-value problem and on a suitable choice of the system of functions* ψ_n. In some cases this method works very well, and assumed series converges very well, while in some cases infinite series either converges very slowly or does not converge at all.

Blasius series/modified Blasius series: In boundary-layer theory H. Blasius [40] was among the first few who recognized the asymptotic behavior of the solutions to the boundary-layer problems. He proposed the solution for the case of boundary layer on a cylindrical body in the form of a power series; it was further developed by K. Hiemenz [87] and L. Howarth [7]. In this method they assumed the velocity of the potential flow in the form of a power series in x, where x denotes the distance from the stagnation point measured along the contour. The velocity profile in the boundary layer is also represented as a similar power series in x, where the coefficients are assumed to be functions of the coordinate y, measured at right angles to the wall (Blasius series). It is important to note in this connection that L. Howarth [7] succeeded in finding a substitution for the velocity profile which confers universal validity on the y-dependent coefficients. In other words, by a suitable assumption regarding the power series, its coefficients have been made independent of the particulars of the cylindrical body, so that the resulting functions could be evaluated and presented in the form of tables. Thus the calculation of the boundary layer for a given shape becomes very simple if use is made of the tables, provided that the tabulation extends over a sufficiently large number of terms of the series.

The usefulness of Blasius' method is, however, severely restricted by the fact that, precisely in the most important case of very slender body shapes, a large number of terms is required; in fact, their number is so large that it ceases to be practicable to tabulate them all with a reasonable amount of numerical work. This occurs because the potential velocity increases steeply at the leading edge and then varies very slowly over a considerable distance downstream. Application of this procedure is given in Blasius [40, 41]. Subsequent work on Blasius' series includes the contribution from N. Froessling [88], A. Ulrich [89], A. N. Tifford [90], L. Howarth

[7], K. Hiemenz [87] and I. Tani [91] .

Goertler series: The Blasius series described above is suitable for the calculation of boundary layers on all cylinders provided that the flow starts with the stagnation point. On the other hand, the series expansion given by L.Howarth and I.Tani are suitable for only the flat plate. A generalization of all hitherto known series expansions was given by H. Goertler [92, 93] who also improved the convergence of the new series with respect to the old ones by introducing new variables.

Meksyn's asymptotic method: Meksyn [94] also acknowledged the fact that solutions to boundary-layer problems are asymptotic in nature, *i.e.,* the boundary-layer functions are rapidly decreasing functions of the coordinate η, normal to the solid boundary. They can, therefore, be treated as asymptotic solutions for the η variable of the boundary-layer equations; they are also slowly varying functions with respect to the coordinate ξ along the boundary; the equation for the ξ variable can be easily solved step by step. An essential part of the solution consists of an evaluation of definite integrals; it is done by the method of steepest descent; the results obtained are usually divergent; their numerical value is found by Euler's transformation. Further details of this method are given in Meksyn [94].

Homotopy analysis method (HAM): This method is proposed by Liao [95] in his Ph.D. dissertation. Contrary to perturbation techniques which are strongly dependent on small parameters in considered nonlinear equations, it is independent of these parameters. This method has been applied to many boundary-layer problems with reasaonable accuracy, such as the Darcy or non-Darcy free convection heat and mass transfer in porous medium (see Wang *et al.* [122]), liquid film on a unsteady stretching surface [96]. The method is in principle based on Taylor's series with respect to an embedding parameter. As a brief view on this method, consider $\tilde{N}$ is a nonlinear differential operator, let $h \neq 0$ and p be complex numbers, and *A(p)* and *B(p)* be two complex functions analytic in the region $|p| \leq 1$, which satisfy

$$A(0) = B(0)\,, \quad A(1) = B(1) = 1\,, \tag{2.60}$$

respectively. Let

$$A(p) = \sum_{k=1}^{\infty} \alpha_{1,k} p^k\,, \quad B(p) = \sum_{k=1}^{\infty} \beta_{1,k} p^k \tag{2.61}$$

denote Maclaurin's series of $A(p)$ and $B(p)$ respectively. The complex functions $A(p)$ and $B(p)$ are called the embedding functions and p is the embedding parameter.

Consider the nonlinear differential equation in general form

$$\tilde{N}(u(r)) = 0\,, \quad r \in \Omega\,, \tag{2.62}$$

where $\tilde{N}$ is a differential operator and $u(r)$ is a solution defined in the region $r \in \Omega$. Applying the HAM to solve it, we first need to construct the following family of equations:

$$[1 - B(p)]\pounds[\theta(r,p) - u_0(r)] = \hbar A(p)\tilde{N}[\theta(r,p)]\,, \tag{2.63}$$

where $\pounds$ is a properly selected auxiliary linear operator satisfying

$$\pounds(0) = 0\,, \tag{2.64}$$

$\hbar \neq 0$ is an auxillary parameter, and $u_0(r)$ us an initial approximation. According to the definition of the embedding functions $A(p)$ and $B(p)$, Eq. (2.63) gives

$$\theta(r,0) = u_0(r) \tag{2.65}$$

when $p = 0$. Similarly, when $p = 1$, Eq. (2.63) is the same as Eq. (2.62) so that we have

$$\theta(r,1) = u(r)\,. \tag{2.66}$$

Suppose that Eq. (2.62) has solution $\theta(r,p)$ that converges for all $0 \leq p \leq 1$ for properly selected $\hbar, A(p)$ and $B(p)$. Suppose further that $\theta(r,p)$ is infinitely differentiable at $p = 0$, that is

$$\theta_0^k(r) = \frac{\partial^k \theta(r,p)}{\partial p^k}|_{p=0}\ , \quad k = 1,2,3\ldots\,. \tag{2.67}$$

Thus as p increases from 0 to 1, the solution $\theta(r,p)$ of Eq. (2.63) varies continuously from the initial approximation $u_0(r)$ to the solution $u(r)$ of the original Eq. (2.62). Clearly, Eqs. (2.65) and (2.66) give an indirect relation between the initial approximation $u_0(r)$ and the general solution $u(r)$. Thus HAM depends on finding a direct relationship between the two solutions [95].

Integral analysis of the boundary layer: The exact boundary-layer equations are not always possible to solve. In 1921 von Kármán derived a momentum equation by integrating the boundary-layer equations across the boundary layer, and thus reducing the partial differential equation to an ordinary differential equation; this enables us to find an approximate solution of the exact solution. Such approximate methods can be devised if we do not insist on satisfying the differential equations for every fluid particle. Instead, the boundary-layer equation is satisfied in a stratum near the wall and near the region of transition to the external flow by satisfying the boundary conditions, together with certain compatibility conditions. In the remaining region of fluid in the boundary layer only a mean over the differential equation is satisfied, the mean being taken over the whole thickness of the boundary layer. Such a mean value is

obtained from the momentum equation which is, in turn, derived from the equation of motion by integration over the boundary-layer thickness. Since this equation will be often used in the approximate methods, to be discussed later, we shall deduce it now, writing it in its modern form. The equation is known as the *momentum integral equation* of boundary-layer thoery, or as von Kármán's integral condition [124].

We shall restrict ourselves to the case of steady, two-dimensional, and incompressible flow, *i.e.,* we shall refer to the following equations:

$$u\frac{\partial u}{\partial x}+v\frac{\partial u}{\partial y}=-\frac{1}{\rho}\frac{dp}{dx}+\nu\frac{\partial^2 u}{\partial y^2}\,, \tag{2.68}$$

$$\frac{\partial u}{\partial x}+\frac{\partial v}{\partial y}=0\,. \tag{2.69}$$

Upon integrating the equation of motion (2.68) with respect to y, from $y=0$ (wall) to $y=h$, where the layer $y=h$ is everywhere outside the boundary-layer, we obtain:

$$\int_0^h\left(u\frac{\partial u}{\partial x}+v\frac{\partial u}{\partial y}-U\frac{dU}{dx}\right)dy=-\frac{\tau_0}{\rho}\,. \tag{2.70}$$

The shear stress at the wall, τ_0, has been substituted for $\mu(\partial u/\partial y)_0$, so that Eq. (2.70) is seen to be valid both for laminar and turbulent flows, on condition that in the latter case u and v denote the time averages of the respective velocity components. The normal velocity component, v, can be replaced by $v=-\int_0^y\mu(\partial u/\partial x)dy$, as seen from the equation of continuity, and, consequently, we have

$$\int_0^h\left(u\frac{\partial u}{\partial x}-\frac{\partial u}{\partial y}\int_0^y\frac{\partial u}{\partial x}dy-U\frac{dU}{dx}\right)dy=-\frac{\tau_0}{\rho}\,. \tag{2.71}$$

Integrating by parts and going through mathematical manipulation, we obtain the following:

$$\int_0^h\frac{\partial}{\partial x}[u(U-u)]dy+\frac{dU}{dx}\int_0^h(U-u)dy=\frac{\tau_0}{\rho}\,. \tag{2.72}$$

Since in both integrals the integrand vanishes outside the boundary layer, it is permissible to put $h\to\infty$.

We now introduce the displacement thickness δ^* and the momentum thickness θ. They are defined by

$$\delta^*U=\int_0^\infty(U-u)dy\quad\text{displacement thickness}\,, \tag{2.73}$$

$$\theta U^2 = \int_0^\infty u(U-u)dy \quad \text{momentum thickness}\,. \tag{2.74}$$

It will be noted that in the first term of the equation (2.72), differentiation with respect to x, and integration with respect to y, may be interchanged as the upper limit h is independent of x. Hence,

$$\frac{\tau_0}{\rho} = \frac{d}{dx}(U^2\theta) + \delta^* U\frac{dU}{dx}\,. \tag{2.75}$$

This is the *momentum integral equation for two-dimensional incompressible boundary layers.* As long as no statement is made concerning τ_0, Eq. (2.75) applies to laminar and turbulent boundary layers alike. This modern form of the momentum integral equation was first given by H. Gruschwitz [114]. It finds its application in the approximate theories for laminar and turbulent boundary layers (see Schlichting [9]). It can be extended to symmetrical boundary layers also.

Using a similar approach, K. Wieghardt [115] deduced in recent times an *energy integral equation* for laminar boundary layers. This equation is obtained by multiplying the equation of motion by u and then integrating from $y = 0$ to $y = h > \delta(x)$. Substituting, again, v from the equation of continuity, we obtain

$$\rho\int_0^h \left[u^2\frac{\partial u}{\partial x} - u\frac{\partial u}{\partial y}\left(\int_0^y \frac{\partial u}{\partial x}\right) - uU\frac{dU}{dx}\right]dy = \mu\int_0^h \frac{\partial^2 u}{\partial y^2}dy\,, \tag{2.76}$$

which will transform into following after series of mathematical operations:

$$\frac{1}{2}\rho\frac{d}{dx}\int_0^\infty u(U^2-u^2)dy = \mu\int_0^\infty \left(\frac{\partial u}{\partial y}^2\right)dy. \tag{2.77}$$

The upper limit of integration could here, too, be replaced by $y = \infty$ because the integrands become equal to zero outside the boundary layer. The quantity $\mu(\partial u/\partial y)^2$ represents the energy, per unit volume and time, which is transformed into heat by friction. The term $(1/2)\rho(U^2-u^2)$ on the left-hand side represents the loss in mechanical energy (kinetic and pressure energy) taking place in the boundary layer as compared with the potential flow. Hence the term $(1/2)\rho\int_0^\infty (U^2-u^2)dy$ represents the flux of dissipated energy, and the left-hand side represents the rate of change of the flux of dissipated energy per unit length in the x direction.

If, in addition to the displacement and momentum thickness from Eqs. (2.73) and (2.74) respectively, we introduce the dissipation energy thickness δ^{**} from the definition

$$U^3\delta^{**} = \int_0^\infty u(U^2-u^2)dy \quad (\text{energy thickness})\,, \tag{2.78}$$

we can write the energy integral equation (2.78) in the following simplified form:

$$\frac{d}{dx}(U^3\delta^{**}) = 2\nu \int_0^\infty \left(\frac{\partial u}{\partial x}\right)^2 dy\,, \tag{2.79}$$

which represents the energy equation for two-dimensional laminar boundary layers in incompressible flow.

Thus, if a linear velocity distribution is considered, we find: displacement thickness $\delta^* = (1/2)\delta$; momentum thickness $\theta = (1/6)\delta$; Energy thickness $\delta^{**} = (1/4)\delta$. Pohlhausen (1921) [118] was the first, who applied von Kármán's equation to solve boundary-layer problems. Polhausen's procedure was subsequently partly modified by Holstein and Bohlen (1940) [117]. The details of this method can be found in Schlichting (1958) [119].

The momentum equation gives good results for accelerated flow, but it is less satisfactory for retarded flow. The position of the separation point, in the case when the method leads to such a point, is usually downstream of the separation point found by an exact solution. Extension of von Kármán's procedure to all boundary-layer problems (heat transfer, compressible flow, three-dimensional flow) is given in heat transfer [120], compressible flow [121] and three-dimensional flow [116]

Green's functions; Equivalent Integral Equations: It is a very usual practice of solving initial value problems by integral equations. The integral equations are then evaluated by applying quadrature formulae. The same however, can be applied to boundary-value problems, but the derivation of equivalent integral equations is complicated. It is based on determination of the Green's function for a linear/nonlinear boundary-value problem. The Green's function for a linear boundary-value problem is roughly analogous to the inverse of the coefficient matrix in a linear system of equations. For nonlinear boundary-value problems several ways in which Green's function can be used to reduce nonlinear BVPs to integral equations are discussed in Keller [70], Collatz [65] and Courant-Hilbert [72]. In brief, let the boundary-value problem be, for example,

$$Ly = f(x, y, y')\,, \tag{2.80}$$

$$y(a) = y(b) = 0\,, \tag{2.81}$$

where L is a differential operator. Then the Green's function, $g(x, \xi)$, is a function such that the solution of (2.80) is given by

$$y(x) = -\int_a^b g(x,\xi) f(\xi, y(\xi), y'(\xi))\ \mathrm{d}\xi\,. \tag{2.82}$$

If the boundary conditions are replaced by inhomogeneous conditions, then the corresponding integral equation (2.82) is modified by the addition of an inhomogeneous term.

Numerical methods

The purpose of this section is to describe in some detail the methods for the numerical solution of two-point boundary-value problems for linear and nonlinear ordinary differential equations. Two-point boundary-value problems occur in a number of areas of applied mathematics, theoretical physics, and engineering; among them boundary layers, the study of stellar interiors, and control and optimization theory are the significant ones. Since it is usually impossible to obtain analytical (closed-form) solutions to two-point boundary-value problems met in practice, these problems must be attacked by numerical methods.

In contrast to initial value problems for ordinary differential equations in which all the conditions are specified for one value of the independent variable (the initial point), two-point boundary-value problems, as the name implies, have the property that conditions are specified at two values of the independent variable (the initial point and the final point; collectively, the boundary points).

This apparently minor change can lead to profound changes in the behavior of the differential equations. It is not hard to give examples of linear differential equations that possess unique solutions as initial value problems, but which may have no solution, a unique solution, or an infinite number of solutions as two-point boundary-value problems. For example, the initial value problem

$$\ddot{y} + y = 0\,,\; y(0) = c_1\,,\; \dot{y}(0) = c_2 \tag{2.83}$$

has the unique solution $y(x) = c_1 \cos x + c_2 \sin x$ for any set of values c_1, c_2. However the boundary-value problem

$$\ddot{y} + y = 0\,,\; y(0) = 1\,,\; y(\pi) = 0 \tag{2.84}$$

has no solution; the problem

$$\ddot{y} + y = 0\,,\; y(0) = 1\,,\; y(2) = 0 \tag{2.85}$$

has the unique solution $y(x) = \cos x - (\cot 2) \sin x$; while the problem

$$\ddot{y} + y = 0\,,\; y(0) = 0\,,\; y(\pi) = 0 \tag{2.86}$$

has an infinite number of solutions $y(x) = B \sin x$, where B may have any value.

In the examples above, values of the solution at the two ends of the interval were specified, and different combinations of end points and values of the solution led to different conditions of existence and uniqueness of solutions. The specification of the derivative of the solution, rather than the value of the solution itself, may also lead to different conclusions with regard to the existence and uniqueness of solutions of two-point boundary-value problems.

In view of the complicated behavior that solutions of two-point boundary-value problems can exhibit, it should not be surprising that the theory of the existence and uniqueness of solutions of these problems is in a less satisfactory condition than the corresponding theory for initial value problems. And it should be expected that the numerical solution of a two-point boundary-value problem for a given ordinary differential equation will in general be a more difficult matter than the numerical solution of the corresponding initial value problem.

There now exist a number of efficient methods for the step-by-step numerical integration of initial value problems. The standard procedures include Runge-Kutta and multi-step methods such as Hamming's modification of Milne's method. These methods have in common that the solution is computed at a succession of values of the independent variable, say $x_1, x_2, x_3, ...$, where x_0 is the initial point. The initial conditions at x_0 contain sufficient information for the solution to be computed at x_1; and so on. (The progression of the solution from x_0 to x_1 to x_2, etc., explains why initial value problems are sometimes called "marching" problems.) Iteration at the points x_i is sometimes used to improve the numerical accuracy, but no "guessing" is involved because the method has already furnished a good first approximation. In two-point boundary-value problems, on the other hand, there is not sufficient information at the initial point to start a step-by-step solution; hence a way must be found to determine the missing initial conditions, or an approach other than step-by-step integration must be used. Also, iteration is more likely to be an essential feature of a method for the solution of two-point boundary-value problems, and it is usual that missing initial conditions or even solution profiles must be guessed, with no other *a priori* knowledge.

Two-point boundary-value problems have been attacked by a variety of numerical techniques, among them:

Interpolation methods: Solutions of the differential equations are found by numerical integration for sets of values of the missing initial conditions. These solutions will not in general satisfy the prescribed boundary conditions. The correct values of the missing initial conditions are then found by inverse interpolation [65, 64].

Shooting methods: They take their name from the situation in the two-point boundary-

value problem for a single second-order differential equation with initial and final values of the solution prescribed. Varying the initial slope gives rise to a set of profiles which suggest the trajectory of a projectile "shot" from the initial point. That initial slope is sought which results in the trajectory "hitting" the target; that is, the final boundary value [70, 123].

This hit-or-miss method is of course unsuitable for the solution of two-point boundary-value problems on high-speed digital computers. What is needed is a more systematic way to vary the missing conditions based on the amount by which the final values are missed. The shooting methods we are concerned with have this property. In fact, linear problems can be solved by shooting methods without iteration, and the iterations necessary for nonlinear problems can be shown to converge under appropriate conditions.

For nonlinear differential equations, shooting methods are a good choice. The methods are quite general and are applicable to wide variety of differential equations. It is not necessary for the applicability of shooting methods that the equations be of special types such as even-order self-adjoint. Despite this, shooting methods, like all methods, have their limitations. Shooting methods sometimes fail to converge for the problems which are sensitive to initial conditions.

Several different shooting methods have been presented in the literature, the most popular choices among them are Runge-Kutta and Newton-Raphson methods.

Theoretically, we can solve all boundary-value problems by initial value processes. Generally, initial value systems are formed from the boundary-value problems by adding sufficient guessed conditions at one point. These conditions are adjusted by some algorithm until the required relations are satisfied at the other point. For such problems a Runge-Kutta method is easily applied. The other popular choices are multistep methods proposed by Bashforth and Adams, Predictor-corrector methods, Gill's method and Milne's method. An excellent comprehensive dicussion about the numerical solutions of differential equations can be found in Bennett *et al.* [108], Collatz [65], Fox [64], Levy and Baggott [109], Milne [112], Mikeladze [113], von Sanden [111] and Henrici [110].

2.3 Objective

In the previous section we discussed both approximate and numerical methods. These methods are capable of producing reasonable solutions of the nonlinear differential equations. However, these methods do not offer much insight in obtaining the analytical solutions to the nonlinear ODEs.

In the case of approximate methods, we have some success in obtaining solutions in the form

of series (Goertler and Blasius series), but, that too is restricted for wedge profile boundary-layer problems, while von Karman's integral equations uses an arbitrary expression for velocity profiles. Nevertheless, there are a number of problems, especially the boundary-layer flows, which pose two-point boundary-value problems (BVP) in similarity form. No general method yet exists to obtain exact solutions of these BVPs. Several attempts have been made to solve problems of flow past a flat plate (Blasius equation), Falkner–Skan wedge flows, etc.; but none of these yield exact analytical solutions. Apart from this there are also various scenarios in heat transfer, for instance laminar film condensation over a vertical plate, which are also in similarity form and lead to nonlinear ordinary differential equation. Even in these cases no analytical method has yet been formulated. Moreover, the advent of supercomputing has further driven away the interest of the scientific community to explore exact solutions of the Navier–Stokes equations. But there is always a need for exact solutions because of the following two reasons:

1. The solutions represent fundamental fluid-dynamic flows. Also, owing to the uniform validity of exact solutions, the basic phenomena described by Navier–Stokes equations can be more closely studied.

2. Exact solutions serve as standards for checking the accuracies of the many approximate methods, whether they are numerical, asymptotic, or empirical. Current advances in computer technology make the complete numerical integration of Navier–Stokes equations more feasible. However, the accuracy of the results can only be ascertained by a comparison with an appropriate exact solution.

In this research we present a novel approach for deriving analytical solutions to transprot equations expressed in similarity variables. We apply a fixed-point iteration procedure to these transformed equations by formally solving for the highest derivative term and then integrating to obtain an expression for the solution in terms of a previous estimate. We are able to analytically obtain the Lipschitz condition for this iteration procedure and, from this, deduce a range of values for the outer limit of the solution domain for which the fixed-point iteration is guaranteed to converge.

Chapter 3
Mathematical Formulation

In numerical analysis we often use fixed-point iteration to seek the solution of nonlinear ordinary differential equations, but usually do not employ this method when seeking analytical solutions. In this research effort, we have used fixed-point iteration [143] to find the solution of some transport equations (based on boundary-layer theory) in similarity form.

In successive approximation methods we begin with a function called the iteration function, which maps one approximation into a better approximation, thus creating a sequence of possible solutions to the problem. Mathematically, a fixed-point can be described as any point that is mapped back to itself by the mapping. Thus, let $f : \mathcal{D} \longrightarrow \mathcal{D}$, $\mathcal{D} \subset \mathbb{R}^{\mathbb{N}}$, and $x = f(x)$. Then x is said to be a fixed-point of f in $\mathcal{D}$. In other words, a fixed-point is mapped back to itself by the mapping. From the mapping we can write $x = f(x)$ or

$$x - f(x) = 0\,. \tag{3.1}$$

Now if we apply the following iteration scheme:

$$x_1 = f(x_0)$$
$$x_2 = f(x_1)$$
$$x_3 = f(x_2)$$
$$\vdots$$
$$x_m = f(x_{m-1})$$
$$\vdots$$

where x_0 is an initial guess. This iteration procedure will generate the sequence x_m of approximations to the fixed-point x^*. Geometrically, the fixed-points of a function $f(x)$ are the point(s) of intersection of the curve $z = f(x)$ and the line $y = x$ as shown in Fig. 3.1. Clearly, there exists $x = x^*$ such that $y = z$ is the fixed-point of f; that is, $x^* = f(x^*)$. Thus, if we begin

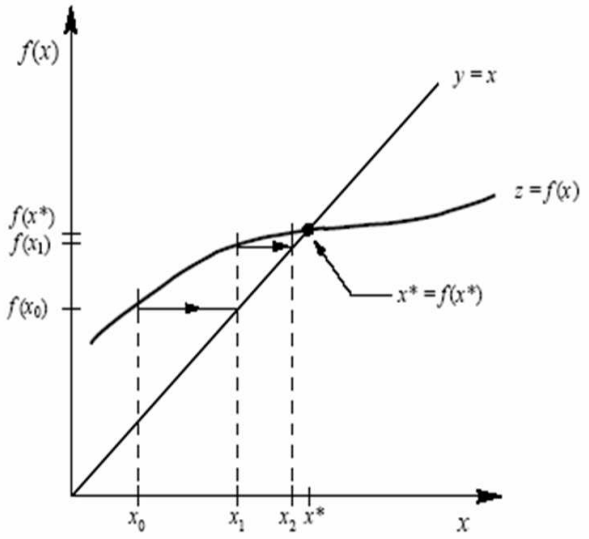

Figure 3.1 Graphical illustration of fixed-point iteration [143].

with x_0 as an initial guess, we find $f(x_0)$ on the curve $z = f(x)$. But according to the iteration scheme, $x_1 = f(x_0)$, so we move horizontally to the curve $y = x$. This locates the next iterate, x_1 on the x-axis, as shown in the figure. This process can now be repeated by again moving vertically to $z = f(x)$ to evaluate $f(x_1)$ and thus a new approximation x_2. An important feature of this iteration procedure is that it converges very fast. For the success of a fixed-point iteration scheme, an iteration function should have a slope less than unity in a neighbourhood of the fixed-point. In such cases, f is said to be a contraction. The following principle [143] provides the sufficient condition for convergence of fixed-point iterations in finite-dimensional spaces of dimension N.

Contraction Mapping Principle: Let f be continuous on a compact subset $\mathcal{D} \subset \mathbb{R}^N$ with $f : \mathcal{D} \longrightarrow \mathcal{D}$, and suppose $\exists$ a positive constant $L < 1 \ni$

$$\|f(y) - f(x)\| \leq L\|y - x\| \ \forall\, x, y \in \mathcal{D}\,. \tag{3.2}$$

Then $\exists$ *a unique* $x^* \in \mathcal{D} \ni x^* = f(x^*)$ *and the sequence* $\{x_m\}_{m=0}^{\infty}$ generated by $x_{m+1} = f(x_m)$ converges to x^* from any guess, $x_0 \in \mathcal{D}$. Here L is a Lipschitz constant whose mathematical significance can be understood via the following inequality:

The inequality,

$$\|f(y) - f(x)\| \leq L\|y - x\| \ \forall\, x, y \in \mathcal{D} \tag{3.3}$$

is called a Lipschitz condition, and L *is the Lipschitz constant.*

This theorem reveals two important aspects of the convergence of iterations. The first is that satisfying $L < 1$ is a sufficient condition but not a necessary condition for the convergence of the corresponding iterations. The second is of mapping f which if holds Eq. (3.2) throughout in any set $\mathcal{D}$, signifies that x^* is the unique fixed-point of f in $\mathcal{D}$. This means that the iterations will converge to x^* using any starting guess, whatever, as long as it is element of the set $\mathcal{D}$. It should be noted that f is considered continuous in $\mathcal{D}$. We now discuss "how to estimate" the Lipschitz constant for a given function f.

Calculation of Lipschitz constant: We have assumed that f is only continuous in $\mathcal{D}$, but if we assume that it also possesses a bounded derivative in this domain [143], then the mean value theorem provides the following relationship for $\mathcal{D} \subset \mathbb{R}^1$: if

$$f(b) - f(a) = f'(\xi)(b-a)\,, \quad \text{for some } \xi \in (a,b) \tag{3.4}$$

then

$$|f(b) - f(a)| = |f'(\xi)||b-a| \leq \left(\max_{x\in[a,b]} |f'(x)|\right) |b-a|\,, \tag{3.5}$$

and we take

$$L = \max_{x\in[a,b]} |f'(x)|\,. \tag{3.6}$$

However, this discussion of fixed-point iteration in number spaces can also be applied to the polynomial spaces. The only exception that we will observe here is in the iteration of the solution in the polynomial space instead of number space. This in turn implies here that at each iteration a polynomial of different degree will be obtained. Hence if $\mathcal{D} \subset \mathbb{P}$ then we will be iterating f with the mapping $f - F(f) = 0$, where f is a polynomial. Thus, we get a sequence of polynomials (of different degrees) at each iteration which will converge to a fixed solution.

3.1 Analytical Iteration Method (AIM)

In this section we will describe an analytical procedure to analyze boundary-value problems in similarity form, which are third-order nonlinear ordinary differential equations. We term our method of finding analytical solutions as "Analytical Iteration Method (AIM)." This method is based on fixed-point iteration over spaces of polynomials. We start our analytical procedure with the original ordinary differential equation re-written for the highest derivative and integrate it to find the solution. As a result of this integration, constants of integration appear in the solution; these constants are evaluated using boundary conditions specified for the physical problem. Once we have this new solution, we can obtain all the derivatives appearing in the above-mentioned, re-written ordinary differential equation and repeat the procedure.

Following the above discussion, we begin with the following nonlinear ordinary differential equation:

$$F(\eta, f) = 0 \tag{3.7}$$

and split it into the two components

$$\mathcal{L}(f) + \mathcal{N}(f) = 0\,, \tag{3.8}$$

where $\mathcal{L}$ and $\mathcal{N}$ are the linear and nonlinear parts of F, respectively. For the 3^{rd} order nonlinear equations, the splitting of the problem into linear and nonlinear parts is given by

$$\mathcal{L}(f) = f'''\,, \tag{3.9}$$

$$\mathcal{N}(f) = F - \mathcal{L}(f)\,. \tag{3.10}$$

The above splitting is done for separating the linear part and integrating it to obtain the initial guess for the solution of nonlinear Eq. (3.7). Thus

$$\mathcal{L}(f) = f''' = 0\,. \tag{3.11}$$

Integrating the above equation thrice with respect to η will generate a polynomial of the following form:

$$f_0(\eta) = C_{10} + C_{20}\eta + C_{30}\eta^2 \tag{3.12}$$

along with its first and second derivatives as

$$f_0'(\eta) = C_{20} + 2C_{30}\eta\,, \tag{3.13}$$

$$f_0''(\eta) = 2C_{30}\,, \tag{3.14}$$

respectively. Here C_{10}, C_{20} and C_{30} are constants of integration and will be evaluated using boundary conditons. In this way an initial solution is obtained, which can be used to obtain the next approximation for the solution of Eq. (3.7). In symbolic notation this iteration procedure for the first iteration can be summarized as follows:

Let f_0, f_0' and f_0'' be the *zeroth approximation* of the solution and its derivatives, respectively. We now rewrite the the original ordinary differential equation for the highest derivative with all the other derivatives substituted by the derivatives obtained at the zeroth approximation. Integrating this equation will yield the *first approximation*,

$$f_1(\eta) = -\mathcal{L}^{-1}[\mathcal{N}(f_0(\eta))] + C_{11} + C_{21}\eta + C_{31}\eta^2\,. \tag{3.15}$$

with

$$f_1'(\eta) = \int \int \mathcal{N}(f_0(\eta))\, dz\, dy + C_{21} + 2C_{31}\eta \tag{3.16}$$

and

$$f_1''(\eta) = \int \mathcal{N}(f_0(\eta))\, dz + 2C_{31} \tag{3.17}$$

as the first and second derivatives,respectively of this first approximation. Here $\mathcal{L}^{-1} = \int \int \int dz\ dy\ dx$, and C_{11}, C_{21} and C_{31} are constants of integration obtained at the first iteration which will be evaluated as before. This procedure can now be generalized to generate a series for obtaining a solution of the equation (3.7). Thus we can express the n^{th} approximatiom of the solution as

$$f_n(\eta) = -\mathcal{L}^{-1}[\mathcal{N}(f_{n-1}(\eta))] + C_{1n} + C_{2n}\eta + C_{3n}\eta^2\,. \tag{3.18}$$

3.1.1 Convergence of AIM

It is clearly evident that to begin the above analytical procedure we need to have an initial guess of the solution function and its derivatives, all of which appear in the equation written for the highest derivative. For this initial guess we solve the linear part of the nonlinear ordinary differential equation. This linear part in boundary-layer flows contains the highest derivative. Integrating this linear part yields an initial guess of the solution and its derivatives. For this initial guess to be the solution of the given nonlinear ordinary differential equation, the following convergence analysis is performed:

Let f be the solution of a nonlinear ordinary differential equation

$$F(\eta, f) = 0\,,$$

where $f \in \mathbb{P}$; *i.e.,* $f(\eta)$ is in a space of polynomials. We say f satisfies a *Lipschitz condition* on $\mathbb{P}$ if $\exists\ L < l$, where l is some definite number, such that

$$\|F(f) - F(g)\| \leq L\,\|f - g\| \quad \forall\ f, g \in \mathbb{P}.$$

Since all $f, g \in \mathbb{P}$ are in C^∞ we can take

$$L = \max_{f \in \mathbb{P}} \|F'(f)\|\ , \tag{3.19}$$

if F is sufficiently regular. Since we will be implementing fixed-point iteration, which underlies the theory of "contraction mapping," the value of the Lipschitz constant is constrained by $L < 1$ for convergence. This will reduce Eq. (3.19) to an inequality, which can be solved for

the maximum domain size η_{max}. Once we know η_{max} for a given nonlinear ordinary differential equation, we can apply the analytical procedure alluded to before to solve it. It should be worthwhile to mention here that this analysis only suggests the sufficient condition and not the necessary condition for the convergence of iterations thus leading to varied rates of convergence of iterations for values of $\eta \in (0, \eta_{max}]$. Moreover, this whole analysis depends on the initial guess of the solution and its derivatives, which are not converged. Therefore it gives only a rough estimate about the maximum size of domain η_{max} instead of a precise one. However, given the simplicity of this analysis and its reasonable estimate about the radius of convergence of AIM, it can be applied to different boundary-layer flows having governing equations in similarity form. For the present thesis two cases are discussed: laminar film condensation over a vertical plate and flow past a flat plate (Blasius equation). In the next chapter, both of these equations and their solution procedures via AIM are discussed in great detail.

Chapter 4
Condensation

Condensation is defined as the removal of heat from a system in such a manner that vapor is converted into liquid. This may happen when vapor is cooled sufficiently below the saturation temperature to induce the nucleation of droplets. Such nucleation may occur homogeneously within the vapor or heterogeneously on entrained particulate matter. Heterogeneous nucleation may also occur on the walls of the system, particularly if these are cooled as in the case of a surface condenser. In this latter case there are two forms of heterogeneous condensation, drop-wise condensation and film-wise condensation, corresponding to the analogous cases in evaporation: nucleate boiling and film boiling. Film-wise condensation occurs on a cooled surface which is easily wetted. On non-wetted surfaces the vapor condenses in drops which grow by further condensation and coalescence, then roll over the surface. New drops then form to take their place. In the next few paragraphs a brief introduction of both drop-wise and film-wise condensation is outlined.

It is quite possible for a thin film of liquid to be adsorbed on all or part of a solid surface. This is very common when adsorption takes place at metal surfaces. Apart from this, polarity of a fluid also enhances the tendency of adorsbtion at the surface, for example, water is the fluid, its polar nature can enhance the tendency of water molecules to attach to portions of the solid surface. These distinct sites of adsorbed liquid molecules on the solid surface can thus serve as nuclei for condensation of the liquid phase when the vapor is supersaturated. The process of drop-wise condensation on the surface begin as the formation of very small droplets on the surface at these sites. The most common example of drop-wise condensation process is the condensation of water vapor present in the air on a cold beverage glass. This is usually interpreted as being a direct consequence of the fact that the liquid poorly wets the glass, except at nuclei locations where water molecules have adsorbed to crevices. Thus drop-wise condensation may occur when the surface is poorly wetted by the liquid phase of the surrounding vapor. In practice, this can be achieved for steam by (1) injecting a nonwetting chemical into the vapor, which subsequently deposits on the surface; (2) introducing a substance such as a fatty acid or wax on to the solid surface; or (3) by permanently coating the surface with a low-surface energy polymer or a noble metal.

As said earlier, in drop-wise condensation, the condensate is usually observed to appear in

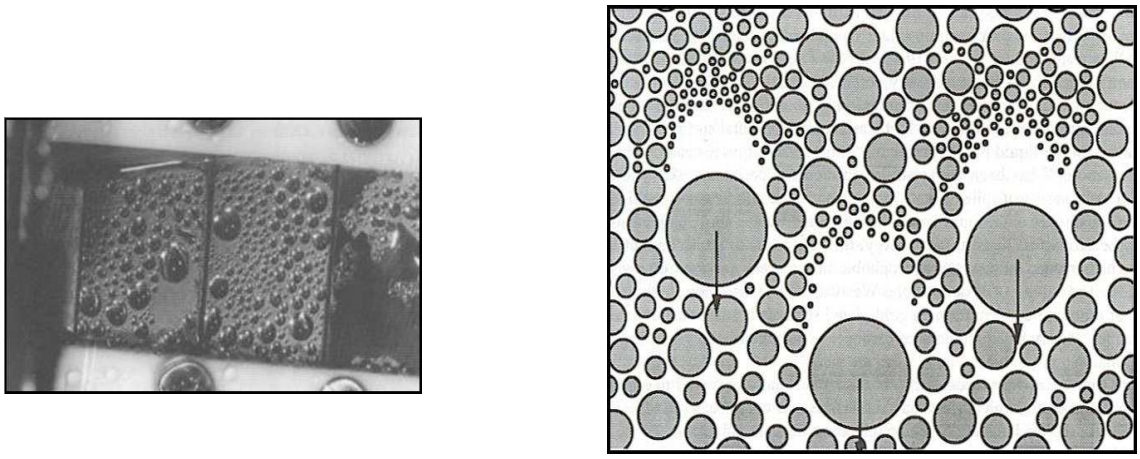

Figure 4.1 Drop-wise condensation from Carey [134].

the form of droplets, which grow on the surface and coalesce with adjacent droplets. When droplets become large enough, they are generally removed from the surface by the action of gravity or drag forces resulting from the motion of the surrounding gas. As drops roll or fall from the surface, they combine with other droplets in their path and thus sweeping the surface clean of droplets. New droplets then begin to grow on the freshly exposed solid surface. This sweeping and renewal of the droplet growth process is responsible for the high heat transfer coefficients associated with drop-wise condensation. Fig. 4.1 shows the appearance of dropwise condensation. As a matter of fact, dropwise condensaton and its mechanism is a topic of much debate. Excellent discussion of this subject are given in the works of Euken [137], McCormick and Baer [138], Umur and Griffith [139], Silver [141], and Welch and Westwater [140].

4.1 Film-wise condensation

In film-wise condensation, the liquid phase forms a thin film on the cold surface. In other words, the liquid phase fully wets a cold surface in contact with a vapor near saturation conditions 4.2. As this process of condensation takes place at the interface of a liquid film covering the solid surface, the removal of latent heat of vaporization occurs at the interface only. Thus the rate of condensation is equal to the rate at which heat is transported across the liquid film from the interface to the surface. This process of laminar film condensation on a vertical plate was first analyzed by Nusselt [142] in 1916 neglecting the acceleration terms and the nonlinear temperature distribution in the liquid film.

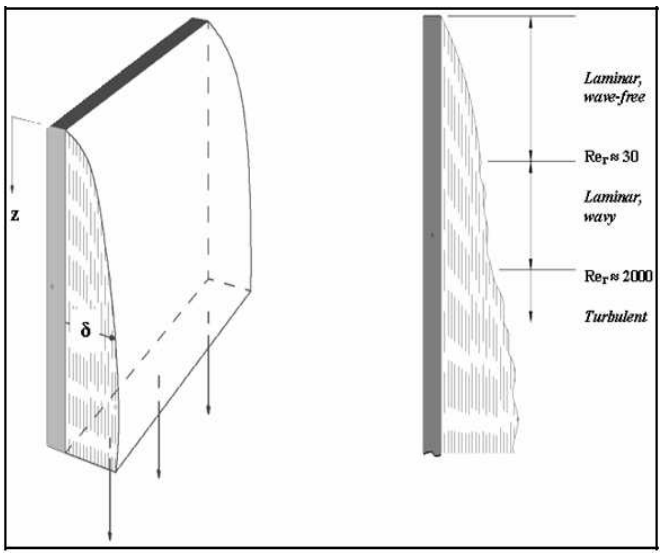

Figure 4.2 Film-wise condensation from [136].

4.1.1 Nusselt's classical model

The Nusselt analysis [142] of laminar film condensation on a vertical surface is shown in Fig. 4.3. The surface exposed to a stationary ambient saturated vapor is taken to be isothermal with a temperature below the saturation temperature (of vapor).

A simple force balance on the shaded film element (4.3) yields

$$(\delta - y)dx(\rho_l - \rho_v)g = \mu_l \frac{du}{dy}dx\,. \tag{4.1}$$

The idealizations of classical Nusselt analysis are as follows:

1. laminar flow,
2. constant properties,
3. subcooling of liquid is negligible in the energy balance,
4. inertia effects are negligible in the momentum balance,
5. the vapor is stationary and exerts no drag,
6. the liquid–vapor interface is smooth,

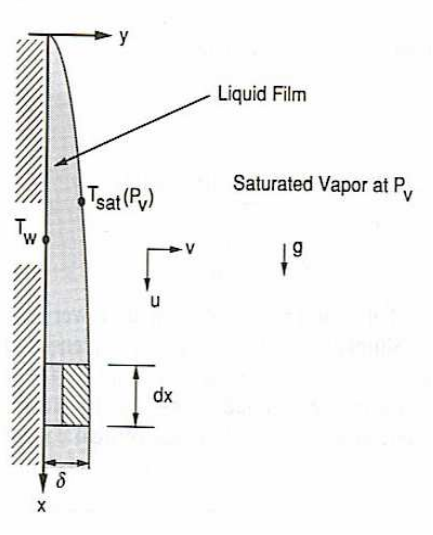

Figure 4.3 Physical model of Film-wise condensation for Nusselt's analysis.

7. heat transfer across film is only by conduction (convection is neglected).

Because heat transfer across the film is by conduction alone, the local heat transfer coefficient is given by $h_l = k_l/\delta$ and local Nusselt number by

$$Nu_x = \frac{h_l x}{k_l} = \left[\frac{\rho_l(\rho_l - \rho_v)g h_{fg} x^3}{4k_l\mu_l(T_{sat} - T_w)}\right]^{\frac{1}{4}} . \tag{4.2}$$

The mean Nusselt number can be obtained as:

$$Nu_m = \frac{h_{lm} x}{k_l} = 0.943\left[\frac{\rho_l(\rho_l - \rho_v)g h_{fg} x^3}{4k_l\mu_l(T_{sat} - T_w)}\right]^{\frac{1}{4}} \tag{4.3}$$

This solution implies invariant physical properties, negligible viscous dissipation and non-rippling flow. Nusselt also derived an (erroneous) first-order correction for the effect of the specific heat of the condensate, a correction for a fixed vapor velocity and a correction for the effect of superheat; and he discussed the effect of non-condensables semi-quantatively. He further asserted that the results for a vertical plate were directly applicable for condensation inside and outside vertical tubes, and by neglecting the effect of surfac tension readily modified his basic solution for condensation outside horizontal tubes.

The basic solution derived by Nusselt has been found to be in good functional accord with subsequent experimental data although the observed rates of heat transfer are somewhat higher than the predicted values, owing primarily to rippling of the film.

Many modifications have been made to the assumptions cited above to incorporate various effects. For example, Nusselt himself assumed the linear temperature distribution in the laminar

film as a first approximation and obtained the relationship for enthalpy change from saturated vapor to liquid at the mean temparature of the liquid film. The mean heat transfer coefficient is

$$h_m = 0.943 \sqrt[4]{\frac{\rho_l(\rho_l - \rho_v) g k_l^3 h_{fg} \left(1 + \frac{3c_{pl}(T_{sat} - T_w)}{8h_{fg}}\right)}{\mu_l x (T_{sat} - T_w)}} \tag{4.4}$$

and the mean Nusselt number is

$$Nu_m = \frac{h_m x}{k_l} = 0.943 \sqrt[4]{\frac{\rho_l(\rho_l - \rho_v) g x^3 h_{fg} \left(1 + \frac{3c_{pl}(T_{sat} - T_w)}{8h_{fg}}\right)}{\mu_l k_l (T_{sat} - T_w)}} . \tag{4.5}$$

Most of the idealizations employed by Nusselt have been investigated theoretically, and many extensions and improvements have been proposed. Bromley [133] derived an improved first-order correction in closed form for the effect of the heat capacity of the condensate. Rosenhow [129] used an alternative procedure to obtain a similar result. Sparrow and Gregg [128] obtained numerical results for the effects of inertia (for Pr from 1 to 100) and heat capacity of the condensate (for $Ja \equiv c_{pl}(T_{sat} - T_w)/h_{fg}$ up to 2) by solving a boundary-layer formulation model for the liquid phase. Koh *et al.* [131] solved a boundary-layer model for both the condensate and vapor numerically and obtained results for a few discrete values for Pr from 0.003 to 810 and Ja from 5×10^{-5} to 1.2. This solution revealed that the terms of the model representing vapor drag become increasingly significant as Pr decreases and are in all cases more significant than those representing the inertia of the condensate. Koh [132] solved the same model approximately, using an integral boundary-layer formulation, and attained results in reasonable agreement with the numerical solution. Chen [130] derived a solution for a modified integral-boundary-layer formulation using a perturbation technique.

4.1.2 Rohsenow's model

Rohsenow in 1956 [129] presented his analysis to obtain the correct nonlinear temperature distribution and heat transfer rates in a liquid condensate film which under the influence of gravity flows downward in essentially laminar flow on vertical plates or tubes. In the analysis, it is assumed that the vapor is saturated with no noncondensable gas present, the wall surface tempaerature is uniform, there is no appreciable vapor shear stress existing at the liquid-vapor interface, and the physical properties of the fluid are constant and uniform. Thus Nusselt's analysis may be improved by determining the actual temperature distribution which is not linear because of the addition of T_{sat} to the outer edge of the film. He solved the energy balance equation by successive approximations for T as a function for δ. Following is the modified mean

heat transfer coefficient of Rohsenow's model:

$$h_m = 0.943 \sqrt[4]{\frac{\rho_l(\rho_l - \rho_v) g k_l^3 h_{fg}^* \left[1 - \frac{1}{10}\frac{c_{pl}\Delta T}{h_{fg}^*} - 0.0328\left(\frac{c_{pl}\Delta T}{h_{fg}^*}\right)^2\right]}{\mu_l x \Delta T \left(1 - \frac{1}{10}\frac{c_{pl}\Delta T}{h_{fg}^*}\right)^4}} \,. \tag{4.6}$$

where

$$h_{fg}^* = h_{fg} + \frac{3}{8} c_{pl}(T_{sat} - T_w) \,. \tag{4.7}$$

For a range $0 < c_{pl}\Delta T/h_{fg} < 1.0$ this equation is very closely approximated by

$$h_m = 0.943 \sqrt[4]{\frac{\rho_l(\rho_l - \rho_v) g k_l^3 h_{fg} \left(1 + 0.68\frac{c_{pl}\Delta T}{h_{fg}}\right)}{\mu_l x \Delta T}} \,. \tag{4.8}$$

4.1.3 Bromley's model

L. A. Bromley [133] derived a first-order correction in closed form for the effect of heat capacity of the condensate. He also correctly included the effect of cross flow on the heat transfer. He used the enthalpy of the liquid at the boiling as a basis. Thus, the heat flow by conduction at a given point y in the condensate film is equal to the decrease in enthalpy of the material between y and y_0 plus the heat liberated by the condensate minus the heat carried by cross flow. Following is the relationship he derived for the mean heat transfer coefficient:

$$h_m = 0.943 \frac{\left(1 + \frac{3}{8}\frac{\Delta T c_{pl}}{h_{fg}}\right)}{\left(1 + \frac{11}{40}\frac{\Delta T c_{pl}}{h_{fg}}\right)^{3/4}} \sqrt[4]{\frac{k_l^3 \rho_l(\rho_l - \rho_v) g h_{fg}}{x \mu_l \Delta T}} \,. \tag{4.9}$$

This approximate equation, on expansion for small values of $\Delta T c_{pl}/h_{fg}$ yields the following:

$$h_m = 0.943 \sqrt[4]{\frac{\rho_l(\rho_l - \rho_v) g k_l^3 h_{fg} \left(1 + 0.675\frac{c_{pl}\Delta T}{h_{fg}}\right)}{\mu_l x \Delta T}} \,, \tag{4.10}$$

which is nearly same as the one Rohsenow showed in his analysis.

4.1.4 Chen's Model

Chen [130] proposed a solution of the condensation problem, including the effect of the drag, due to an initially stationary body of vapor. The method of solution is as follows: the momentum and energy equations are written in integral form using boundary-layer assumptions; these are supplemented by an internal momentum balance for the solution of velocity profiles and an internal energy balance for the solution of temperature profiles. Perturbation methods are employed to solve these equations. The computed velocity profiles show a negative

gradient at the interface, as expected, and the heat-transfer results for low Prandtl numbers are significantly lower than previous theories neglecting the vapor drag. He gave the results in the form of ratio of the Nusselt numbers computed from his model and from the classical model of Nusselt. Thus

$$\frac{h_m}{h_{m,00}} = \left(\frac{1+0.68\xi+0.02\xi\zeta}{1+0.85\xi-0.15\xi\zeta}\right)^{1/4} \tag{4.11}$$

where $h_{m,00}$ represent the values for $\xi = 0$, $\zeta = 0$.

4.1.5 Koh's model

Koh, Sparrow and Harnett [131] analyzed the film condensation problem by solving the complete liquid and vapor boundary-layer equations simultaneously. By using the integral-method, the task of solving the complicated two-phase boundary-layer differential equations in laminar film condensation has been reduced to the simple work of solving an algebraic equation. In this model they assumed the profile of velocity for both liquid and vapor and equated them at the interface boundary condition. Following is one of the key eepressions which dictates the relationship of the two constants that were considered in their analysis:

$$\frac{1}{2}\left(X_1+\sqrt{X_1^2+X_2^2}\right) = \frac{24+4\frac{\beta_l^2}{\alpha_l}+3\alpha_l\beta_l^2-\frac{1}{2}\beta_l^4}{16-3\alpha_l\beta_l^2}\,, \tag{4.12}$$

where X_1 and X_2 are functions of α_l and β_l. Here α_l and β_l are related to liquid layer thickness δ and u_δ respectively. It is demonstrated by Sparrow and Gregg [128] that δ is related to the physical quantity $c_{pl}\Delta T/h_{fg}$; thus, Eq. (4.12) allows to calculate α_l for any given β_l. Once α_l is known the heat transfer can be found by solving the energy equation.

4.2 Gregg and Sparrow's model

In this section we will describe the model proposed [128] which is the basis of modern analysis of condensation (Chen [130] , Koh et al [131]). The problem of laminar film condensation on a vertical plate is solved using boundary-layer theory. Starting with the boundary-layer (partial differential) equations, a similarity transformation is found which reduces them to ordinary differential equations. An analytical solution for this model of Sparrow and Gregg [128] is obtained via AIM.

4.2.1 Boundary layer analysis of laminar film condensation

A schematic representation of the physical model and coordinate system is shown in Fig. 4.4. A vertical plate is suspended in a large body of pure vapor. The vapor is at its saturation

temperature, T_{sat}. The plate temperature, T_w, ($T_{sat} > T_w$) is taken to be uniform in the main body of the analysis. A continuous laminar film of condensate runs downward along the plate. Velocities in the vapor are assumed to have no effect on the condensate film.

Formulation of model and conservation laws. The equations expressing conservation of mass, momentum, and energy for steady laminar flow in a boundary layer on a vertical plate are, respectively,

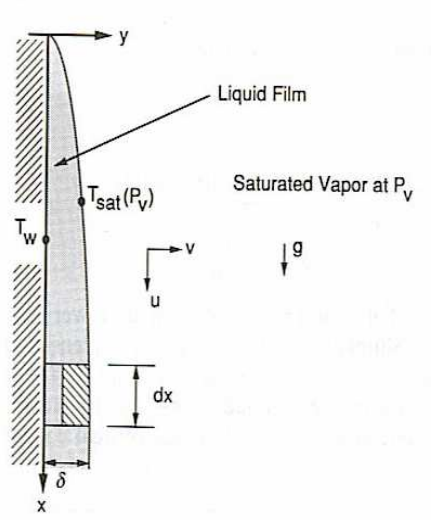

Figure 4.4 Physical model of Film-wise condensation for similarity analysis.

$$\frac{\partial u}{\partial x} + \frac{\partial u}{\partial y} = 0\,, \tag{4.13}$$

$$\rho_l \left(u\frac{\partial u}{\partial x} + v\frac{\partial u}{\partial y} \right) = g(\rho_l - \rho_v) + \mu_l \frac{\partial^2 u}{\partial y^2}\,, \tag{4.14}$$

$$\rho_l c_{pl} \left(u\frac{\partial T}{\partial x} + v\frac{\partial T}{\partial y} \right) = k_l \frac{\partial^2 T}{\partial y^2}\,. \tag{4.15}$$

Except ρ_v, which represents the vapor density, the fluid properties are those of the condensate. Various dissipation has been neglected, as has been the temperature dependence of the fluid properties. The boundary conditions at the cooled plate ($y = 0$), and at the liquid-vapor interface ($y = \delta$) are

$$\text{at } y = 0: \quad u = v = 0\,, \quad T = T_w\,, \tag{4.16}$$

$$\text{at } y = \delta: \quad \frac{\partial u}{\partial y} = 0\,, \quad T = T_{sat}. \tag{4.17}$$

At the plate, the boundary conditions are a consequence of the no-slip condition and the isothermal wall specification. The relations (4.17), which apply for $y = \delta$, specify continuity

of the temperature profiles across the interface and a negligible shear stress exerted by the surrounding vapor on the liquid film. The solution of Eq. (4.13), as usual, may be written in terms of a stream function ψ defined by the relations,

$$u = \frac{\partial \psi}{\partial y}\,, \quad v = -\frac{\partial \psi}{\partial x}\,, \tag{4.18}$$

it follows that the continuity equation (4.13) is automatically satisfied, while the Eqs. (4.14) and (4.15) result in the following pair of partial differential equations for ψ and T as functions of x and y :

$$\frac{\partial \psi}{\partial y}\frac{\partial^2 \psi}{\partial x \partial y} - \frac{\partial \psi}{\partial x}\frac{\partial^2 \psi}{\partial y^2} - = \frac{g(\rho_l - \rho_v)}{\rho_l} + \nu_l \frac{\partial^2 \psi}{\partial y^2}\,, \tag{4.19}$$

$$\frac{\partial \psi}{\partial y}\frac{\partial T}{\partial x} - \frac{\partial \psi}{\partial T}\frac{\partial T}{\partial y} = \alpha \frac{\partial^2 T}{\partial y^2}\,. \tag{4.20}$$

Rather than deal with these two formidable partial differential equations directly, we transform these equations into ordinary differential equations by similarity transformation. Thus, we define a new independent variable η as follows:

$$\eta = cyx^{-1/4}\,, \tag{4.21}$$

with

$$\psi = 4\alpha c x^{3/4} f(\eta)\,, \tag{4.22}$$

and

$$\theta(\eta) = \frac{T_{sat} - T}{T_{sat} - T_w}\,, \tag{4.23}$$

where

$$c = \left[\frac{g c_{pl}(\rho_l - \rho_v)}{4\nu_l k_l}\right]^{1/4}\,. \tag{4.24}$$

The velocity components are related to the similarity variables as

$$u = 4c^2 \alpha x^{1/2} f'(\eta)\,, \tag{4.25}$$

$$v = c\alpha x^{-1/4}[\eta f'(\eta) - 3f(\eta)], \tag{4.26}$$

where the primes indicate differentiation with respect to η.

Under the transformation Eqs. (4.21), (4.22), (4.23) and (4.24), the partial differential equations of momentum (4.19) and energy (4.20) become

$$f''' + \frac{1}{Pr}[3ff'' - 2(f')^2] + 1 = 0\,, \tag{4.27}$$

$$\theta'' + 3f\theta' = 0\,, \tag{4.28}$$

where Pr represents the Prandtl number (Prandtl number enters the problem because the acceleration terms were retained). The boundary conditions (4.16) and (4.17) transform to,

$$f(0) = f'(0) = 0\,, \quad f''(\eta_\delta) = 0\,, \tag{4.29}$$

$$\theta(\eta_\delta) = 0\,, \quad \theta(0) = 1\,, \tag{4.30}$$

where η_δ is the value of η corresponding to $y = \delta$. Evidently, the solution of Eqs. (4.27) and (4.28) subject to the boundary conditions (4.29) and (4.30) depends upon the specification of two parameters, Pr and η_δ. The mathematical problem posed by Eqs. (4.27) and (4.28) with boundary conditions (4.29) and (4.30) is a fifth-order system of nonlinear ordinary differential equations with five boundary conditions. The system is therefore closed if we can specify the location of the interface. However, the location of the interface is not known *a priori*. The interface location is dictated by the transport, and it therefore must be determined as a part of the solution process.

It may also be observed that while the foregoing development has much in common with that for free convection, there do exist some differences:

1. equations (4.27) and (4.28) need not be solved simultaneously, whereas the corresponding free-convection equations require simultaneous solution;

2. the current problem is a two-parameter problem while in convection only the Pr enters.

The additional relation needed to determine the location of interface is obtained from an energy balance over a segment of film. Thus, to relate η_δ to known physical quantities this balance can be written as:

$$\int_0^x \left[k \left(\frac{\partial T}{\partial y} \right)_{y=\delta} \right] dx = \int_0^\delta \rho u h_{fg}\, dy\,. \tag{4.31}$$

The left-hand side represents the heat transferred from the condensate to the plate over a length from $x = 0$ to $x = x$. The term on the right is the energy liberated as latent heat. The assumption of negligible heat conduction across the liquid-vapor interface, which is standard in condensation theory, has been used. In terms of similarity variables defined above, Eq. (4.31) can be written as

$$-\frac{3f(\eta_\delta)}{\theta'(\eta_\delta)} = Ja = \frac{c_{pl}(T_{sat} - T_w)}{h_{fg}} \tag{4.32}$$

where $\theta'(\eta_\delta)$ and $f(\eta_\delta)$ are the values of $d\theta/d\eta$ and f at $\eta = \eta_\delta$. The problem is now closed mathematically. From a solution of Eqs. (4.27) and (4.28) corresponding to given values of η_δ

and Pr, the quantities on the right-hand side of Eq. (4.32) are known. Hence $c_{pl}\Delta T/h_{fg}$ is determined. In other words, for a fixed Pr, there is a unique relation between η_δ and $c_{pl}\Delta T/h_{fg}$.

4.2.2 Analytical solution of condensation equation

In this section, we will demonstrate a procedure to solve Eqs. (4.27) and (4.28) analytically via AIM. Recall that both of the equations (4.27) and (4.28) need not be solved simultaneously. Thus, we will apply AIM first to solve Eq. (4.27) and then to Eq. (4.28). We will start with the splitting of the given nonlinear ordinary differential equation (4.27) into linear and nonlinear parts; thus if

$$F(\eta, f) = f''' + \frac{1}{Pr}[3ff'' - 2(f')^2] + 1 = 0\,, \tag{4.33}$$

splitting this into linear and nonlinear parts will yield

$$\mathcal{L}(f) = f''' + 1\,, \tag{4.34}$$

and

$$\mathcal{N}(f) = F - \mathcal{L}(f) = \frac{1}{Pr}[3ff'' - 2(f')^2]\,. \tag{4.35}$$

Integrating linear part (4.34) will give us an initial guess for the solution and its derivatives (*zeroth approximation*) appearing in Eq. (4.27),

$$f_0 = -\frac{\eta^3}{6} + C_{10}\frac{\eta^2}{2} + C_{20}\eta + C_{30}\,, \tag{4.36}$$

$$f_0' = -\frac{\eta^2}{2} + C_{10}\eta + C_{20}\,, \tag{4.37}$$

$$f_0'' = -\eta + C_{10}\,, \tag{4.38}$$

where C_{10}, C_{20} and C_{30} are constants of integration. These constants are evaluated using boundary conditions (4.16). Thus, as an initial guess to the solution of Eq. (4.27), we obtain the following:

$$f_0 = -\frac{\eta^3}{6} + \eta_\delta\frac{\eta^2}{2}\,, \tag{4.39}$$

$$f_0' = -\frac{\eta^2}{2} + \eta_\delta\eta\,, \tag{4.40}$$

$$f_0'' = -\eta + \eta_\delta\,. \tag{4.41}$$

Once the initial guess for the solution and its derivatives are obtained, we can perform convergence analysis as follows:

Convergence analysis for condensation equation

In the convergence analysis for the momentum equation of condensation, we begin with re-writing the original nonlinear differential equation in terms of the highest derivative, *viz,*

$$f''' = -\frac{3}{Pr} f f'' + \frac{2}{Pr}(f')^2 - 1\,. \tag{4.42}$$

We now integrate Eq. (4.42) and define

$$F(f) \equiv -\frac{3}{Pr}\int_0^{\eta}\int_0^{\zeta}\int_0^{\xi} f'' f\, dx\, dy\, dz + \frac{2}{Pr}\int_0^{\eta}\int_0^{\zeta}\int_0^{\xi} (f')^2\, dx\, dy\, dz - \int_0^{\eta}\int_0^{\zeta}\int_0^{\xi} 1\, dx\, dy\, dz\,. \tag{4.43}$$

or

$$F'(f) = \frac{d}{df}\left[\underbrace{-\frac{3}{Pr}\int_0^{\eta}\int_0^{\zeta}\int_0^{\xi} f'' f\, dx\, dy\, dz}_{I} + \underbrace{\frac{2}{Pr}\int_0^{\eta}\int_0^{\zeta}\int_0^{\xi} (f')^2\, dx\, dy\, dz}_{II} - \underbrace{\int_0^{\eta}\int_0^{\zeta}\int_0^{\xi} 1\, dx\, dy\, dz}_{III}\right]. \tag{4.44}$$

We now simplify each of these I, II and III term. Thus, starting with the I term, we simplify it as follows:

$$\frac{d}{df} I = -\frac{3}{Pr}\frac{d}{df}\int_0^{\eta}\int_0^{\zeta}\int_0^{\xi} f'' f\, dx\, dy\, dz \tag{4.45}$$

or

$$\frac{d}{df} I = -\frac{3}{Pr}\frac{d}{df}\int_0^{\eta}\int_0^{\zeta}\left(f\, f' - \int_0^{\xi}(f')^2\, dx\right) dy\, dz\,. \tag{4.46}$$

The first term of the bracketed expression will remain as it is, while the second term of the bracketed expression of Eq. (4.46) will be combined with the II term, yielding

$$F'(f) = -\frac{3}{Pr}\frac{d}{df}\int_0^{\eta}\int_0^{\zeta} f f'\, dy\, dz + \frac{5}{Pr}\frac{d}{df}\int_0^{\eta}\int_0^{\zeta}\int_0^{\xi}(f')^2\, dx\, dy\, dz - \frac{d}{df}\int_0^{\eta}\int_0^{\zeta}\int_0^{\xi} 1\, dx\, dy\, dz\,. \tag{4.47}$$

Simplifying the above equation further, we obtain

$$F'(f) = -\frac{3}{Pr}\frac{d}{df}\left[\frac{1}{2}\int_0^{\eta} f^2\, dz\right] + \frac{5}{Pr}\frac{d}{df}\int_0^{\eta}\int_0^{\zeta}\int_0^{\xi}(f')^2\, dx\, dy\, dz - \frac{d}{df}\int_0^{\eta}\int_0^{\zeta}\int_0^{\xi} 1\, dx\, dy\, dz\,. \tag{4.48}$$

In the above equation, we will commute the integral operator with the differential operator in the first and the second term on the RHS. Thus,

$$F'(f) = -\frac{3}{Pr}\left[\frac{1}{2}\int_0^{\eta}\frac{d}{df} f^2\, dz\right] + \frac{5}{Pr}\int_0^{\eta}\int_0^{\zeta}\int_0^{\xi}\frac{d}{df}(f')^2\, dx\, dy\, dz - \frac{d}{df}\int_0^{\eta}\int_0^{\zeta}\int_0^{\xi} 1\, dx\, dy\, dz\,. \tag{4.49}$$

The third term on the RHS is differentiated after the integration. It should be noted that while differentiating the second term of the Eq. (4.48), the f' is taken as the function of f. Here f, f' and f'' are initial guesses or the *zeroth approximation* of the solution.

$$F'(f) = -\frac{3}{Pr}\left[\int_0^{\eta}\left(-\frac{\eta^3}{6}+\eta_\delta\frac{\eta^2}{2}\right)dz\right]+\frac{5}{Pr}\int_0^{\eta}\int_0^{\zeta}\int_0^{\xi}\frac{d}{df}\left(\frac{2f}{\eta}-\frac{\eta^2}{6}\right)^2 dx\,dy\,dz+$$
$$\frac{d}{df}\int_0^{\eta}\int_0^{\zeta}\int_0^{\xi} f'''\,dx\,dy\,dz\,. \quad (4.50)$$

Simplyfying Eq. (4.50) we obtain the following expression for the $F'(f)$:

$$F'(f) = \frac{1}{Pr}\left[-\frac{7}{24}\eta^4+\frac{17}{6}\eta^3\eta_\delta\right]+1\,.$$

From the definition of L^1 norm for polynomial spaces, we can write

$$\max\|F'(f)\|_1 = \int_0^{\eta_\delta}\left|\frac{1}{Pr}\left[-\frac{7}{24}\eta^4+\frac{17}{6}\eta^3\eta_\delta\right]+1\right|d\eta$$

or

$$\max\|F'(f)\|_1 = \frac{78\eta_\delta^5}{120Pr}+\eta_\delta\,, \quad (4.51)$$

where the term inside the $|\cdot|$ is monotone. If we consider the expression inside $|\cdot|$ as

$$G(\eta) = \frac{1}{Pr}\left[-\frac{7}{24}\eta^4+\frac{17}{6}\eta^3\eta_\delta\right]+1 \quad (4.52)$$

then this $G(\eta)$ is monotone in $[0,\ \eta_\delta]$ if

$$G(0) < G(\eta_\delta)\ \text{ for }\ 0<\eta_\delta\,. \quad (4.53)$$

Thus evaluating $G(0)$ and $G(\eta_\delta$

$$G(0) = 1 \quad (4.54)$$

and

$$G(\eta_\delta) = \frac{61}{24}\eta_\delta^4+1\,, \quad (4.55)$$

since $(61/24)\eta_\delta^4$ is a positive quantity, the function $G(\eta)$ satisfies the condition of monotonocity (4.53). Hence, we can now apply the following Lipschitz condition to the Eq. (4.51):

$$L = \max\|F'(f)\|_1 \text{ where } L<1 \text{ for convergence}\,, \quad (4.56)$$

$$\frac{78\eta_\delta^5}{120Pr}+\eta_\delta<1\,. \quad (4.57)$$

This is a fifth-degree polynomial, that has five roots, but as it is known that $\eta_\delta > 0$, so we will adopt only positive values. The above relationship of Pr and η_δ defines the stability of the AIM. However, different trends in the stability of the AIM are observed for different Prandtl numbers. All these trends and their discussions are included in detail in the results section (Refer to the discussion of Fig. 4.25).

Analytical iteration method for condensation equation

We will now begin the analytical iterations by integrating Eq. (4.42) thrice. The constants of integration as a result of this successive integration will be evaluated via given boundary conditions (4.29). Recalling the general symbolic form of the nth approximation of the AIM (3.18), we can express the first iteration for the momentum equation as

First iteration

$$f_1 = -\int\int\int \frac{1}{Pr}[3f_0 f_0'' - 2(f_0')^2]\,dx\,dy\,dz - \int\int\int 1\,dx\,dy\,dz + C_{10}\frac{\eta^2}{2} + C_{20}\eta + C_{30}\,, \quad (4.58)$$

We can express the right-hand side of Eq. (4.58) in terms of η by substituting for f, f' and f'' from Eqs. (4.39), (4.40) and (4.41). Following are the solutions obtained for Eq. (4.27) after the first itearation of AIM :

$$f_1 = -\frac{\eta^3}{6} + \frac{\eta_\delta^2}{Pr}\frac{\eta^5}{120} + C_1\frac{\eta^2}{2}\,, \quad (4.59)$$

$$f_1' = -\frac{\eta^2}{2} + \frac{\eta_\delta^2}{Pr}\frac{\eta^4}{24} + C_1\eta\,, \quad (4.60)$$

$$f_2'' = -\eta + \frac{\eta_\delta^2}{Pr}\frac{\eta^3}{6} + C_1\,, \quad (4.61)$$

where

$$C_1 = \eta_\delta - \frac{\eta_\delta^5}{6Pr}\,. \quad (4.62)$$

Thus, we now have a new set of f, f' and f'' which can be used for carrying out the next iteration, and so on. This iteration procedure can be repeated up to 5 iterations and 2 iterations for the Eqs. (4.27) and (4.28), respectively. The inability of not performing more number of iterations is the computation limitation. This limitation arises because of the very large polynomial obtained at the end of the 5th iteration. This polynomial has 122 terms in it. It should be mentioned here that all the successive iterations, and hence the integrations in the AIM, are done using MAPLE [144]. Eventhough there is a limitation on performing the number of iterations in AIM, it is capable of producing accurate and converged solutions for a large number of Prandtl numbers. Thus, once we have the converged solution from the momentum

equation in terms of f, it is substituted into the energy equation (4.28). We now apply AIM to the energy equation by integrating the linear part of it to obtain an initial guess for its solution. Thus,

$$\theta_0'' = 0\,, \tag{4.63}$$

with the following associated boundary conditions:

$$\theta(0) = 1\,, \quad \theta(\eta_\delta) = 0\,.$$

Integrating this linear part and using the boundary conditions mentioned above, leads to polynomials $\mathcal{P}(\eta)$s for the $\theta(\eta)$ and the $\theta'(\eta)$:

$$\theta_0 = \frac{-1}{\eta_\delta}\eta + 1\,, \tag{4.64}$$

$$\theta_0' = \frac{-1}{\eta_\delta}\,. \tag{4.65}$$

This θ' and the converged solution of momentum equation f can be used to evaluate a new θ by setting up the analytical iterations in the following manner:

$$\theta_1'' = -3f\theta_0'\ , \tag{4.66}$$

$$\theta_1' = -\int 3f\theta_0'\,dx + A_1\,, \tag{4.67}$$

$$\theta_1 = -\int\int 3f\theta_0'\,dx\,dy + A_1\eta + B_1\,. \tag{4.68}$$

Here A_1 and B_1 are the constants of integration that will be evaluated using boundary conditions (4.30). Thus again, an iteration procedure can be set up for the energy equation until we get the converged solution for θ. This iteration procedure for θ converges in only 2 iterations for a wide range of Prandtl numbers. Moreover, it is worthwhile to mention here that not more than 2 iterations can be performed for θ. This is because of the large polynomial (509 terms) obtained at the end of 2^{nd} iteration.

4.2.3 Results for condensation equation

We will divide the discussion of the results in two parts. In the first part, we present the results for the high Prandtl numbers, *i.e.,* $Pr \geq 1$. In the second part, we discuss the low Prandtl numbers which are suitable for liquid metals, *i.e.,* $Pr < 0.03$.

High Prandtl numbers

Since condensation over a vertical plate involves a process of heat transfer, it would be more useful to report the results in the form of a variation of the local heat transfer coefficient or

the local Nusselt number. A plot of this variation of the local Nusselt number, Nu_x, with Ja for various Pr is shown in Fig. 4.5. In the plots shown in Fig. 4.5, the local Nusselt number is represented in terms of $\theta'(0)$. This $\theta'(0)$ can be obtained directly from the solution of the energy equation (4.28). These plots can also be viewed as the variation of the local heat transfer coefficient h_x with Ja. To be more explicit about the relationship between Nu_x and h_x and between Nu_x and $\theta'(0)$, the following relations are given below in terms of similarity variables:

$$Nu_x = \frac{h_x x}{k} = [-\theta'(0)] \left[\frac{g c_{pl} (\rho_l - \rho_v) x^3}{4 \nu k_l} \right]^{\frac{1}{4}} \tag{4.69}$$

or

$$Nu_x \left[\frac{g c_{pl} (\rho_l - \rho_v) x^3}{4 \nu k_l} \right]^{-\frac{1}{4}} = -\theta'(0)\,, \tag{4.70}$$

where ρ_l is condensate density, ρ_v is vapor density, x is distance along the plate from the leading edge, ν is kinematic viscosity, k_l is thermal conductivity and g is the acceleration due to gravity. The right-hand side of Eq. (4.70) is found from the solution of Eq. (4.27) and is a function of Pr and of η_δ, or of Pr and Ja. Thus variation of Nu_x with Ja can be seen in the plot of $\theta'(0)$ *vs.* Ja. Each of the Figs. 4.5 (a), (b) and (c) shows the variation of $\theta'(0)$ with Ja for 3 different values of the Prandtl numbers ($Pr = 1$, 10, 100) for AIM. These results match favorably with those of the Runge–Kutta numerical scheme as shown in Fig. 4.5.

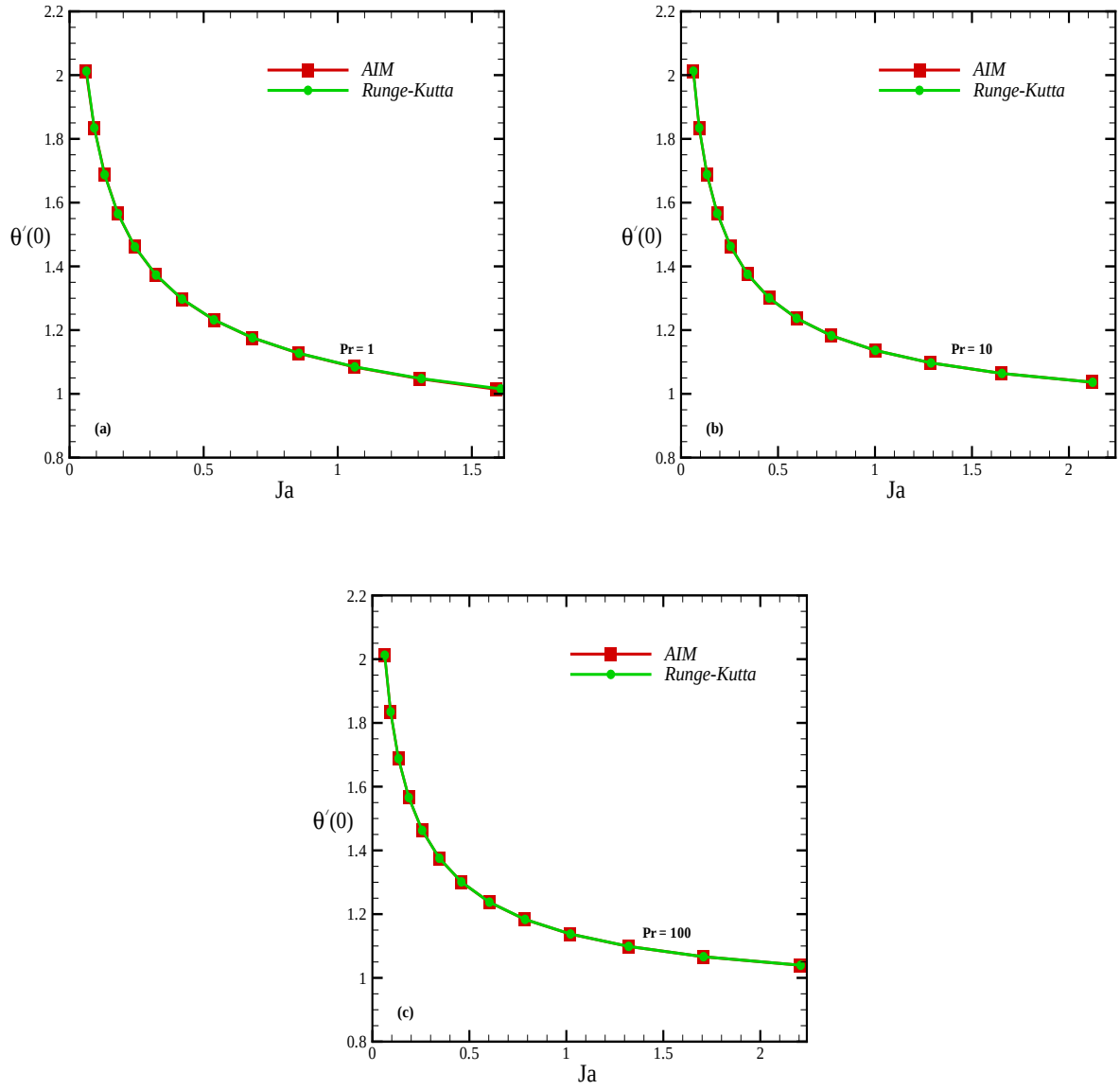

Figure 4.5 Comparison of profiles of local Nusselt number vs. Jacob number obtained from the AIM and the Runge–Kutta for $Pr = 1, 10, 100$.

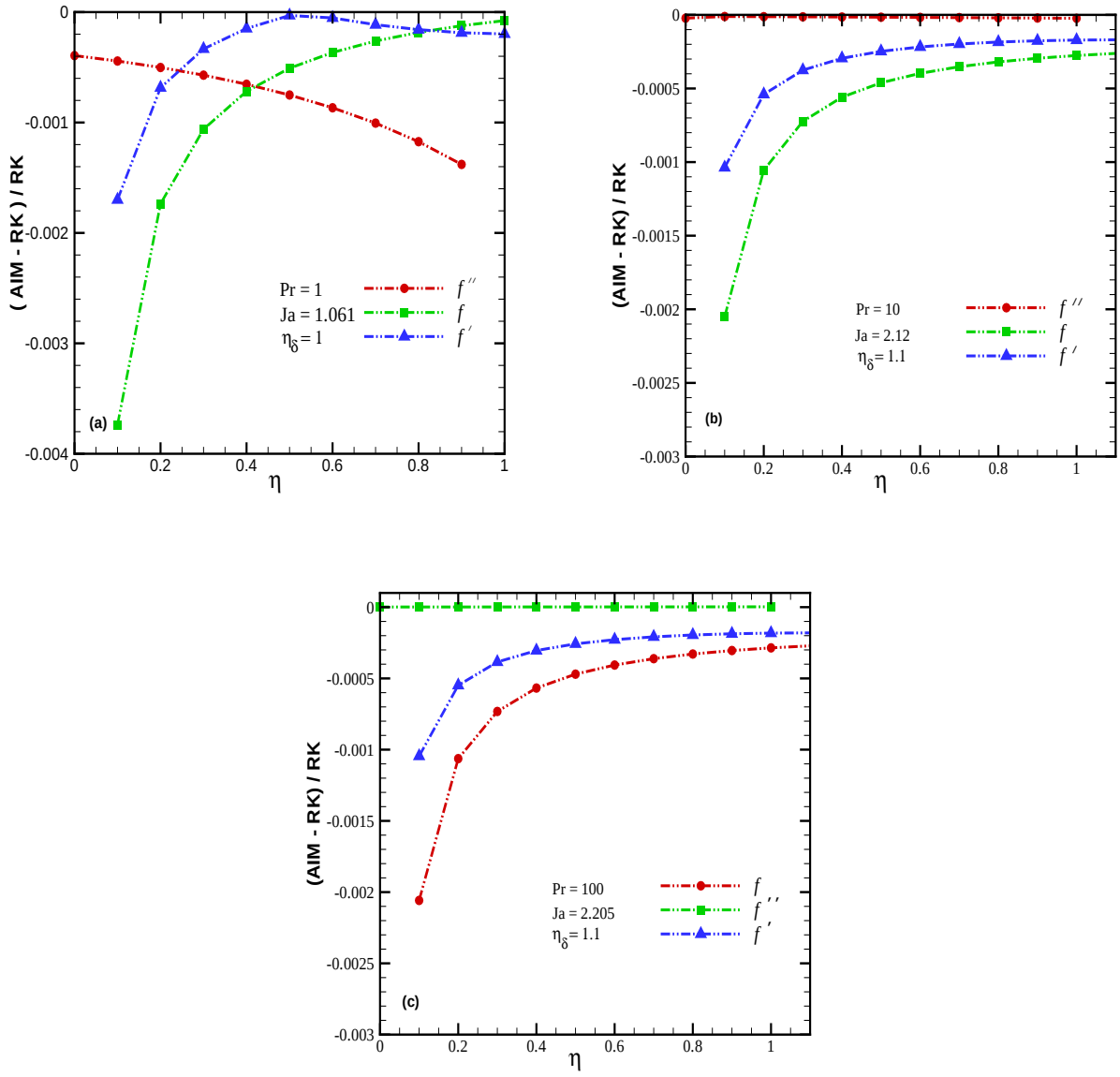

Figure 4.6 Relative error between the solutions of the AIM and the Runge–Kutta w.r.t. the Runge–Kutta for $Pr = 1, 10, 100$.

However, for more detailed comparisons of the solutions obtained from the AIM and the Runge–Kutta numerical scheme, plots of the relative error of the AIM and the Runge–Kutta with respect to the Runge–Kutta for each of f, f' and f'' are shown in Fig. 4.6. These errors are calculated at different points of the domain for all the 3 Prandtl numbers ($Pr = 1$, 10, 100). The maximum error for each of the solution (f, f' and f'') is found to be of the order of $\approx 10^{-3}$ ($Pr = 1$), $\approx 10^{-4}$ ($Pr = 10$) and $\approx 10^{-5}$ ($Pr = 100$). Thus from the accuracy point of view, AIM converges rapidly for Prandtl numbers $Pr > 1$.

We now discuss the convergence behavior of each of these 3 Prandtl numbers. We will start with $Pr = 1$ and $Ja = 1.061$. The convergence behavior for each of f, f' and f'' is shown .

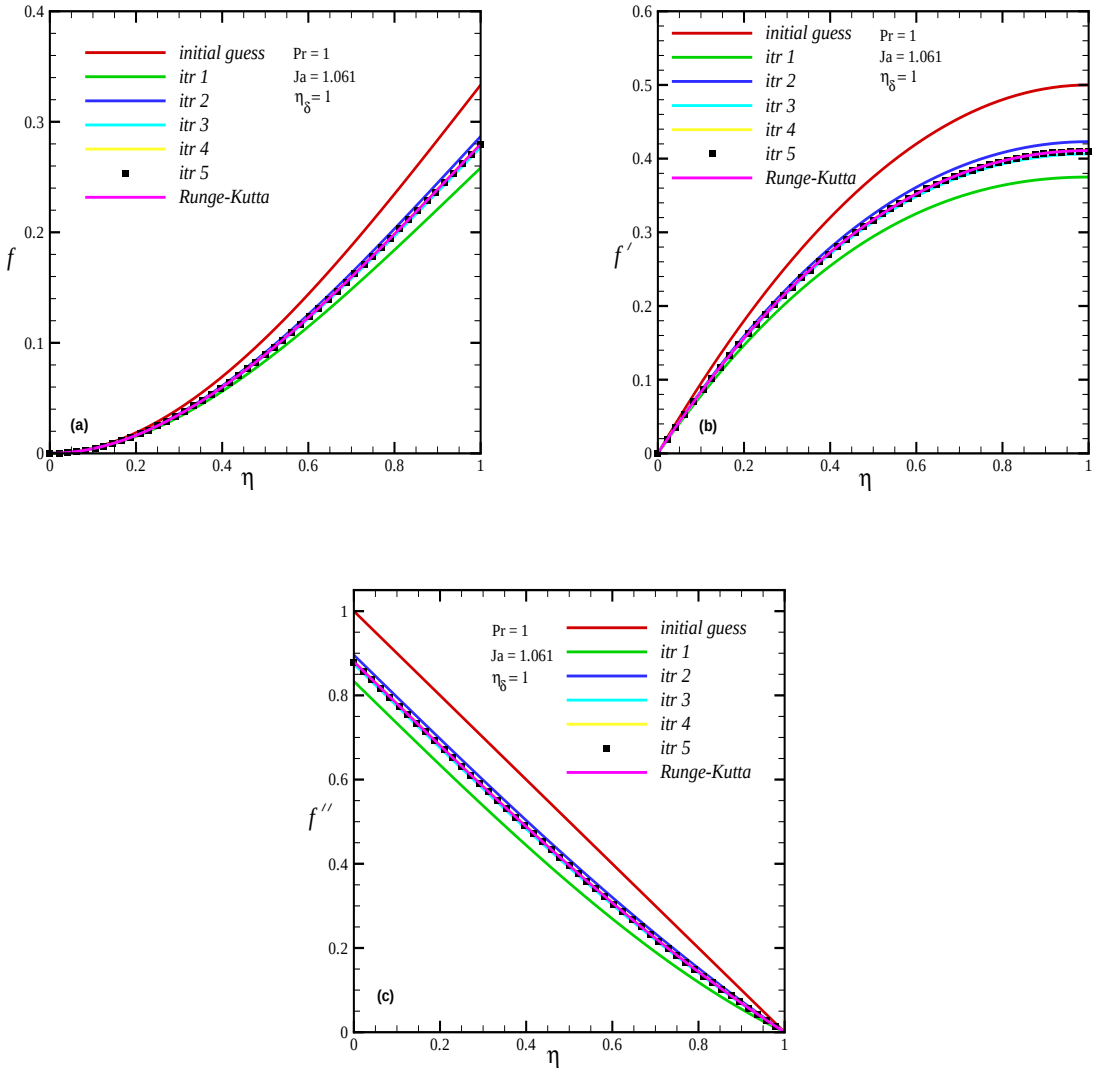

Figure 4.7 Convergence of the iterations of the AIM for f, f' and f'' for $Pr = 1$.

4.7. The figure shows the solutions obtained at various iterations of the AIM. A Runge–Kutta solution has also been superimposed in each of these plots of f, f' and f''. This numerical solution from the Runge–Kutta as shown in Fig. 4.7 is found to be in an agreement with the converged solution of AIM obtained at the 5th iteration. However, in order to understand this convergence behavior of AIM it is necessary to investigate the trend of its iteration error. Fig. 4.8 shows relative error plots for f, f' and f'' calculated throughout the domain at each of the 5 iterations. Here quantity inside the bracket on y-axis is defined as follows:

$$\text{iteration error}\,(f'') = \frac{|f''^{(n+1)} - f''^{(n)}|}{f''^{(n+1)}}\,, \tag{4.71}$$

$$\text{iteration error}\,(f') = \frac{|f'^{(n+1)} - f'^{(n)}|}{f'^{(n+1)}}\,, \tag{4.72}$$

and

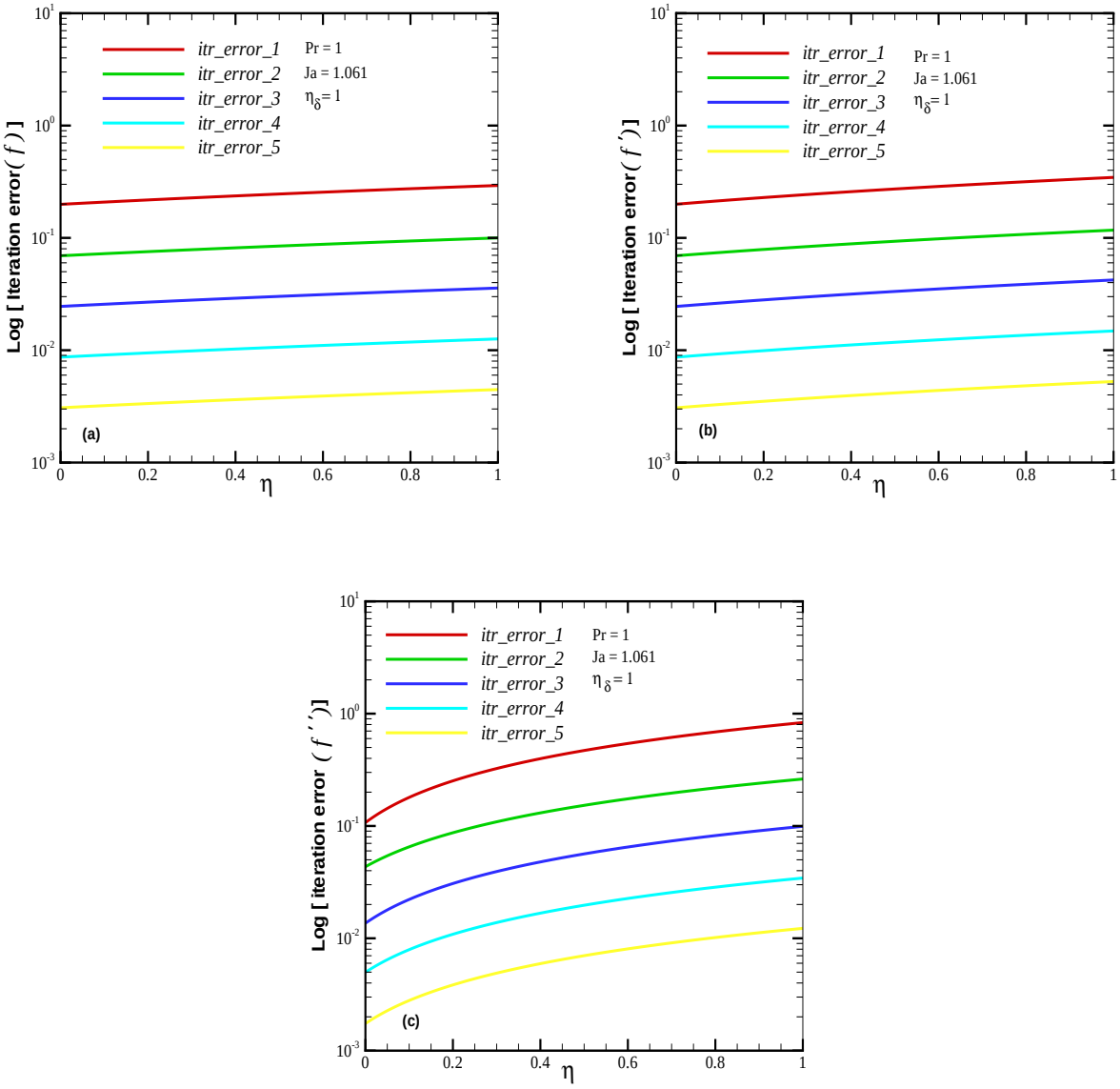

Figure 4.8 Iteration error profiles of f, f' and f'' for $Pr = 1$.

$$\text{iteration error}\,(f) = \frac{|f^{(n+1)} - f^{(n)}|}{f^{(n+1)}}\,. \tag{4.73}$$

Here n represents the iteration number. The *itr_error_1* in each of these plots is a relative difference between the solution obtained after the first iteration and the initial guess w.r.t. the first iteration, while the rest of the plot lines are the relative errors calculated between consecutive iterations. It should be noted that in each of these plots, y-axis is scaled in *log*. It is quite evident from the figures that at each iteration, there is a significant decrease in the iteration error. Due to the fact that we can perform only 5 iterations because of the computation limit, results of 5 iterations are shown. However, from the behavior of the iteration error in Fig. 4.8, it is clear that if we can perform more number of iterations more accurate solutions can

be obtained from AIM. Similar trends of the iteration errors are obtained in the iterations for the dimensionless temperature θ, see Fig. 4.9 (b). In Fig. 4.9 (a) convergence of temperature distribution along the film is shown for $Pr = 1$ and $Ja = 1.061$. As mentioned earlier because of the computation limitation only 2 iterations for θ are performed and hence the results for only 2 iterations are shown. The solution converges very rapidly and is found to be in good agreement with the solution obtained from the Runge–Kutta numerical scheme (see Fig. 4.9 (a)).

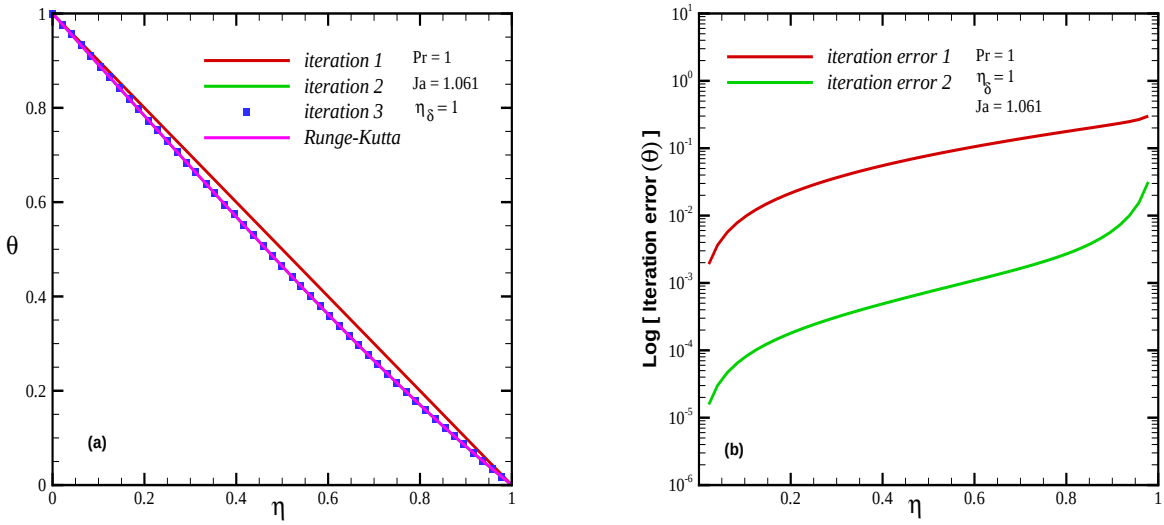

Figure 4.9 Iteration error profiles of θ for $Pr = 1$.

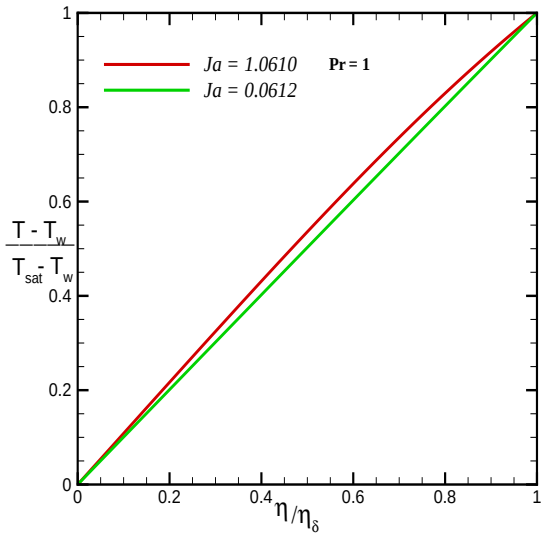

Figure 4.10 Temperature distribution for two different Jacob numbers.

Furthermore, as a standard result that is frequently reported in the literature of the condensation, a variation of this temperature distribution with film thickness δ or Ja is shown for two different values of Ja for $Pr = 1$ in Fig. 4.10. The temperature profiles are essentially a straight line. However with increasing values of Ja increasing deviations from linearity are found. This fact has already been confirmed by different authors [128, 129], consolidating further the accuracy of our solution procedure. The similar trends are found in the convergence of solutions and iteration errors for other higher Prandtl numbers too. As an example, we have taken into account two cases of Prandtl numbers *i.e.,* $Pr = 10$ and $Pr = 100$. The results for $Pr = 10$ and $Ja = 2.12$ are shown in Fig. 4.11. This Fig. 4.11 shows the convergence of the solution for f, f' and f''. It is obvious from the figure that the solution has begun to converge from the first iteration. All the successive iterations for each of the f, f' and f'' converged very quickly to an exact solution. These converged solutions of the AIM are compared, and found to be in an excellent agreement with those obtained from the Runge–Kutta 4th order numerical scheme as shown in Fig. 4.11.

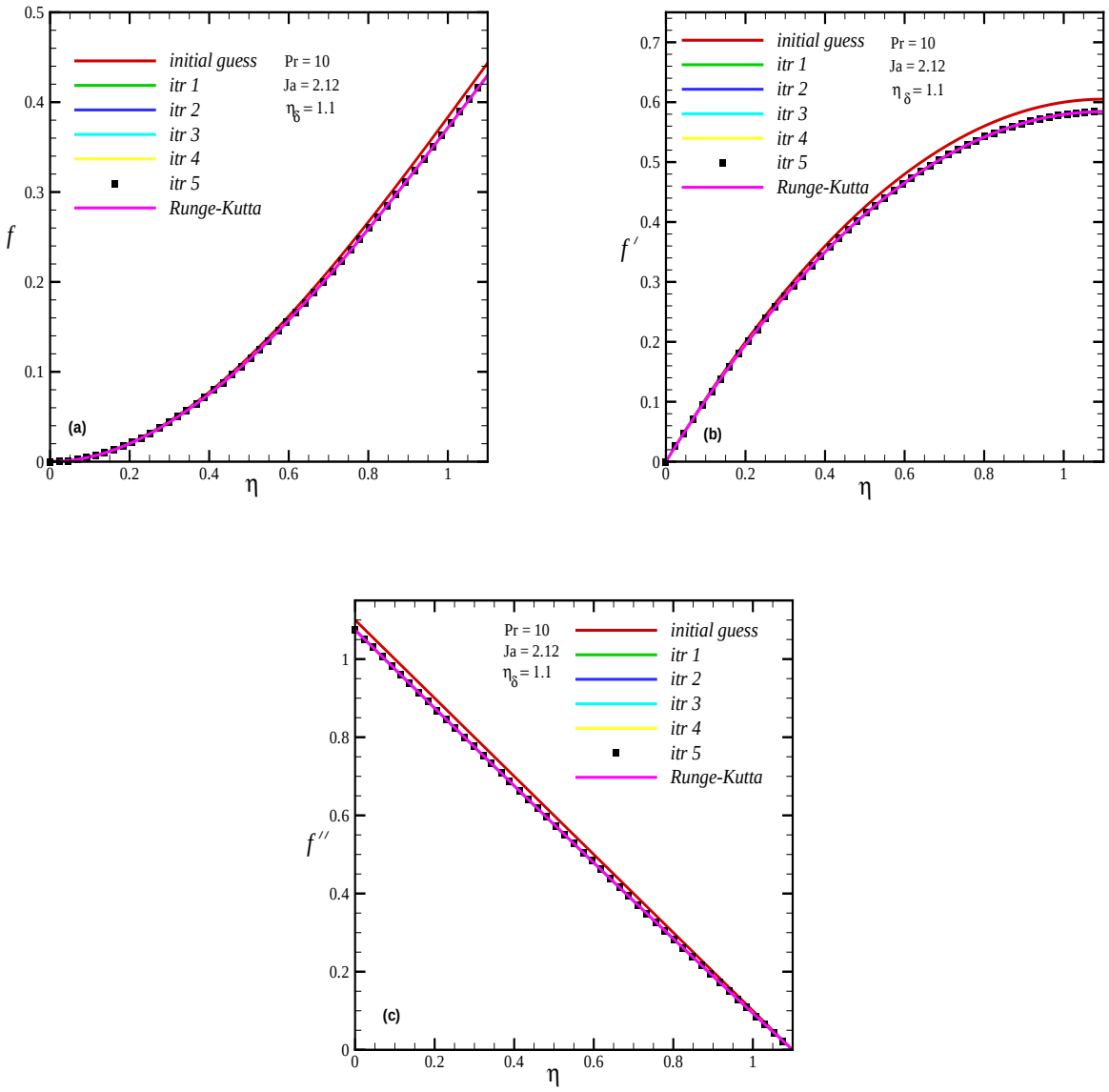

Figure 4.11 Convergence of the iterations of the AIM for f, f' and f'' for $Pr = 10$.

The next results in line for this Prandtl number are the plots of iteration error for f, f' and f''. In Fig. 4.12 iteration errors for f, f' and f'' are plotted as before. The variation of iteration error in this case is not very different from the one we discussed in $Pr = 1$. Here also the quantity inside the bracket on y-axis is defined as follows:

$$\text{iteration error}\,(f'') = \frac{|f''^{(n+1)} - f''^{(n)}|}{f''^{(n+1)}}\,, \tag{4.74}$$

$$\text{iteration error}\,(f') = \frac{|f'^{(n+1)} - f'^{(n)}|}{f'^{(n+1)}}\,, \tag{4.75}$$

and

$$\text{iteration error}\,(f) = \frac{|f^{(n+1)} - f^{(n)}|}{f^{(n+1)}}\,. \tag{4.76}$$

It is evident from these iteration error plots that AIM is converging quite beautifully for this

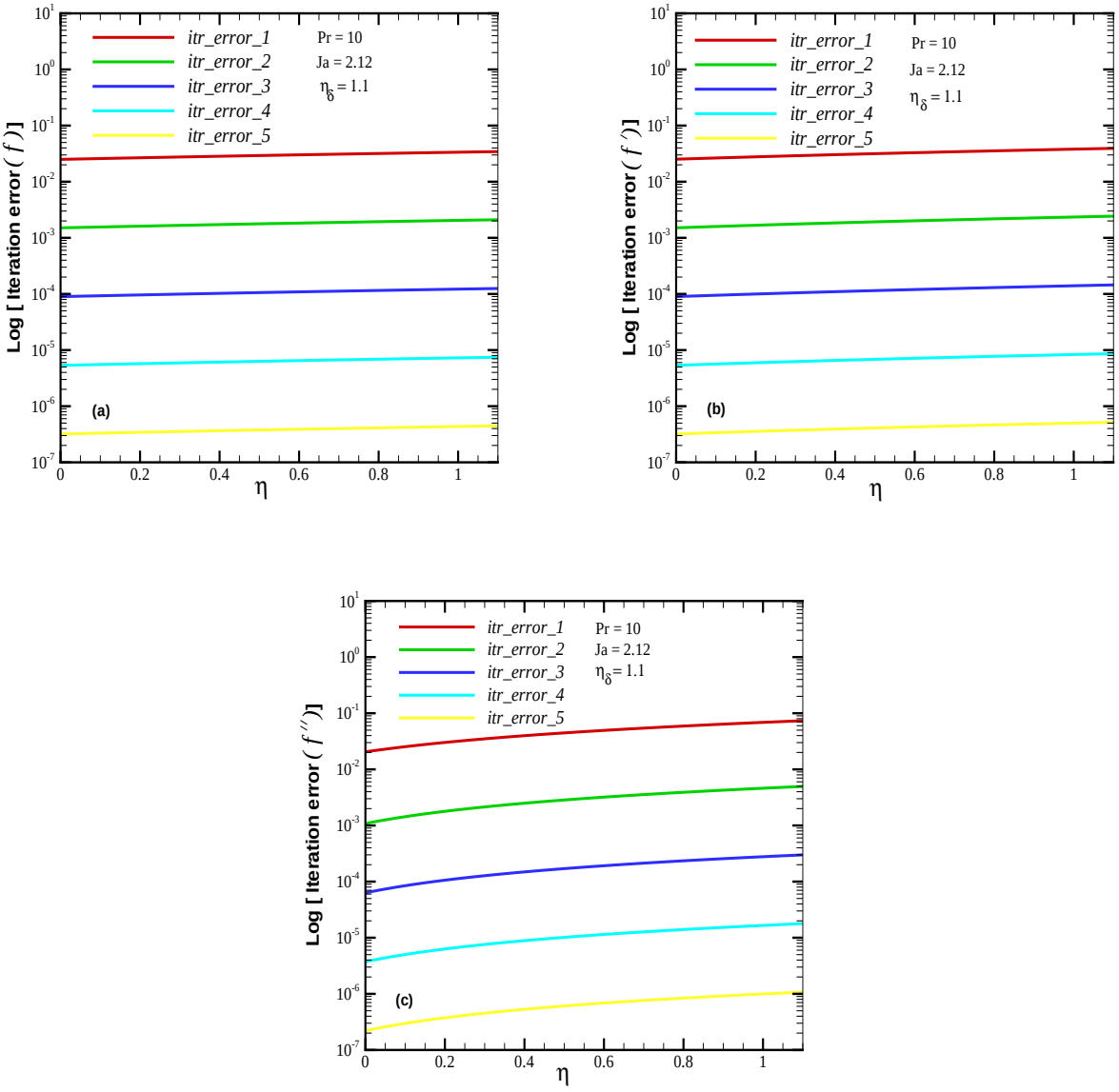

Figure 4.12 Iteration error profiles of f, f' and f'' for $Pr = 10$.

Prandtl number and in fact, it is able to obtain results of approximately $\approx 10^{-7}$ tolerance at the end of the 5th iteration. We now discuss the convergence of iterations and variation of iteration error for dimensionless temperature θ. It can be seen that the solution converges quickly with a maximum error of $\approx 10^{-2}$ at the end of the 2nd iteration. Despite of this large maximum error this solution is very close to the one obtained from the Runge–Kutta numerical scheme. The reason for this close confirmity is the rapid convergence of the AIM, which can be seen in the iteration error plot of θ, where going from first iteration to the second has almost decreased the maximum error by 500%. Thus we can expect that in the *3rd* iteration, the relative error between the iterations will be of the order of $\approx 10^{-6}$. This in turn implies that the current

solution at the 2nd iteration is very accurate and converged. It should be noted that the y-axis in Fig. 4.13 is scaled in *log* and

$$\text{iteration error}\,(\theta) = \frac{|\theta^{(n+1)} - \theta^{(n)}|}{\theta^{(n+1)}}\,. \tag{4.77}$$

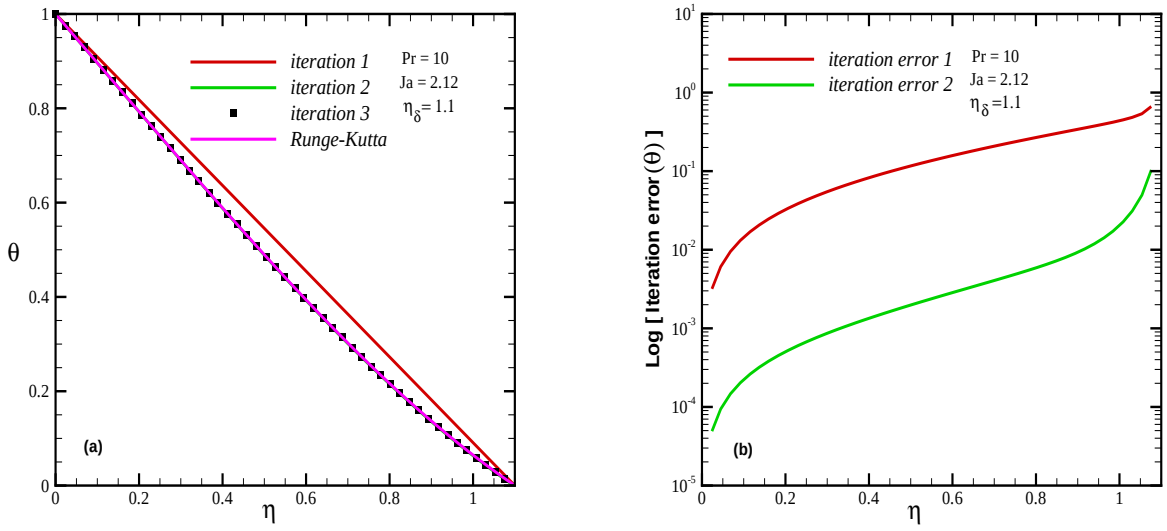

Figure 4.13 Iteration error profiles of θ for $Pr = 10$.

Moving further to the Prandtl number of 100, we have found the similar behavior in the convergence of solution profiles of f, f', f'' and θ. In fact from the profiles of f, f' and f'', shown in Fig. 4.14, it can be easily concluded that the solution of the (4.27) is approaching towards the solution of the equation with no acceleration terms in it *i.e.*,

$$f''' + 1 = 0\,.$$

So, it is reasonable to expect increasing effects due to the retention of acceleration terms at the lower Prandtl numbers. However, for the purpose of comparison, we are presenting all the results for $Pr = 100$, that are discussed for $Pr = 1$ and $Pr = 10$. The plots of convergence of iterations for this case are found to be convergent from the beginning. This can be observed in Fig. 4.14 where all the 5 iterations along with the Runge–Kutta numerical solution are overlapping each other. It should be noted that the present value of the Jacob number is very high and generally the values of much lower Jacob number than this are of practical importance. This further means that lower η_δs are required for such situations. This decrease, or lowering of η_δs, results in a more rapid convergence along with increased accuracy.

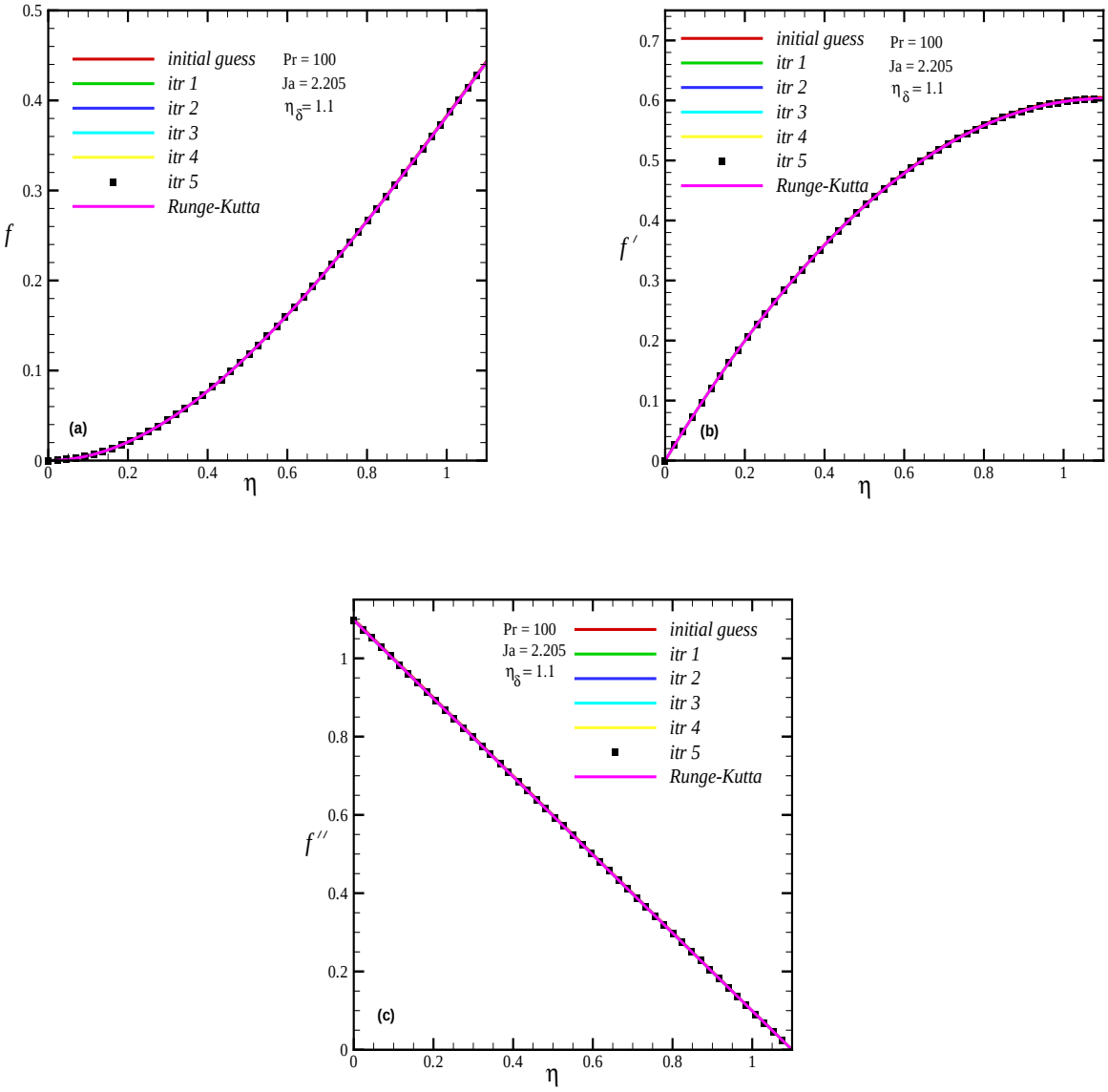

Figure 4.14 Convergence of iterations of the AIM for f, f' and f'' for $Pr = 100$.

In the next Fig. 4.15, iteration error for 5 iterations of the AIM can be seen for $Pr = 100$. As a matter of fact, we have not shown the iterative error between the 4th and the 5th iteration in this plot, as it is zero. This error cannot be shown on the y-axis, as it is scaled in *log*. The quantity on y-axis in each of these plots is same as defined for $Pr = 1$ and $Pr = 10$.

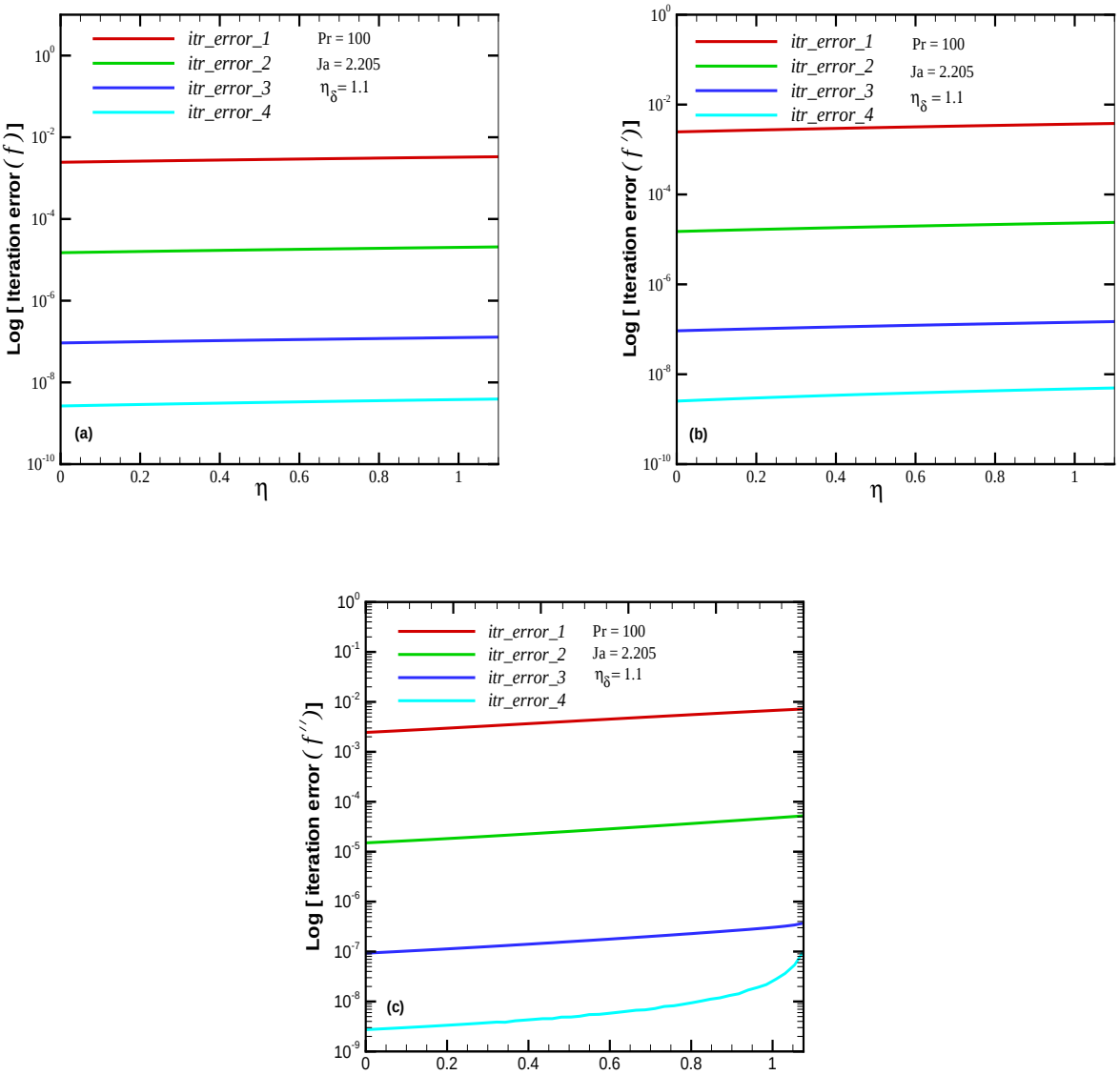

Figure 4.15 Iteration error profiles of f, f' and f'' for $Pr = 100$.

The temperature distribution across the condensate layer are also of some interest. The convergence results for the dimensionless temperature θ are shown in Fig. 4.16 (a). In Fig. 4.16 (b), variations of the iteration error in the entire domain, are plotted. It can be seen from the comparison of 4.16 (b) and 4.13 (b) that for the same value of η_δ, higher Prandtl numbers converged more rapidly towards the exact solution. The y-axis here too is defined as before.

The next important result in this discussion of high Prandtl numbers is of the variation

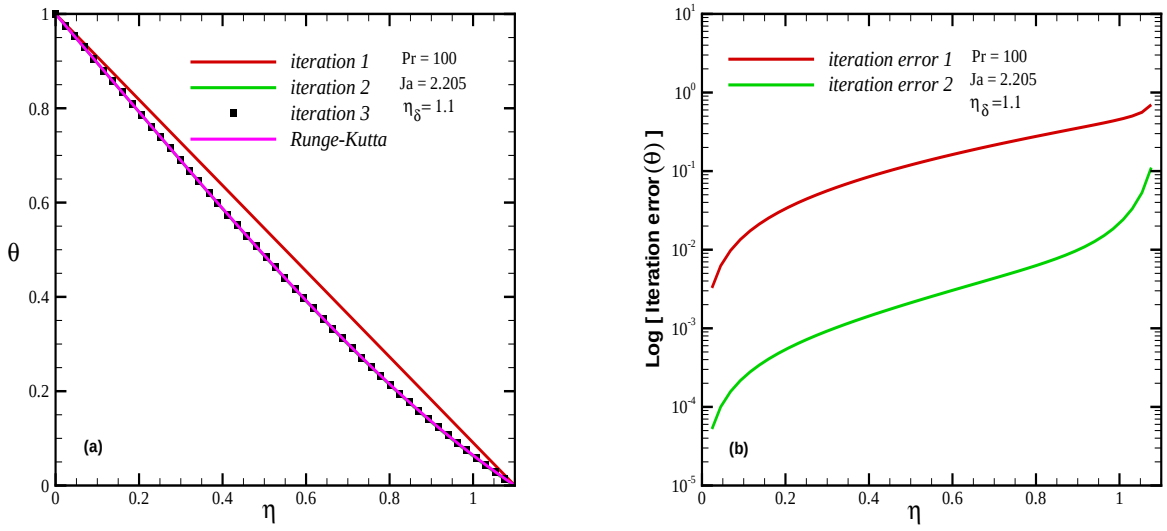

Figure 4.16 Iteration error profiles of θ for $Pr = 100$.

of the Jacob number Ja with respect to condensate film thickness (η_δ) for each fixed Prandtl number. Recalling Eq. (4.57), the following are the critical values of η_δ for the above discussed Prandtl numbers:

For $Pr = 1$

$$(\eta_\delta)_{critical} = 0.78 \tag{4.78}$$

For $Pr = 10$

$$(\eta_\delta)_{critical} = 0.92 \tag{4.79}$$

For $Pr = 100$

$$(\eta_\delta)_{critical} = 0.99 \tag{4.80}$$

which suggest that the AIM will give the converged solution for a fixed Prandtl number (say $Pr = 10$) if the thickness of the condensate layer is less than $(\eta_\delta)_{critical}$ (i.e., $\eta_\delta < 0.92$, for $Pr = 10$). But because of the reasons pointed out in convergence analysis, we found AIM stable for $\eta_\delta \in [0.5\,, 1.1]$ for all the three Prandtl numbers. This range gives Jacob numbers $0 < Ja < 1.7$ for $Pr = 1$, $0 < Ja < 2.1$ for $Pr = 10$ and $0 < Ja < 2.2$ for $Pr = 100$ as shown in Fig. 4.17 which covers most of the practical situations.

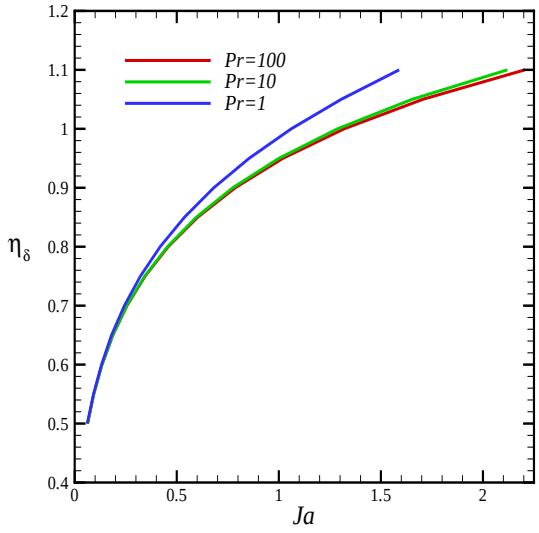

Figure 4.17 Variation of the Jacob number with respect to the condensate film thickness.

We now present solutions for momentum equation and energy equation in the form of following polynomials:

Momentum equation

$$f = \left(\frac{\eta_\delta^2}{Pr}\right)\frac{\eta^5}{120} - \frac{\eta^3}{6} + C_1\frac{\eta^2}{2} \tag{4.81}$$

Energy equation

$$\theta = \left(\frac{\eta_\delta}{Pr}\right)\frac{\eta^7}{1680} - \frac{1}{\eta_\delta}\frac{\eta^5}{120} + \frac{C_1}{\eta_\delta}\frac{\eta^4}{8} + A_1\eta + B_1 \tag{4.82}$$

where

$$A_1 = \left(\frac{17}{840}\right)\frac{\eta_\delta^7}{Pr} - \frac{\eta_\delta^3}{10} - \frac{1}{\eta_\delta}\,, \tag{4.83}$$

$$B_1 = 1 \tag{4.84}$$

and

$$C_1 = -\frac{\eta_\delta^5}{6Pr} + \eta_\delta\,. \tag{4.85}$$

These solutions are able to produce results which are accurate up to two places of decimal for the range of Prandtl numbers greater than 8 *i.e.,* $Pr > 8$ with $\eta_\delta \leq 1.1$. These polynomials are obtained at the end of the first iteration for both momentum and energy equations. It is evident from Fig. 4.18 that these polynomials are able to produce reasonable solutions for $1 \leq Pr < 8$ having $\eta_\delta < 1$, and highly accurate solutions for $Pr > 8$ having $\eta_\delta \geq 1.1$.

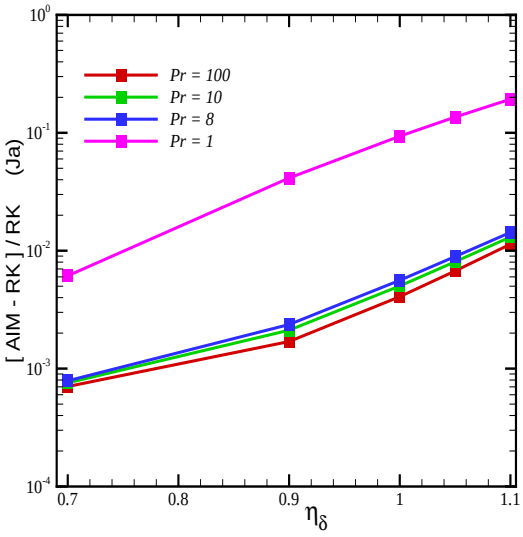

Figure 4.18 Relative error between solutions obtained from first iteration of AIM and converged Runge–Kutta numerical scheme.

Low Prandtl numbers

In the previous section, we showed that the laminar film condensation problem in boundary layer formulation for high Prandtl numbers can be solved analytically via AIM. We now describe the applicability of the AIM to the Prandtl numbers, which corresponds to liquid metals, *i.e.,* $Pr \in [0.003\,, 0.03]$. We have chosen two Prandtl numbers, $Pr = 0.03$ and $Pr = 0.008$, from this range. Eqs. (4.27) and (4.28) are solved for these two Prandtl numbers via AIM and the results are shown in Fig. 4.19 as the variation of the Nusselt number obtained from the Sparrow and Gregg's model with respect to the Nusselt number obtained from the classical Nusselt model, which predicts that

$$Nu_x \left[\frac{\frac{c_{pl}\Delta T}{h_{fg}}}{\frac{(\rho_l - \rho_v)x^3}{4\nu k_l}} \right]^{\frac{1}{4}} = 1\,. \tag{4.86}$$

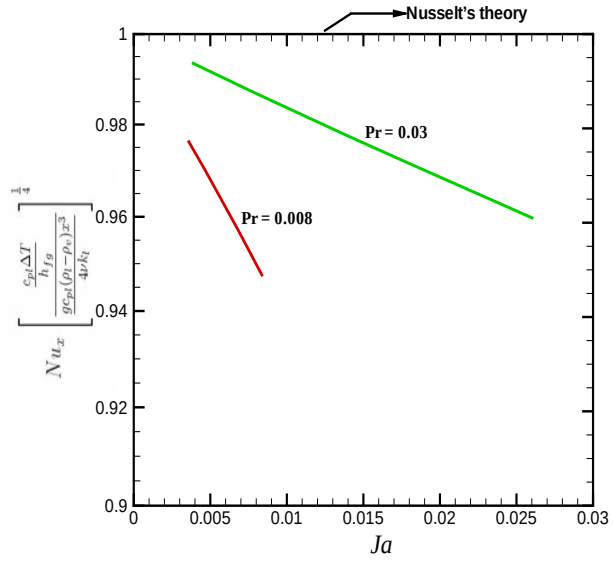

Figure 4.19 Local heat transfer results for low Prandtl nmuber.

For small values of Ja, *i.e.,* relatively thin condensate films, Nusselts theory gives results in close accord with those of the complete boundary-layer solutions. As Ja increases, *i.e.,* thicker films, the inertia affects lead to a dropping off of the Nusselt number. Heat transfer results corresponding to these solutions are presented in Fig. 4.19 in terms of the local Nusselt number. The ordinate variable is chosen to provide a direct comparison with Nusselt's simple theory.

We now discuss the results for Prandtl numbers 0.03 and 0.008 obtained via AIM. For both the cases only results of f' and f'' are discussed. Thus starting with $Pr = 0.008$, we show the convergence of the solution for this Prandtl number in the next two figures. In Fig. 4.20 profiles for both f' and f'' are plotted for $Ja = 0.0067$. The converged solution from the

Runge–Kutta numerical scheme is also shown in the figure. In both the cases of f' and f'' a good agreement between the numerical solution and the analytical solution is obtained. Similar

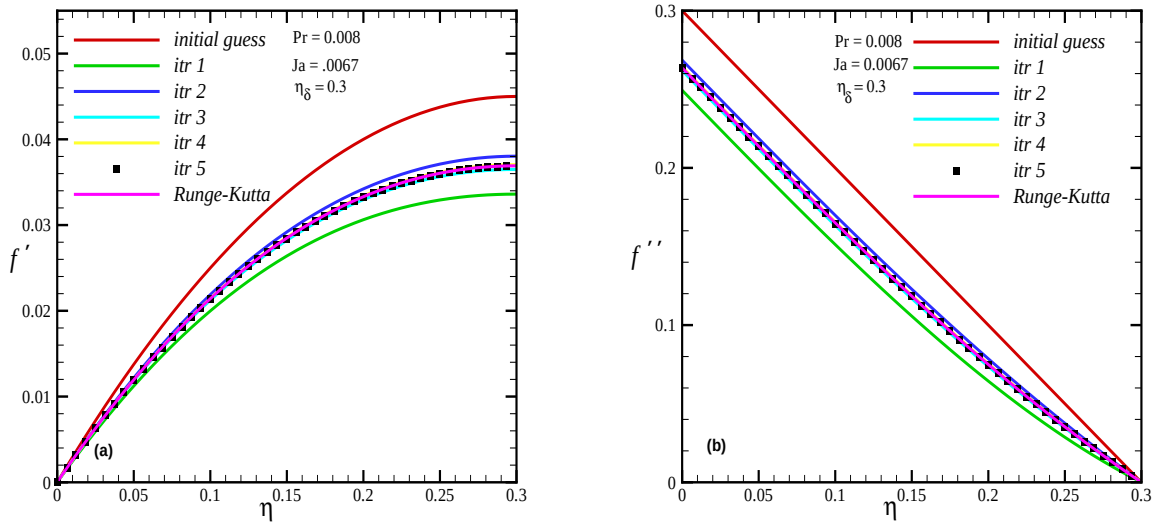

Figure 4.20 Iteration error profiles of f' and f'' for $Pr = 0.008$.

pattern of convergence is found in the results for $Pr = 0.03$ and $Ja = 0.022$. It can be seen from the plots that after the 1st iteration, solution for both f' and f'' is converging rapidly to the exact solution (see Fig. 4.21).

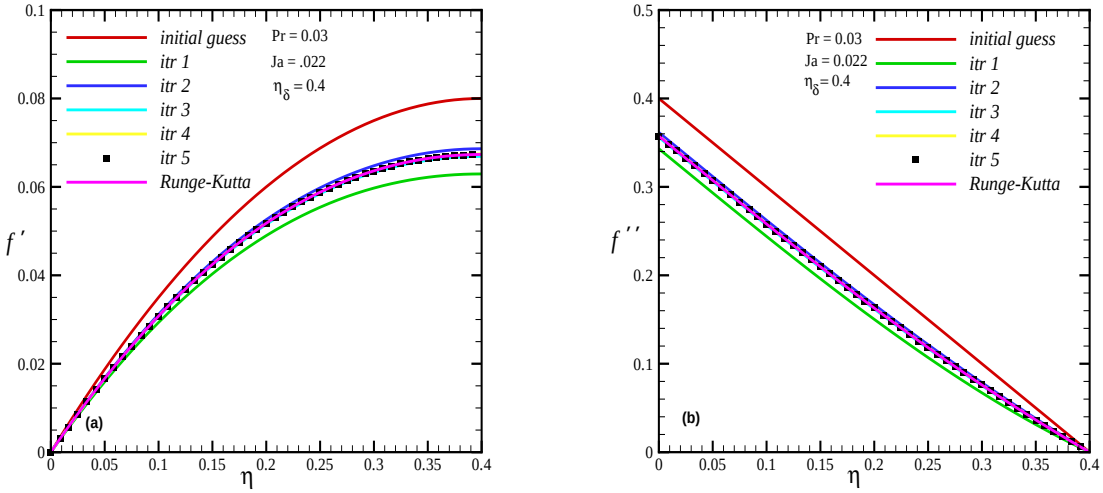

Figure 4.21 Iteration error profiles of f and f'' for $Pr = 0.03$.

For the direct comparison between the solutions obtained numerically and analytically, relative error plots between the solutions obtained from the Runge-Kutta numerical scheme and the AIM are shown in Fig. 4.22 for both the Prandtl numbers. In each case maximum error is found to be of the order of 10^{-3} (see Fig. 4.22).

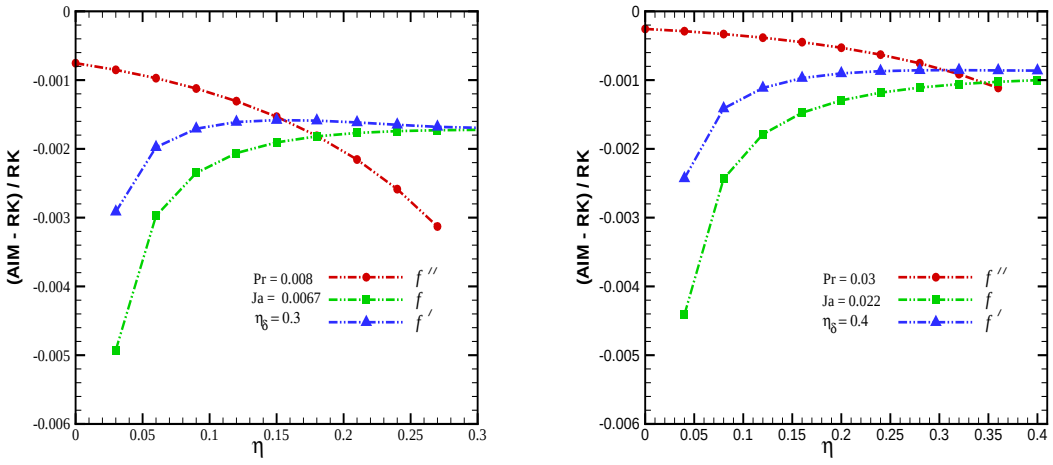

Figure 4.22 Relative error profiles of the AIM and the Runge–Kutta numerical scheme for f, f' and f'' for $Pr = 0.008$ and $Pr = 0.03$.

Here it would be worthwhile to mention that in both the cases, the Jacob numbers taken into account are low, as higher Jacob numbers cause decrease in the accuracy and the stability of the AIM. We now show this effect of increasing Jacob number on the accuracy of the results obtained via AIM and the Runge–Kutta numerical scheme. For this we compare the solution of the second derivative f'' obtained from the AIM with that of the Runge–Kutta numerical scheme for different Jacob numbers. This solution is calculated at the surface of the vertical plate. The plots show a trend of decrease in the relative error of the results for a given Prandtl number with the increase in the Jacob number. In fact the relative error reaches to its minimum for some Jacob number whereafter it starts to increase.

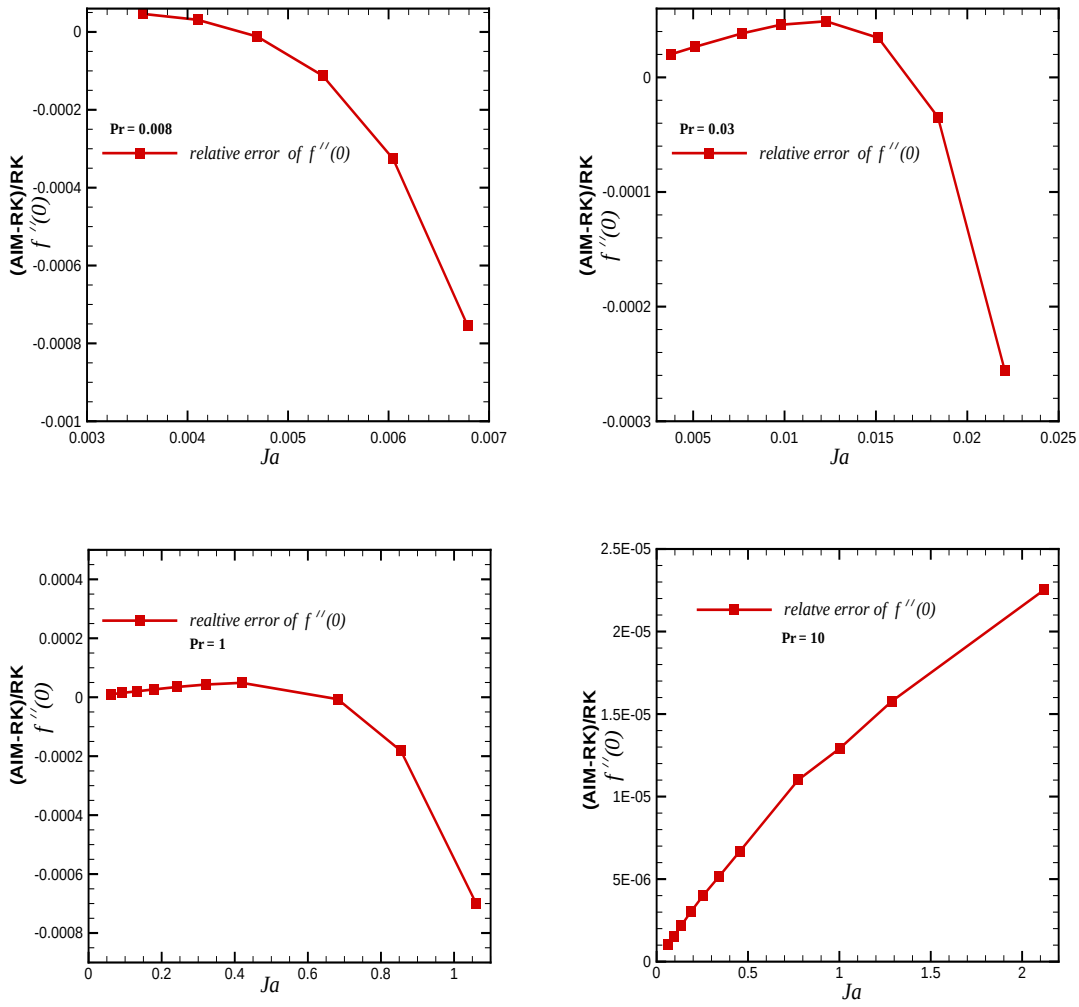

Figure 4.23 Variation of relative error of $f''(0)$ with respect to the Jacob number for various Prandtl numbers.

We now discuss the special case of $Pr = 0$ and the accuracy of its solution obtained via AIM with respect to the Runge–Kutta numerical scheme. However, it should be noted that for this case we have to eliminate the Pr from the denominator of momentum equation (4.27). Thus if in the similarity transformation if we define constant c as $c = g(\rho - \rho_v)/4\nu^2\rho$, we obtain the following equations of momentum and energy respectively:

$$f''' + 3ff'' - 2(f')^2 + 1 = 0\,, \tag{4.87}$$

$$\theta'' + 3\,Pr\,f\theta' = 0\,. \tag{4.88}$$

The Jacob number can now be defined as

$$Ja = 3Pr\frac{f(\eta_\delta)}{\theta'(\eta_\delta)}\,. \tag{4.89}$$

Here note that Eq. (4.88) can be solved exactly for θ by substituting $Pr = 0$. Following are the solutions for the energy equation for $Pr = 0$:

$$\theta = -\frac{\eta}{\eta_\delta} + 1\,, \quad \theta' = -\frac{1}{\eta_\delta}\,. \tag{4.90}$$

The result for this Prandtl number is shown in the form of variation of modified Jacob number which is Ja/Pr with respect to Nusselt number (Nu) or $\theta'(0)$ in Fig. 4.24. Results from both the AIM and the Runge–Kutta numerical scheme are plotted. It is obvious from the Fig. 4.24 that the results of the two schemes are in agreement.

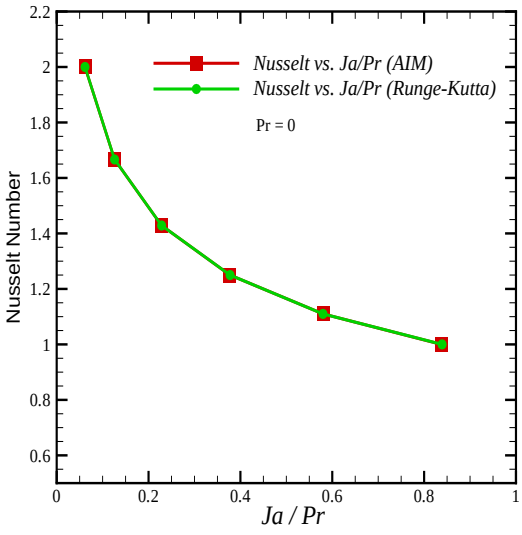

Figure 4.24 Relative error between solutions obtained from first iteration of AIM and converged Runge–Kutta numerical scheme.

Extending further the discussion of the accuracy of the AIM in low ($Pr < 0.03$) and high ($Pr > 1$) Prandtl numbers, we now present the stability plot for the above method. In Fig. 4.25 stability regions for the Prandtl numbers range from 0.03 to 10 are shown. In these plots

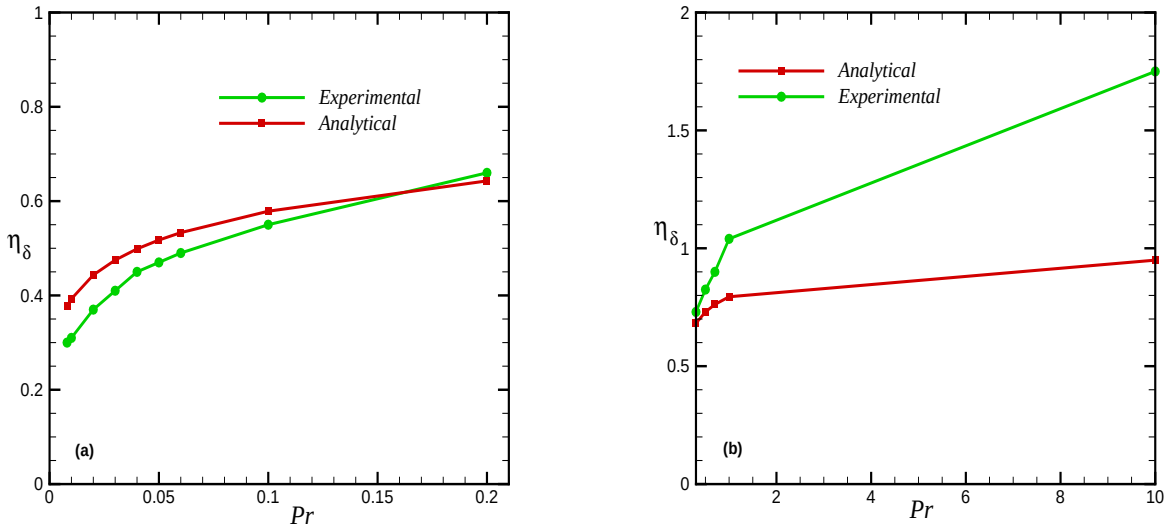

Figure 4.25 Stability plots of low and high Prandtl numbers.

the data plotted in red line is the data obtained from *stability equation* (4.57), which defines the stability region for each Prandtl number. According to this stability analysis if we select a η_δ less than the $(\eta_\delta)_{critical}$ determined from Eq. (4.57), AIM is guaranteed to give a converged solution. However, we have seen that for low Prandtl numbers this analysis overpredicts the value of $(\eta_\delta)_{critical}$ and underpredicts it for high Prandtl numbers. In fact, we have found that in the case of $Pr = 0.008$, AIM gives converged solution till the value of $\eta_\delta \approx 0.3$ while the analysis (4.57) preditcs it to be ≤ 0.397. Similarly for $Pr = 0.03$ it is found to be $\eta_\delta \approx 0.4$ instead of 0.47. Thus it would be worthwhile to report a result about the stability of the AIM based on some assumption for its successful application to a given set of Pr and η_δ. Fig. 4.25 is the graph of such stable region for the AIM to operate with a maximum iteration error of 10^{-2} in the solution of f'' at the end of 5th iteration for any Prandtl number lying between [0.03, 10]. Fig. 4.25 (a) shows the stable region for the range of Prandtl numbers $Pr \in [0.008, 0.2]$ while Fig. 4.25 (b) represents the stability for $Pr \in [0.3, 10]$. In both the figures, if for a particular Pr we select a value of η_δ less than the value of η_δ, which corresponds to a given Pr on the green line, AIM is guaranteed to give a converged solution with a maximum error of $\leq 10^{-2}$. The significance of this discussion lies in the fact that even though the iteration error in the solutions obtained via AIM is of the order of 10^{-2} they agree very well with the solutions obtained from

the Runge–Kutta 4th order numerical scheme, which is accurate up to the tolerance of 10^{-8}.

Chapter 5
Analytical solution for a flow over flat plate

In the early 20^{th} century, the mechanics of fluid developed in two different directions. One of these approach was guided by *theoretical hydrodynamics* which was evolved from Euler's equations of motion for a frictionless, non-viscous fluid and which achieved a high degree of completeness. The results of this so-called classical science of hydrodynamics however were found to be in contradiction to the experimental results. This anamolous behavior in the two results was particularly seen in the problems of pressure losses in pipes and channels and in the drag of a body which moves through a mass of fluid. Thus practical engineers, prompted by the need to solve the important problems arising from the rapid progress in technology, developed their own highly empirical science of hydraulics. The science of hydraulics was based on a large number of experimental data and differed greatly in its methods and in its objects from the science of theoretical hydrodynamics.

At the beginning of the present century, L. Prandtl distinguished himself by showing how to unify these two divergent branches of fluid dynamics. He achieved a high degree of correlation between theory and experiment and paved the way to the remarkably successful development of fluid mechanics which has taken place over the past 50 years. He proved that the flow about a solid body can be divided into two regions: a very thin layer in the neighbourhood of the body (*boundary layer*) where friction plays an essential part, and the remaining region outside this layer, where friction may be neglected. With the aid of this hypothesis, Prandtl succeeded in giving a physically penetrating explaination of the importance of viscosity in the assessment of drag and paved the way for the theoretical analysis of viscous flows, achieving at the same time a maximum degree of simplification of the attendant mathematical difficulties.

The boundary layer theory finds its application in the calculation of the skin friction drag which acts on a body as it is moved through the fluid: for example, the drag experienced by the flat plate at zero incidence, the drag of a ship, of an airplane or turbine blade. Boundary-layer flow has the peculiar property that under certain conditions, the flow in the immediate neighbourhood of a solid wall becomes reversed, causing the boundary layer to separate from it. Boundary layer theory gives an answer to the very important question of what shape must a body be given in order to avoid this detrimental sepration.

5.1 Flow over a flat plate (Blasius equation)

The simplest example of the application of the boundary-layer equations is the flow past a flat plate. Historically, this was the first example illustrating the application of Prandtl's boundary layer theory; it was discussed by H. Blasius [40] in his doctoral thesis. Let the leading edge of the plate be at $x = 0$, following are the assumptions taken into account:

1. a steady potential flow has constant velocity U in the x direction, and, therefore, $dp/dx = 0$.
2. an infinitely thin flat plate is placed into this flow so that the plate is parallel to the potential flow (*0 angle of incidence*).

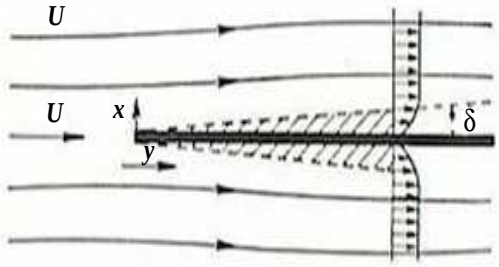

Figure 5.1 Boundary layer along a flat plate.

Because of the vicosity, the flow will retard, creating a boundary layer on either side of the plate. Here only the boundary layer on one side of the plate is considered. The flow is assumed to be laminar. Thus the N.-S. equations for this flow,

$$u\frac{\partial u}{\partial x} + v\frac{\partial u}{\partial y} = \cancelto{0}{-\frac{1}{\rho}\frac{dp}{dx}} + \nu\frac{\partial^2 u}{\partial y^2}\,, \tag{5.1}$$

$$\frac{\partial u}{\partial x} + \frac{\partial v}{\partial y} = 0\,, \tag{5.2}$$

with tangential and normal velocities vanish at boundary: tangential velocity = free stream velocity far from plate *i.e.,*

$$u|_{y=0} = 0\,, \quad v|_{y=0} = 0\,, \quad u|_{y=\infty} = U\,. \tag{5.3}$$

Since the system under consideration has no preferred length, it is reasonable to suppose that the velocity profiles at varying distances from the leading edge are similar to each other, which means that the velocity curves $u(y)$ for varying distances x can be made identical by selecting suitable scale factors for u and y appear quite naturally as the free stream velocity, U, and the

boundary layer thickness, $\delta(x)$, respectively. It will be noted that the latter increases with the current distance x. Hence the principle of similarity of velocity profiles in the boundary layer can be written as $u/U = \phi(y/\delta)$, where the function ϕ must be the same at all distances x from the leading edge.

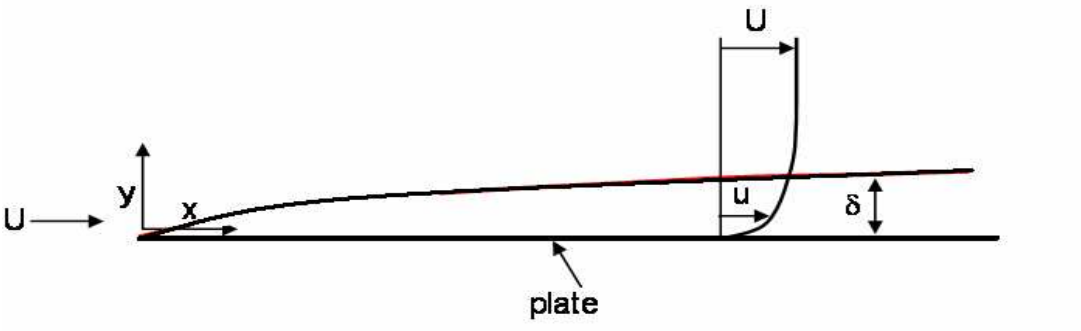

Figure 5.2 Sketch of a boundary layer along a flat plate.

Until now, we have not given a precise definition of boundary layer thickness. Here we use δ to denote *nominal boundary thickness*, which is defined to be the value of y at which $u = 0.99U$, *i.e.,*

$$u(x, y)|_{y=\delta} = 0.99U\,. \tag{5.4}$$

As we have seen in the first chapter in the case of a suddenly accelerated plate, that $\delta \sim \sqrt{\nu t}$, where t denotes the time from the start of the motion. In this case we will consider it as the time which a fluid particle takes in reaching from the leading edge to the point x. For a particle outside the boundary layer this is $t = x/U$, so that we may put $\delta \sim \sqrt{\nu x/U}$. We now introduce the new dimensionless similarity variable $\eta = y/\delta$ or,

$$\eta = y\sqrt{\frac{U}{2\nu x}}\,. \tag{5.5}$$

The stream function of the flow, $\psi = \int u\,dy|_{x=const}$, should increase as δ, or $x^{1/2}$, and can be put as,

$$\psi = \sqrt{2\nu U x}\, f(\eta) \tag{5.6}$$

where $f(\eta)$ denotes the dimensionless stream function. Thus the velocity components become:

$$u = \frac{\partial \psi}{\partial y} = \frac{\partial \psi}{\partial \eta}\frac{\partial \eta}{\partial y} = U f'(\eta)\,, \tag{5.7}$$

$$v = -\frac{\partial \psi}{\partial x} = \sqrt{\frac{\nu U}{2x}}(\eta f - f') \tag{5.8}$$

where the prime denotes differentiation with respect to η. Here u is of the order of U while v is of small order, $U/\sqrt{Re_x}$. Substitution of u and v from Eqs. (5.7) and (5.8) into the boundary layer momentum relation (5.1) yields,

$$-\frac{U^2}{x}\eta f' f'' + \frac{U^2}{x}(\eta f' - f)f'' = \nu\frac{U^2}{x\nu}f''' \,. \tag{5.9}$$

After simplification, the following ordinary diffrential equation is obtained:

$$f''' + f f'' = 0 \,. \tag{5.10}$$

Referring to Eq. (5.3) , the no-slip conditions $u|_{y=0} = 0$, $v|_{y=0} = 0$, and the freestream-merge condition, $u|_{y=\infty} = U$, convert to

$$f'(0) = f(0) = 0 \,, \quad f'(\infty) = 1 \,. \tag{5.11}$$

Equation (5.10) is the celebrated nonlinear *Blasius equation* for flat-plate flow. Thus both partial differential equations have been transformed into an ordinary differential equation via similarity transformation. The resulting differential equation is nonlinear and of third order. The three boundary conditions are, therefore, sufficient to determine the solution completely. A Number of techniques that are prevalent for solving this equation have already been discussed in chapter 2. However, in the next section we have attempted to solve this equation via AIM. It should be noted that in the Blasius equation, the thickness of boundary layer is not well defined. In the case of flow over a flat plate, this $\eta \to \infty$ is taken at $\eta = \eta_{max} = 6.0$. However, we have found our solution technique to be convergent up to $\eta_{max} = 3.5$. Although this radius of convergence of $\eta_{max} = 3.5$ is restrictive in capturing the solution for the complete flow in the boundary layer, it provides a reasonable idea about the 99% of the flow within the boundary layer.

5.1.1 Analytical solution of the Blasius equation

To begin the analytical procedure, we find the initial guess for the solution or the *zeroth approximation*. To do this, we solve the linear part of Eq. (5.10) which is

$$\mathcal{L}(f) = f''' \,, \tag{5.12}$$

and equate it to zero. Integrating this linear part thrice will give us a *zeroth approximation* for the solution,

$$f_0 = C_{10}\frac{\eta^2}{2} + C_{20}\eta + C_{30} \,, \tag{5.13}$$

$$f_0' = C_{10}\eta + C_{20}\,, \tag{5.14}$$

$$f_0'' = C_{10}\,. \tag{5.15}$$

We will now evaluate each of these constants of integration C_{10}, C_{20} and C_{30} using the boundary conditions given by Eq. (5.11), as follows:

$$C_{10} = \frac{1}{\eta_{max}}\,, \quad C_{20} = 0\,, \quad C_{30} = 0\,, \tag{5.16}$$

which on substitution into Eqs. (5.13), (5.14) and (5.15) yields,

$$f_0(\eta) = \frac{\eta^2}{2\eta_{max}}\,, \quad f_0'(\eta) = \frac{\eta}{\eta_{max}}\,, \quad f_0''(\eta) = \frac{1}{\eta_{max}}\,. \tag{5.17}$$

This solution of linear part will be used for the convergence analysis and as an initial guess for solving Eq. (5.10) via AIM.

Convergence analysis for the Blasius equation

After obtaining the initial guess, we will perform the following convergence analysis. Thus rewriting Eq. (5.10) for the highest derivative,

$$f''' = -ff''\,. \tag{5.18}$$

We solve the above equation for $f(\eta)$ by integrating $f'''(\eta)$ thrice. We get,

$$\int_0^\eta \int_0^\zeta \int_0^\xi f'''\,dx\,dy\,dz = -\int_0^\eta \int_0^\zeta \int_0^\xi f''f\,dx\,dy\,dz\,,$$

$$f = -\int_0^\eta \int_0^\zeta \int_0^\xi f''f\,dx\,dy\,dz,$$

$$F(f) = -\int_0^\eta \int_0^\zeta \int_0^\xi f''f\,dx\,dy\,dz\,. \tag{5.19}$$

This $F(f)$ will converge if it obeys the following *Lipschitz condition*,

$$\|F(f) - F(g)\| \leq L\,\|f - g\| \quad \forall\, f, g \in \mathbb{P}\,, \tag{5.20}$$

where *Lipschitz constant* L is defined by

$$L = \max_{f\in\mathbb{P}} \|F'(f)\|\,.$$

$F'(f)$ can be expressed by differentiating Eq. (5.19) as

$$F'(f) = -\frac{d}{df}\int_0^{\eta}\int_0^{\zeta}\int_0^{\xi} f'' f \, dx \, dy \, dz \,. \tag{5.21}$$

Here $f(\eta)$ and $f''(\eta)$ are the initial guesses obtained from linear part *i.e.,* Eq. (5.17). Thus substituting their value in Eq. (5.21) yields,

$$F'(f) = -\frac{d}{df}\int_0^{\eta}\int_0^{\zeta}\int_0^{\xi} \frac{C_1^2}{2}\eta^2 \, dx \, dy \, dz \,, \tag{5.22}$$

$$F'(f) = -\frac{d}{df}\int_0^{\eta} \frac{C_1^2}{2}\frac{\eta^4}{12} \, dz \,, \tag{5.23}$$

but we know that

$$f^2 = \frac{C_1^2}{4}\eta^4 \,, \tag{5.24}$$

therefore we can write Eq. (5.23) as

$$F'(f) = -\frac{1}{6}\frac{d}{df}\int_0^{\eta} f^2 \, dz \,. \tag{5.25}$$

Commuting the integral operator with the differential operator and differentiating the integrand w.r.t. f in Eq. (5.25), we get the following:

$$F'(f) = -\frac{1}{6}\int_0^{\eta} 2f \, dz \,, \tag{5.26}$$

$$F'(f) = -\frac{1}{3}\int_0^{\eta} f \, dz \,, \tag{5.27}$$

$$F'(f) = -\frac{C_1\eta^3}{18} \,. \tag{5.28}$$

From the definition of L^1 norm we can write

$$\max \|F'(f)\|_1 = \frac{C_1}{18}\int_0^{\eta_{max}} \left|-\eta^3\right| \, d\eta \,, \tag{5.29}$$

$$\max \|F'(f)\|_1 = \frac{C_1\eta_{max}^4}{72} \,, \tag{5.30}$$

here $C_1 = 1/\eta_{max}$ and the term inside the $|\cdot|$ is monotone. Thus

$$L = \max_{f\in\mathbb{P}} \|F'(f)\| \text{ where } L < 1 \text{ for convergence} \,, \tag{5.31}$$

or

$$\frac{\eta_{max}^3}{72} < 1 \Rightarrow \eta_{max} < 4.16\,. \tag{5.32}$$

This is a third-degree polynomial that has three values, but as $\eta_{max} > 0$, we consider only positive values. In the given case of flow over a flat-plate, these values should be less than 4.16. The significance of the relationship (5.32) and hence of the critical value of $\eta_{max} < 4.16$ lies in the fact that if we take boundary layer thickness more than 4.16, the AIM will not give converged solutions of the Blasius equation. However, in our application of AIM to the Blasius equation, we have found the converged solutions for the values of η_{max} up to 3.5. We now discuss the solution procedure for $\eta_{max} = 3.5$ in the next section.

Analytical iteration method for Blasius equation

As outlined earlier, to start the analytical iterations we solve the original nonlinear ordinary differential equation for the highest derivative *i.e.,*

$$f_1''' = -f_0 f_0''\,. \tag{5.33}$$

The right hand side of the above equation can be reduced to a polynomial by substituting the values of f anf f'' from Eq. (5.17). The equation can now be integrated thrice to yield a new polynomial with terms containing constants of integration. These constants of integration can be evaluated via boundary conditions as before. Following are the solutions obtained after the first iteration.

$$f_1 = -\frac{\eta^5}{120\eta_{max}^2} + \eta_{max}\frac{\eta^2}{48}\,, \tag{5.34}$$

$$f_1' = -\frac{\eta^4}{24\eta_{max}^2} + \eta_{max}\frac{\eta}{24}\,, \tag{5.35}$$

$$f_1'' = -\frac{\eta^3}{6\eta_{max}^2} + \frac{\eta_{max}}{24}\,. \tag{5.36}$$

These new solutions will begin a new analytical iteration. In this way we develop an iteration method which will be repeated until two successive polynomials are sufficiently close in $L^1(0, \eta_{max})$ to satisfy a specified convergence criterion. The specified criterion in the present case is taken as the iteration error of shear stress at the wall should not be greater than 10^{-2}. In this case also we have a limitation on the number of iterations because of the limitation in computing power. The maximum number up to which MAPLE [144] can iterate the solution is 9. The number of terms present in the polynomial at the end of 9^{th} iteration is 512.

5.1.2 Results and discussions for Blasius equation

In the convergence analysis for the Blasius equation, we found that AIM will converge for any value of η_{max} less than 4.16. However, in practice it is found to be convergent for the values

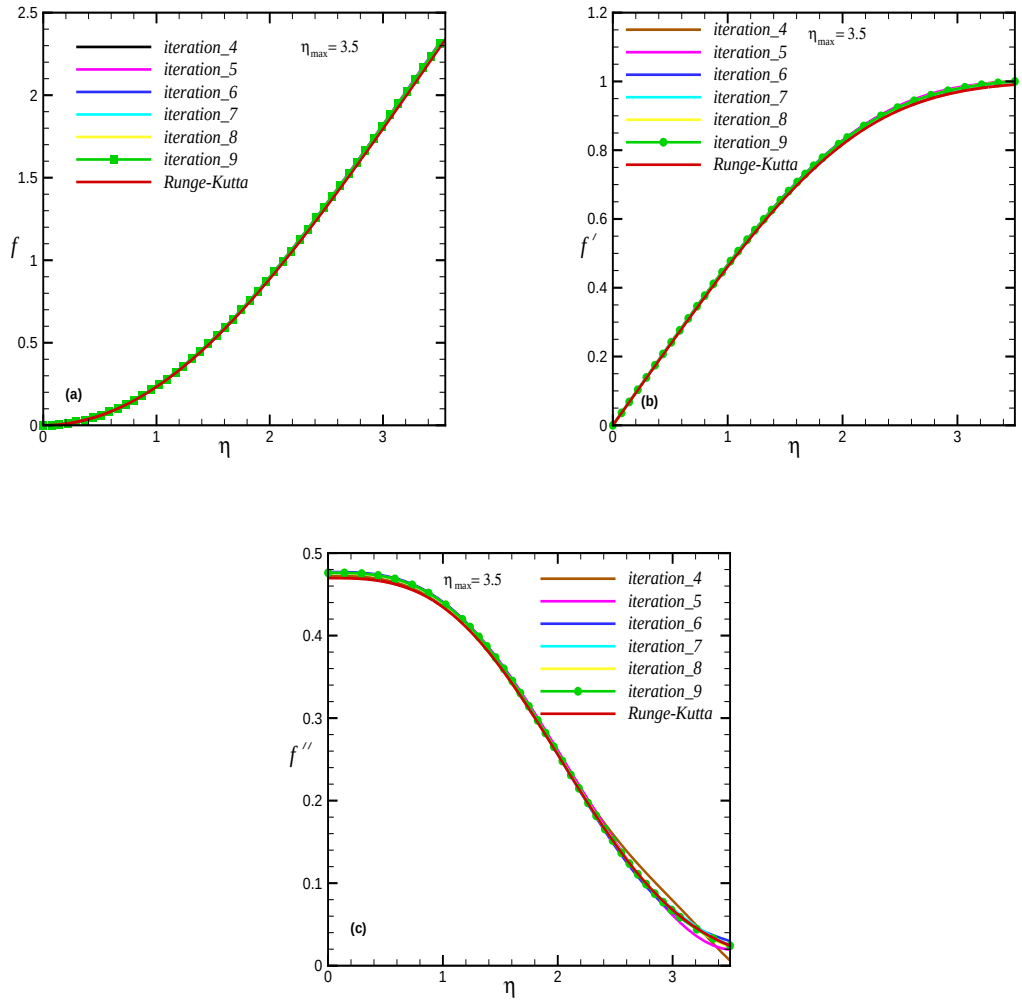

Figure 5.3 Convergence of the iterations of the AIM for f, f' and f'' for $\eta_{max} = 3.5$.

up to $\eta_{max} = 3.5$. This indicates that AIM cannot predict the exact solution of the Blasius equation for the entire domain. However, this value of $\eta_{max} = 3.5$ is sufficient to capture the solution of 99% of the boundary layer. In Fig. 5.3, convergence of the solution for each of the f, f' and f'' is shown. In these plots, iterations numbering from 4th till 9th are shown. At the end of the 9th iteration, a good agreement between the solutions of the Runge–Kutta and the AIM can be seen. However, to judge the relative accuracy of the solutions at various iterations, in the next figure iteration errors of the solution of the Blasius equation are plotted for each of the f, f' and f''. It can be seen from the relative error plots for f and f' that the maximum error is of the order of 10^{-3}. In the case of shear stress f'', the solution is converging with a

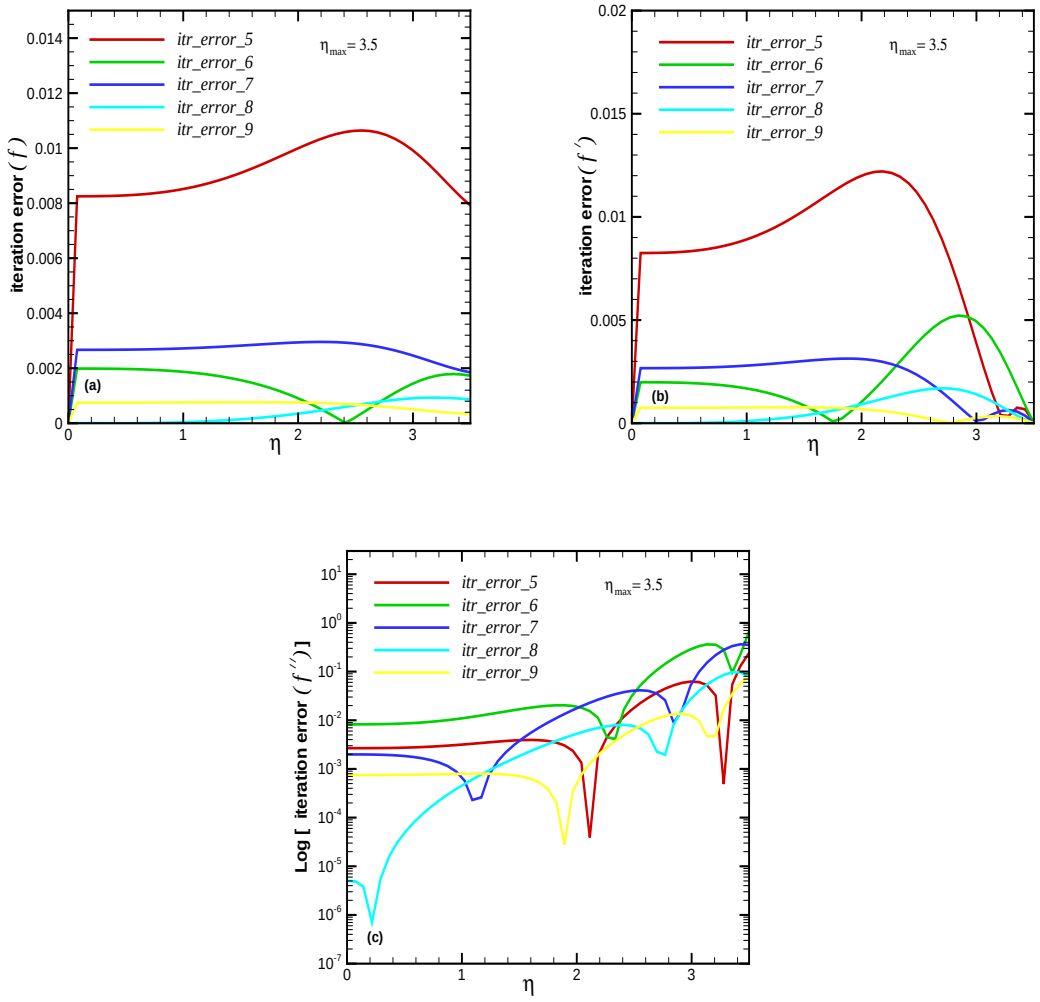

Figure 5.4 Iteration error profiles of f, f' and f'' for $\eta_{max} = 3.5$.

maximum error of $\approx 10^{-2}$. It should be noted that the maximum error in case of f'' ocurrs near the edge of the boundary layer. This can be explained from the fact that we are considering the infinity boundary condition at 3.5 *i.e.*, $f'(3.5) = 1.0$, which is actually $f'(3.5) = 0.99$ in real flow conditions. Although this error seems to be small in f', it gets more pronounced in its next derivative which is f'' and thus affects the solution. We now compare the converged solutions obtained via AIM with those of the 4th order Runge–Kutta numerical scheme. In this case, also, we have found a reasonable agreement between the solutions of stream function f, velocity profile f', and shear stress profile f'' (see Fig 5.5). Here the maximum error is found to be of the order of 10^{-2} for each of the f, f' and f''. The results obtained from the Runge–Kutta 4th order numerical scheme are for $\eta_{max} = 6.0$, and are accurate up to 8 decimal places. It can be seen from Fig. 5.5 that all solutions of the two methods are in good agreement. Moving further, we now compare the different parameters of the boundary layer that can be obtained from f, f'

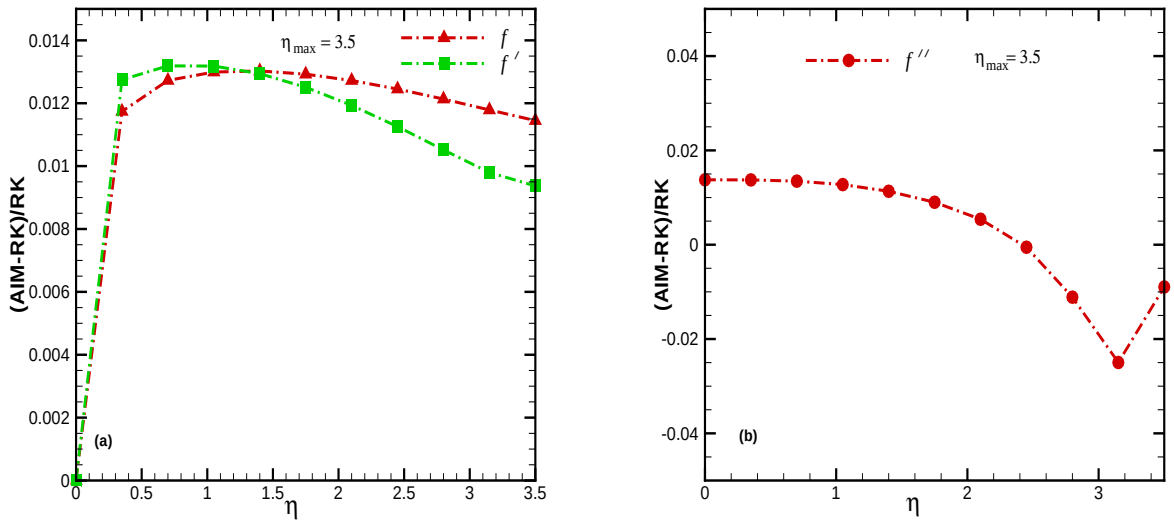

Figure 5.5 Relative error between the solutions of the AIM and the Runge–Kutta w.r.t. the Runge–Kutta for $\eta_{max} = 3.5$.

Table 5.1 Relative error between the boundary layer parameters obtained from the AIM and the Runge–Kutta w.r.t. the Runge–Kutta for $\eta_{max} = 3.5$.

Parameters	AIM	Runge–Kutta	Relative error
$\delta_{99\%}/x$	$\approx 4.54/\sqrt{Re_x}$	$\approx 5.0/\sqrt{Re_x}$	9.2
δ^*/x	$\approx 1.6788/\sqrt{Re_x}$	$\approx 1.7208/\sqrt{Re_x}$	2.44
θ/x	$\approx 0.673/\sqrt{Re_x}$	$\approx 0.664/\sqrt{Re_x}$	1.35
C_f	$\approx 0.673/\sqrt{Re_x}$	$\approx 0.664/\sqrt{Re_x}$	1.35

and f''. We note that $f' = 0.99$ occur at $\eta \approx 3.5$ when the boundary layer thickness is taken to be 6.0. However, in our case it occurs at $\eta \approx 3.21$ as we have taken $\eta_{max} = 3.5$. The table 5.1 shows the results of the coefficient of friction at the wall (C_f) and the ratio of momentum and displacement thickness to the distance x along the plate. These results are obtained for each of the Runge–Kutta and the AIM. The relative errors of all these parameters are also included in table 5.1. It can be seen that barring the relative error of $\delta_{99\%}$, other parameters differ only by $\approx 2\%$ from the actual values. This error in all the parameters is directly related to the restrictive radius of convergence. The restriction on the radius of convergence of AIM can be explained from the viewpoint of the *singularity* present in the Blasius equation. As it belongs to a class of boundary-layer problems over an infinite interval, the radius of convergence can only be defined for some specific domain size, which is $\eta_{max} \approx 4.16$ in our analysis. However, this radius of convergence is found to be overpredictive than the actual $\eta_{max} \approx 3.5$. One of the reasons of this overprediction is the basis of convergence analysis, which uses an initial guess

as a solution of the given nonlinear ordinary differential equation. This assumption works well when the initial guess and the converged solution are close, but underpredicts/overpredicts the domain size when they are not close, as we have seen in the case of the Blasius equation.

Chapter 6
Summary and conclusions

In this chapter, a summary of the present research will be given. We will then present a list of conclusions drawn from the research. Finally, a brief note on future work that can be done as a consequence of this research will be presented.

6.1 Summary

1. In chapter I, a brief introduction of transport equations and their solutions via similarity transformation was presented. This chapter also presented the background information and significance of similarity transformations.

2. In Chapter II, we presented some background information to enable the reader to understand the motivation behind this work as much as possible. In particular, relevant previous work on the exact solutions for the N.-S. equations was presented. Included were discussions on the various methods to solve the nonlinear ordinary differential equations: approximate methods and numerical methods. The approximate methods included variational methods, Galerkin procedure, collocation methods, quasilinearization, regular perturbation method, Cauchy–Picard iteration, series solutions, homotopy analysis method, integral analysis method and Green's functions. In the numerical methods section, we gave the brief account of interpolation methods, shooting methods, and several references to the other numerical methods.

3. The classical theory of fixed-point iteration in the polynomial spaces was discussed in chapter III. An analytical iteration method (AIM) for solving nonlinear ordinary differential equations was developed in this chapter. The linear part of the nonlinear ordinary differential equation was separated, and was used to obtain the initial guess for the nonlinear ordinary differential equation. An analytical iteration procedure was then set up for obtaining the exact analytical solution. A convergence criterion for estimating the radius of convergence for this method was also been deduced.

4. In chapter IV, the process of film-wise condensation was discussed. Different models (Nusselt's classical, Rohsenow's, Bromley's, Chen's, Koh's, and Sparrow and Greggs's models) of film-wise condensation were outlined. An analytical solution (by applying

AIM) was given to Sparrow and Gregg's boundary layer model of film-wise condensation. The results of this analytical method were compared and explained with the numerical results of the 4th order Runge–Kutta numerical scheme. The analytical iteration method was first applied to the high Prandtl numbers 1, 10 and 100, and then extended to the low Prandtl numbers of 0.03 and 0.008.

5. In Chapter V, we developed an analytical iteration method for solving the Blasius equation. The problem was solved for 99% of the boundary layer. The results obtained from the AIM were compared with the Runge–Kutta numerical scheme. Various other parameters, for instance, displacement thickness, momentum thickness and shear stress at the wall were also compared and explained.

6.2 Conclusions

1. The "Analytical Iteration Method (AIM)" proposed by us was found to be successful in obtaining solutions of the transport equations in the similarity form. The solutions of two celebrated equations, film-wise condensation and flow over a flat-plate, were obtained. These solutions were found in good agreement with the numerical results.

2. In the case of film-wise condensation, results for both high and low Prandtl numbers were reported. In the case of high Prandtl numbers of 1, 10 and 100, the solutions obtained from the AIM were found in an excellent agreement with that of the Runge–Kutta numerical scheme. The solutions were reported in terms of the variation of the Nusselt number with respect to the Jacob number. The range of film thickness for high Prandtl numbers was taken as $\eta_\delta = [0.5, 1.1]$. This range covers most of the practical situations.

3. Several other forms of results, for instance, variation of stream function and its derivatives with respect to film thickness, were also explained and compared with the corresponding Runge–Kutta results. Dimensionless temperature varaition for different Jacob numbers for a given Prandtl number was also shown and found to be deviating from linearity with the increasing Jacob numbers.

4. The convergence of iterations in high Prandtl numbers was found to be high. In fact in moving from *Pr=1* to *Pr=10*, the iterations converged immediately after the first iteration.

5. For low Prandtl numbers, two Prandtl numbers 0.03 and 0.008 were selected. The results were shown as the variation of the Nusselt number obtained via AIM for Sparrow

and Gregg's model with respect to the Nusselt number obtained from Nusselt's model. Dropping off of the Nusselt number in the results showed the effects of inertia in these comparisons.

6. Effects of increasing the Jacob number on the accuracy of the AIM w.r.t. the Runge–Kutta were discussed. The results showed the decrease in the accuracy for the high Jacob numbers. The results were compared for f'' at the vertical plate.

7. Stability plots for Prandtl numbers ranging from 0.03 to 10 were shown. A criteria to obtain reasonably accurate solutions via AIM was also discussed for this range.

8. It was found in the convergence analysis that it overpredicts the critical value of film thickness (η_δ) for low Prandtl numbers. However, in case of high Prandtl numbers this analysis was found to underpredict the film thickness. This lack of consistency in the convergence analysis was due to its dependence on the the initial guess of the solution. As a matter of fact, this initial guess is not a converged solution of the equation; it only provides a rough estimate about the radius of convergence of the solution. Similar deviations in the critical value of boundary layer thickness were observed and explained for the Blasius equation.

6.3 Future work

As alluded to at the beginning of this thesis, this research effort was focused primarily on developing the analytical solutions for transport equations in the similarity form. We have shown that the equations in similarity form can be solved analytically via fixed-point iteration, and the solution can be represented as a polynomial (similar to power series). Further work needs to be done with the other transport equations in the similarity form. This includes the equation of stretching flows, free shear flows, point sink flow and other Falkner–Skan wedge flows. Another perspective of this research can be extended for improving the convergence analysis. However, we would like to mention here that all the analytical integrations for various iterations in AIM are performed via MAPLE. Therefore in the future, if we can go beyond 9 iterations, some of the problems can be solved for the large radius of convergence; for instance, the Blasius equation can be solved for a radius of convergence ≈ 4.0.

BIBLIOGRAPHY

1. R. Berker. *A new solution of the Navier–Stokes equation for the motion of a fluid contained between two parallel plates rotating about the same axis*, Arch. Mech., **31**, pp. 265–280, 1979.

2. R. Berker. *Intégration des és du movement d'un fluide visquex incompressible*, Handbuch der Physik, ed. S. Fluǵg, **VIII/2**, pp. 1–384, Berlin, Springer–Verlag, 1963.

3. R. Berker. *An exact solution of the Navier–Stokes equation–the vortex with curvillinear axis,* Intl. J. Eng. Sci., **20**, pp. 217–230, 1982.

4. G. W. Bluman, J. D. Cole. *Similarity methods for Differential Equations*, New York, Springer–Verlag, pp. 1–332, 1974.

5. V. W. Ekman. *On the influence of the earth's rotation on ocean currents",* Ark. Mat. Astron. Fys. **2**, pp. 1–52, 1905.

6. A. G. Hansen. *Similarity Analyses of Boundary Value Problems in Engineering,* Prentice–Hall, Englewood Cliffs, NJ, 1964.

7. L. Howarth. *The boundary layer in three dimensional flow–Part II. The flow near a stagnation point,* Philos. Mag. Ser. 7, **42**, pp. 1433–1440, 1951.

8. K. R. Rajagopal. *A class of exact solutions to the Navier–Stokes equations,* Intl. J. Eng. Sci., **22**, pp. 451-458, 1984.

9. H. Schlichting. *Boudary-Layer Theory,* McGraw-Hill 6th ed., New York, 1968.

10. H. Schlichting. *Laminare Strahlenausbreitung,* Z. Angew Math. Mech., **13**, pp. 260-263, 1933a.

11. R. K. Shah, A. L. London. *Laminar Flow Forced Convection in Ducts,* Adv. Heat Transfer (Suppl.), New York, Academic, pp. 1–477, 1978.

12. C. Y. Wang. *On a class of exact solutions of the Navier–Stokes equations,* J. Appl. Mech., **33**, pp. 696-698, 1966.

13. C. Y. Wang. *Exact solutions of the unsteady Navier–Stokes equations,* Appl. Mech. Rev., **42**, pp. S269–282, 1989a.

14. C. Y. Wang. *The three-dimensional flow due to a stretching flat surface,* Phys. Fluids, **27**, pp. 1915-1917, 1984.

15. C. Y. Wang. *Shear flow over a convection cells–an exact solution of the Navier–Stokes equations,* ZAMM, 1999a.

16. C. Y. Wang. *Exact solutions of the Navier–Stokes equations–the generalized Beltrami flows, review and extesion,* Acta Mech., **81**, pp. 69–74, 1990b.

17. S. Weinbaum, V. O'Brien. *Exact Navier–Stokes solutions including swirl and cross flow,* Phys. Fluids, **10**, pp. 1438–1447, 1967.

18. G. B. Whitham. *The Navier–Stokes equations of motion in laminary boundary layers,* ed. L. Rosenhead, Oxford, Clarendon, pp. 114–162, 1963.

19. J. H. Lane. Am. J. Sci., **50**, pp. 57, 1870.

20. V. R. Emden. *Gaskugeln,* Springer, Berlin, 1907.

21. L. Kelvin. Proc. Roy. Soc., Edinburgh, **27A**, pp. 375, 1907.

22. S. Chandrashekhar. *Introduction to the Study of Stellar Structure,* Univ. Chicago Press, Illinois, 1939.

23. H. T. Davis. *Introduction to Nonlinear Differential and Integral Equations,* Dover, New York, 1962.

24. A. Andronow, S. Chaikin. *Theory of Oscillations,* Moscow, 1937.

25. J. J. Stoker. *Nonlinear Vibrations in Mechanical and Electrical Systems,* Willey (Interscience), New York, 1950.

26. N. W. MacLachaln. *Ordinary Non-Linear Differential Equations in Engineering and Physical Sciences,* 2nd ed., Oxford Univ. Press, London and New York, 1955.

27. N. M. Kryloff, N. N. Bogoliuboff. *Introduction to Nonlinear Mechanics,* Princeton Univ. Press, Princeton, New Jersey, 1943.

28. N. Minorsky. *Introduction to Non-linear Mechanics,* Edwards, Ann Arbor, Michigan, 1947.

29. N. Minorsky, E. Leimanis. *Dynamics and Nonlinear Mechanics,* Wiley, New York, 1958.

30. N. Minorsky. *Nonlnear Oscillation,* Van Nostrand, Princeton, New Jersey, 1962.

31. W. J. Cunningham. *Introduction to Nonlinear Analysis,* McGraw–Hill, New York, 1958.

32. I. G. Malkin. *Some Problems in the Theory of Nonlinear Oscillatons,* books 1,2 (translated from publ. of State Publishing House of Tech. Theoret. Lit. Moscow, U.S. At. Energy Comm., Washington, D.C., 1956).

33. J. K. Hale. *Nonlinear Oscillations,* McGraw–Hill, New York, 1963.

34. J. P. Lasalle, S. Lefschetz. *Stability by Liapunov's Direct Method with Applications,* Academic Press, New York, 1963.

35. J. P. Lasalle, S. Lefschetz. *Nonlinear Differential Equations and Nonlinear Mechanics,* academic Press, New York, 1963.

36. W. G. Bickley. Phil. Mag., **17**, pp. 603, 1934.

37. von Karman. *The engineer grapples with nonlinear problems,* Bull. Am. Math. Soc., **46**, pp. 615, 1940.

38. L. Prandtl. *Über Flüssigkeitsbewegung bei sehr kleiner Reibung,* Proc. Third Internat. Math. Cong. Heidelberg [English translation in NACA Technical Memo. 452], 1904.

39. L. Prandtl. *Collected Works,* **1-3**, Springer, Berlin, 1961.

40. H. Blasius. *Grenzschichten in Flüssikeiten mit kleiner Rebung,* Z. Angew. Math. Phys., **56**, pp. 1–37 [English translation in NACA Technical Memo. 1256], 1908.

41. H. Blasius. *Das Ähnlichkeitsgesetz bei Reibungsvorgangen in Flüssikeiten,* Forsch. Arb. Ing. Wes., **134**, Berlin, 1913.

42. S. Goldstein. *Concerning Some Solutions of the Boundary Layer Equations in Hydrodynamics,* Proc. Cambridge Phil. Soc., **26**, pp. 1–30, 1930.

43. C. W. Oseen. *Neure Methoden und Ergebnisse in der Hydrodynamik,* Akademische Verlag. Geest & Portig, Leipzig, 1927.

44. O. Reynolds. *On the Dynamical Theory of Incompressible Viscous Fluids and the Determination of the Criterion,* Phil. Trans. Roy. Soc. London Ser. A, **186**, pp. 123-164, 1895.

45. W. F. Ames. *Nonlinear Partial Differential Equations in Engineering,* Academic Press, New York, 1965.

46. W. F. Ames. *Nonlinear Ordinary Differential equations in Transport Processes,* Academic Press, New York, 1968.

47. S. J. Kline. *Similitude and Approximation Theory,* McGraw-Hill, New York, 1965.

48. S. J. Kline, D. E. Abbott. *Simple Methods for Classification and Construction of Similarity Solutions of Partial Differential Equations,* Rept. MD-6, Dept. of Mech. Eng., Stanford University, Stanford, California, AFSOR–TN–60–1163.

49. L. I. Sedov. *Dimensional and Similarity Methods in Mechanics (transl.),* Academic Press, New York, 1960.

50. A. S. Berman. *Laminar flow in channels with porous walls,* J. Appl. Phys., **24**, pp. 1232–1235, 1953.

51. A. S. Berman. *Laminar flow in annulus with porous walls,* J. Appl. Phys., **29**, pp. 71–75, 1958.

52. W. Wuest. *Asymptotische Absaugegrenzschichten an längsangeströmten zylindrischen Körpern,* Ing. Arch., **23**, S. 198–208, 1955.

53. H. G. Lew. *Asymptotic suction characteristics of thr boundary layer over a circular cylinder,* J. Aeronaut. Sci., **23**, pp. 895–897, 1956.

54. M. Yashura. *On the asymptotic solution of the laminar compressible boundary layer over a circular cylinder with uniform suction,* J. Phys. Soc. Jpn., **12**, pp. 102, 1955.

55. J. T. Stuart. *A simple corner flow with suction,* Q. J. Mech. Appl. Math., **19**, pp. 217–220, 1966.

56. A. S. Gupta. *Ekman layer on a porous plate,* Phys. Fluids, **15**, pp. 930–931, 1972.

57. V. Vidyanidhi, S. D. Nigam. *Secondary flow in a rotating channel,* J. Math. Phy. Sci., **1**, pp. 85–94, 1967.

58. V. Vidyanidhi, V. Prasad, V. B. Ramana Rao, V. V. *Secondary flow between two parallel porous walls in a rotating system,* J. Phys. Soc. Jpn., **39**, pp. 1077-1081, 1975.

59. T. N. G. Abbott, K. Walters. *Rheometrical flow systems. part 2. Theory for the orthogonal rheometer, including an exact solution of the Navier–Stokes equations,* j. Fluid Mech., **40**, pp. 205–213, 1970.

60. M. E. Erdogen. *Flow due to eccentric rotating a poroue disk and a fluid at infinity,* J. Appl. Mech., **43**, pp. 203-204, 1976.

61. Kampé de Fériet *Sur quelques cas d'intégration des équations du mouvement plan d'un fluide visquex incompressible,* Proc. Int. Congr. Appl. Mech., 3rd, stockholm, pp. 334-338, 1930.

62. Kampé de Fériet *Determination ds mouvements plans d'un fluide visquex incompressible, uú le tourbillon est constant le long des lignes de courant,* Verh. Intl. Math. Kongr., Zürich, **2**, pp. 298–299, 1932.

63. C. Strakhovitch *On a class of motion of a viscous incompressible liquid,* Prikl. Mat. Mekh., **2**, pp. 74–81 (In Russian), 1955.

64. L. Fox. *Numerical Solution of Two-Point Boundary Problems in Ordinary Differential Equations,* Oxford, London, 1957.

65. L. Collatz. *The Numerical Treatment of Differential Equations,* 3rd ed., Springer–Verlag, Berlin, 1960.

66. R. S. Varga, *Matrix Iterative Analysis,* Prentice-Hall, Englewood Cliffs, N. J., 1962.

67. L. V. Kantrovich, G. P. Akylov. *Functional Analysis in Normed Spaces,* New York, Macmillan, 1964.

68. L. V. Kantrovich, V. I. Krylov. *Approximate Methods of Higher Analysis,* New York, Interscience, 1958.

69. P. Ciarlet, M. Schultz, R. Varga *Numerical methods of high-order accuracy for nonlinear boundary value problems,* Numer. Mathe., **9**, pp. 394-430, 1967.

70. H. Keller *Existence theory for two point boundary value problems,* Bulletin A. M. S., **72**, pp. 728–731, 1966.

71. R. Courant *Variational methods for the solutions of problems pf equilibrium and vibrations,* Bull. Amer. Math. Soc., **49**, pp. 1-23, 1943.

72. R. Courant, D. Hilbert. *Methoden der math,* Physik, **I**, 2nd ed., pp. 302, Berlin, 1931.

73. K. O. Friedrichs, H. B. Keller *A finite difference scheme for generalized Neumann problems. In Numerical Solution of Partial Differential Equations,* J. Bramble, Ed., New York, Academic Press, pp. 1–9, 1966.

74. L. A. Pipes *Applied Mathematics for Engineers and physicists,* 2nd ed. McGraw–Hill, New York, 1958.

75. H. Poincaré. *Mecanique Celeste,* **Vol. I**, Gauthier-Villars, Paris, 1892.

76. J. L. Nowinski, I. A. Ismail. *Developments in Theoretical and Applied Mechanics,* N. A. Shaw, ed., **Vol. II**, pp. 35, Pergamon Press, Oxford, 1965.

77. W. F. Ames, J. L. Sontowski. J. Appl. Mech., **33**, 218, 1966.

78. J. Shohat. J. Appl. Phys., **15**, pp. 568, 1944.

79. R. Bellman. Quart. Appl. Math., **13**, pp. 135, 1955.

80. R. Bellman. *Paper 55-APM-33,* Am. Soc. Mech. Eng., New York, 1955.

81. K. O. Friedrichs *Theory of viscous fluids,* Fluid Dynamics, Chapter 4, Brown Univ. Press, Providence, Rhode Island, 1942.

82. K. O. Friedrichs *Special Topics in Fluid Mechanics,* N. Y. U. Press, New York, 1953.

83. S. Kaplun, P. A. Lagerstrom *Asymptotic expansions of Navier–Stokes solutions for small Reynolds numbers,* J. Math. Mech., **Vol. 6**, pp. 585–593, 1957.

84. F. P. Bretherton. *The motion of long bubbles in tubes,* J. Fluid Mech., **10**, pp. 166, 1961.

85. P. A. Lagerstrom, J. D. Cole. *Examples illustrating expansion procedures for the Navier–Stokes equations,* J. Rat. Mech. Anal., **4**, pp. 817–882, 1955.

86. M. Van Dyke. *Perturbation Methods in Fluid Mechanics,* Academic Press, New York, 1964.

87. K. Hiemenz. *Die Grenzschicht an einem in den gleichförmigen Flüssigkeitsstrom eingetauchten geraden Kreiszylinder. Diss. Göttingen,* Dingl. Polytech. J., 326, 321–324, 344–348, 357–362, 372–376, 391–393, 407–410, 1911.

88. N. Frössling. *Verdunstung, Wärmeübertragung und Geschwindigkeitsverteilung bei zweidimensionaler und rotationssymmetrischer laminarer Grenzschichtströmung,* Lunds. Univ. Arsskr. N. F. Adv. 2, **35**, Nr. 4, 1940.

89. A. Ulrich. *Die ebene laminare Reibungsschict an einem Zylinder,* Arch. Math., **4**, pp. 247–256, 1949.

90. A. N. Tifford. *Heat Transfer and frictional effects in laminar boundary layers,* part 4, Universal Series Solutions, WADC Technical Report, pp. 53–288, 1954.

91. I. Tani. *On the solution of the laminar boundary layer equations,* Jour. Phys. Soc., Japan, **4**, pp. 149–154, 1949.

92. H. Goertler. *A new series for the calculation of steady laminar boundary-layer flows,* Jour. of Math. and Mechanics, **6**, 1, 1957.

93. H. Goertler. *Zahlentafeln universeller Funktionen zur neuen Reihe für die Berechnung laminarer Grenzschichten,* Bericht No. 34 of the Deutsche Versuchsanstalt für Luftfahrt, 1957.

94. D. Meksyn. *New Methods in Laminar Boundary Layer Theory,* Pergamon, London, 1961.

95. S. Liao. *HOMOTOPY ANALYSIS METHOD: A NEW ANALYTIC METHOD FOR NONLINEAR PROBLEMS,* Appl. Math. and Mech., **Vol. 19**, No. 10, Oct. 1998.

96. C. Wang. *Analytic solutions for a liquid filmon an unsteady stretching surface,* Heat Mass Transfer, **42**, pp, 759-766, 2006.

97. D. A. Anderson, J. C. Tannehill and R. H. Pletcher. *Computational Fluid Mechanics and Heat Transfer,* Hemisphere, New York, 1984.

98. M. Holt. *Numerical Methods in Fluid Dynamics,* Springer, New York, 1984.

99. C. Y. Chow. *An Introduction to Computational Fluid Mechanics,* Wiley, New York, 1979.

100. T. K. Bose. *Computational Fluid Dynamics,* Wiley, New York, 1988.

101. G. A. Sod. *Numerical Methods in Fluid Dynamics,* Cambridge Univ. Press, New York, 1985.

102. S. V. Patankar. *Numerical Heat Transfer and Fluid Flow,* Hemisphere, New York, 1980.

103. A. Cohen, G. E. Stechert and Co. *An introduction to the Lie Theory of One-Parameter Groups,* New York, 1931.

104. L. E. Dickson. *Differential Equations from the Group Standpoint,* Annals of Mathematics, Second Series, **25**, pp. 287-378, 1923.

105. L. Boltzmann. *Ann. Physik,* **53:959**, 1894.

106. G. Birkhoff. *Hydrodynamics,* Princeton Univ. Press, Princeton, New Jersey, Ch. V, 1950.

107. T. V. Davies, E. M. James *Nonlinear Differential Equations,* Addison-Wesley, Reading, Massachusetts, 1966.

108. A. A. Bennett, W. E. Milne, H. Bateman. *Numerical Integration of Diffrential Equations,* Dover, New York, 1956.

109. H. Levy, E. A. Baggott *Numerical Studies in Differential Equations,* Dover, New York, 1956.

110. P. Henrici. *Discrete Variable Methods in Ordinary Differential Equations,* Wiley, New York, 1962.

111. von Sanden. *Praxis der Differentialgleichungen,* 4th ed. de Gruyter, Berlin, 1955.

112. W. E. Milne *Numerical Solution of Differential Equations,* Wiley, New York, 1953.

113. S. E. Mikeladze. *New Methods of Integration of Differential Equtations and Their Applications to Problems in Theory of Elasticity,* (in Russian), Gosudarstv. Izdat Tehn.-Teor. Lit., Moscow, 1951.

114. E. Gruschwitz. *Die turbulente Reibungssschicht in ebener Strómung bei Druckabfall und Druckanstieg,* Ing.-Arch., **2**, pp. 321, 1931.

115. K. Weighardt. *Über einen Energiesatz zyr Berechnung laminarer Grenzschichten,* Ing.-Arch., **16**, pp. 231, 1948.

116. A. Mager *Generalization of boundary layer momentum-integral equations to three-dimensional flows including those of rotating systems,* NACA Rep., No. **1067**, 1952.

117. H. Holstein, T. Bohlen. *Lilienthal-Berichit,* S **10**, pp. 5-16, 1940.

118. K. Pohlhausen. *Z. Angrew. Math. Mech.,* **1**, pp. 252, 1921.

119. H. Schlichting. *Grenzsschicht-Theorie,* 3rd ed., G. Barun, Karlsruhe, 1958.

120. F. M. White. *Heat and Mass Transfer,* Addison-Wisley, Reading Mass., 1988.

121. F. M. White. *Viscous Fluid Flow ,* 2nd ed., McGraw-Hill, New York, 1991.

122. C. Wang, S. J. Liao, J. M. Zhu. *An explicit analytic solution for the combined heat and mass transfer by natural convection from a vertical wall in a non-Darcy porous medium,* Intl. J. Heat Mass transfer, **46**, pp. 4813-4822, 2003.

123. S. M. Roberts, J. S. Shipman. TWO-POINT BONDARY VALUE PROBLEMS: SHOOTING METHODS, Elsevier, New York, 1972.

124. von Kármán. *Über laminare and turbulente Reibung,* ZAMM, **1**, 233, 1921.

125. G. B. Jeffrey. *The two-dimensional steady motion of a viscous fluid,* Philos. Mag. Ser., **6 29**, pp. 455-65, 1915.

126. L. J. Crane. *Flow past a stretching plate,* ZAMP, **21**, pp. 645-647, 1970.

127. I. S. Gradshteyn, I. M. Ryzhik. *Table of Integrals, Series and Products,* Academic Press, New York, 1965.

128. E. M. Sparrow, J. L. Gregg. *A Boundary-Layer Treatment of Laminar Film Condensation,* J. Heat Transfer, Trans. ASME, Series C, **81**, pp. 13–18. 1959.

129. W. M. Rohsenow. *Heat Transfer and Temperature Distribution in Laminar-Film Condensation,* Trans. ASME, **78**, pp. 1645-1648, 1958.

130. M. M. Chen. *An Analytical Study of Laminar Film Condensation: Part 1-Flat Plates,* J. Heat Transfer, **83**, pp. 48–54, 1961.

131. J. C. Y. Koh, E. M. Sparrow, J. P. Harnett. *The two phase boundary layer in laminar film condensation,* Intl. J. Heat Transfer, **2**, pp. 69–82, 1961.

132. J. C. Y. Koh. *An Integral Treatment of Two-Phase Boundary Layer in Film Condensation,* J. Heat Transfer, **83**, pp. 359–362, 1961.

133. L. A. Bromley. *Effect of Heat Capacity of Condensate,* Industrial and Engineering Chemistry, **44**, pp. 2966, 1952.

134. V. P. Carey. *LIQUID-VAPOR PHASE-CHANGE PHENOMENA,* Series in Chemical and Mechanical Engineering, HPC, Washington, 1992.

135. J. G. Collier, J. R. Thome. *Convective Boiling and Condensation,* 3rd ed., Oxford Science Publications, 1994.

136. http://www.wlv.com/products/databook/db3/data/db3ch7.pdf

137. A. Eucken. *Naturwisseenschaften,* **25**, pp. 209, 1937.

138. J. L. McCormick, E. Baer. *On the mechanism of heat transfer in drop-wise condensation,* J. Colloid Sci., **18**, pp. 208–216, 1963.

139. A. Umur, P. Griffith. *Mechanism of drop-wise condensation,* J. Heat Transfer, **87**, pp. 275–282, 1965.

140. J. F. Welch, J. W. Westwater. *Microscopic study of drop-wise condensation,* Int. Developments in Heat Transfer, Proc. Int. Heat Transfer Conf., ASME, Part II, pp. 302–309, 1961.

141. R. S. Silver. *An approach to a general theory of surface condensers,* Proc. Inst. Mech. Eng., **178**, pp. 339-376, 1964.

142. W. Nusselt. *Die Oberflachen Kondensation des Wasserdampfes,* Zeitschrift des Vereines Deutscher Ingenieure, **60**, pp. 541–569, 1916.

143. J. M. McDonough. *LECTURES IN BASIC COMPUTATIONAL NUMERICAL ANALYSIS,* Univ. Kentucky, Lexington, KY, 2004.

144. *MAPLE 10,* Maplesoft Corporation, Waterloo, Ontario, Canada.

VITA

Abhishek Tiwari

Abhishek Tiwari was born on March 31, 1979 in Jabalpur (M. P.), India. He received a bachelors' degree from Rajiv Gandhi Proudyogiki Vishwavidyalaya, Madhya Pradesh, India in July of 2002. Currently he is completing work on a Masters degree in the Department of Mechanical Engineering at the University of Kentucky.

Professional Positions Held

Faculty of Mathematics, July 2003 - July 2004

Institute of Management Studies

Gwalior, Madhya Pradesh, India.

Teaching Assistant, Spring 2005 - Spring 2006

Advanced Computational Fluid Dynamics Group

Department of Mechanical Engineering, University of Kentucky, Lexington, KY.

Graduate Research Student, Spring 2006 - Spring 2007

Advanced Computational Fluid Dynamics Group

Department of Mechanical Engineering, University of Kentucky, Lexington, KY.

Scholastic Honors

Kentucky Graduate Scholarship, Fall 2004 - Fall 2006

University of Kentucky, Lexington, KY.

Professional Society Membership

American Society of Mechanical Engineers

Papers and Conferences

1. Abhishek Tiwari, Kaveh A. TAgavi and J. M. McDonough, "Analytical Methods for Transport Equations in Similarity Form," 2007 ASME-JSME Thermal Engineering Summer Heat Transfer Conference, Vancouver, British Columbia, Canada, July 8-12, 2007.

2. Abhishek Tiwari and J. M. McDonough, "A Schur Complement/Domain Decomposition Elliptic Solver," Dayton-Cincinnati Aerospace Science Symposium, Dayton, OH, March 2006.

3. Abhishek Tiwari and J. M. McDonough, "Numerical Techniques for Bubble Dynamics," Dayton-Cincinnati Aerospace Science Symposium, Dayton, OH, March 2005.

Undergraduate Projects

1. Study and comparison of Braking Systems in Automobiles, June 2002.